THE INTERACTIONS OF OLIGOPEPTIDE AMIDES AND ANTHRACYCLINES WITH DNA

By

STEVENS WHITE PEARCE

A DISSERTATION PRESENTED TO THE GRADUATE COUNCIL
OF THE UNIVERSITY OF FLORIDA
IN PARTIAL FULFILLMENT OF THE REQUIREMENTS FOR THE
DEGREE OF DOCTOR OF PHILOSOPHY

UNIVERSITY OF FLORIDA

1977

TO MY FAMILY

ACKNOWLEDGMENTS

The author extends his appreciation to Professor Edmond J. Gabbay for his guidance and support during the past four years. Thanks are extended to all those who have helped in the author's graduate studies, especially Dr. P. Adawadkar, Mr. M. Adkins, Mr. R. Dugan, Dr. J. Dugan, Mr. R. Fingerle, Ms. L. Gabbay, Mr. D. Grier, Dr. L. Kapicak, Ms. A. Kennedy, Mr. D. O'Brein, Ms. C. Petzinger, Ms. J. Raudenbush, Mr. R. Sheardy, and Professor D. W. Wilson.

The completion of this course of study would not have been possible without the support and encouragement of the author's family.

Table of Contents

List of Tables

Table		Page
15.	Effect of pH on the Rate of Hydrolysis of the Blycosidic Bond of the Anthracyclines at 50°C	90
16.	Biological Activity of the Anthracyclines against Mouse Lymphocytic Leukemia	93
17.	Biological Activity of the Anthracyclines against Mouse Lymphocytic Leukemia	94

List of Figures

Figure Page

Abstract of Dissertation Presented to the Graduate Council of the University of Florida in Partial Fulfillment of the Requirements for the Degree of Doctor of Philosophy

THE INTERACTIONS OF OLIGOPEPTIDE AMIDES AND ANTHRACYCLINES WITH DNA

By

Stevens White Pearce

March 1977

Chairman: Edmond J. Gabbay
Major Department: Chemistry

The first part of the thesis discusses the interaction specificities of sixteen oligopeptide amides with salmon sperm DNA. The peptides are of defined sequence with a N-terminal L-lysyl-L-phenylalanine. The extent of upfield chemical shift and signal line broadening of the ^{1}H nmr signals of the aromatic protons of the peptide (in the presence of excess DNA) are found to depend on the primary sequence and chirality of the α carbons of the amino acids in the oligopeptide amides. Viscometric titrations of DNA with the peptides show that in all cases the peptide causes a reduction in helical length; however, there is a greater change with peptides which contain a D-amino acid, instead of L, in the 3 position from the N-terminal. Peptides with a D-amino acid in the 3 position also exhibit stronger binding affinity to DNA and

greater stabilization of the helix-coil transition than do peptides with only L-amino acids. The results obtained with the different di-, tri-, tetra-, penta-, and hexapeptides are found to be consistent with a model whereby the peptide assumes a slightly modified single-stranded β-sheet structure which is wrapped around the nucleic acid helix in a manner similar to that described by M. H. F. Wilkins ((1956) Cold Spring Harbor Symp. Quant. Biol., 21, 75).

The second part of this thesis involves the study of 11 new anthracycline derivatives, daunorubicin, and adriamycin with DNA. The anthracyclines, daunorubicin, and adriamycin undergo hydrolysis of the glycosidic bond leading to water insoluble aglycones which have been suggested to be the cause of the drugs' accumulative toxicity. The derivatives which have been prepared lead to water soluble aglycones upon glycosidic hydrolysis, thus, reducing the biological half-life.

The anthracyclines in the presence of DNA exhibit an induced circular dichroism and a red shift in the maxima. The visible absorption spectra of the anthracyclines show a pronounced hypochromic effect upon the addition of DNA. It is shown that the extent of hypochromism in the electronic transition of the anthracycline upon binding to DNA is directly proportional to the apparent binding affinity, K_a, of the drug to DNA as determined by spectral titration methods.

Both the rate of dissociation of DNA-anthracycline complexes and the effect of the anthracyclines on the activity of DNA-dependent *E. coli* RNA polymerase were examined.

It is found that the rate of dissociation of the drug from DNA is inversely proportional to the extent of inhibition of the polymerase reaction. This is consistent with the results of W. Muller and D. M. Crothers ((1968) J. Mol. Biol., 35, 251) on the interaction specificities of actinomycin D and its derivatives with DNA.

In vivo tests on the anthracycline against P-388 lymphocytic leukemia show that (i) the optimal dose and toxic dose of the new anthracycline derivatives are higher than for either daunorubicin or adriamycin, (ii) the aglycones have biological activity although much lower than that of the anthracycline, and (iii) two of the newly synthesized anthracycline analogs exhibit greater biological activity than does daunorubicin. The lack of enhanced biological activity of the other analogs may be explained by (i) the inability of the aromatic ring to fully intercalate between the base pairs of DNA due to steric bulk, (ii) the reduced lipid solubility of the analogs, and/or (iii) the increased susceptibility of the analogs to glycosidic hydrolysis as compared to daunorubicin.

CHAPTER I
INTRODUCTION

The determination of the fiber structure of deoxyribonucleic acid in 1953, by Watson and Crick, is undoubtedly a milestone in biological science.[1,2] Watson said of it, "The gene was no longer a mysterious entity whose behavior could be investigated only by breeding experiments. Instead, it became a real molecular object about which chemists could think objectively in the same manner as smaller molecules."[3]

DNA may have a molecular weight into the billions of daltons and if fully extended may be as long as 2 centimeters.[4] In fact, a complete DNA molecule, as it exists inside the cell, is difficult to isolate due to the molecule's extreme length which imparts to it a susceptibility to break under minimal shearing forces.[5] Therefore, during the isolation process the DNA breaks into fragments and studies are usually conducted on the fragments of the initial native molecule. Homogeneous DNA (i.e., DNA with a defined molecular weight and sequence) may be obtained from (i) viral or bacterial sources, (ii) selective isolation of an organism's genome, (e.g., satelite DNA), and (iii) via direct synthetic procedures.

The most common commercial DNA are obtained from calf thymus and salmon sperm. The nucleic acid concentration is generally expressed in units of phosphate per liter and is determined on the basis of the molar extinction coefficient of the bases at 260 nm (e.g., for salmon sperm DNA, ε_p = 6,500).[6]

DNA Structure

Watson and Crick published their concept of the structure of the DNA molecule on the basis of X-ray diffraction data on DNA fibers and on the chemical evidence of Chargaff and Lipschitz.[1,2,7] In fact, without their pioneering work on the chemical approach to discerning the molecular structure of DNA, Watson and Crick would not have been able to propose their structure of DNA, since X-ray analysis of fibers produce low resolution data that must be fitted through use of models.

On work involving DNA from numerous sources, Chargaff and Lipschitz noted that there were certain similarities for DNA's of various species.[7] These observations, known as Chargaff's rules, are that (1) the amount of adenine (A) equals the amount of thymine (T); (2) the amount of guanine (G) equals the amount of cytosine (C); and (3) for a particular species, the A-T/G-C ratio is a constant.

The Watson-Crick model of nucleic acid, seen in Figure 1, consists of two antiparallel polynucleotide strands held together by specific hydrogen bonds formed between the

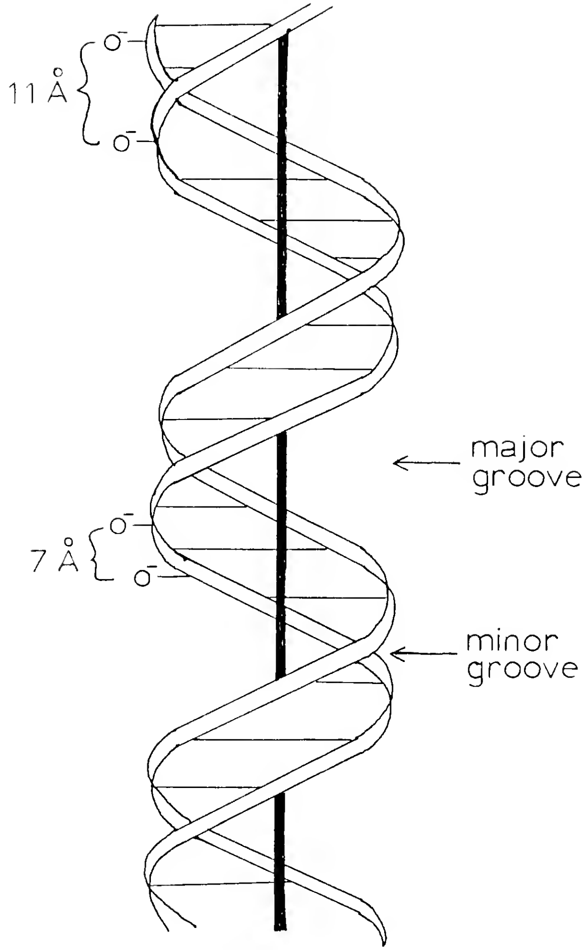

Figure 1. Schematic Representation of the Watson-Crick Double Helix of DNA. The outer helical strands represent the sugar-phosphate backbone, the horizontal lines represent the base-pairs, and the vertical line is the helical axis.

complimentary bases as well as by hydrophobic forces that favor a stacked base geometry. Figure 2 illustrates the specific Watson-Crick base pairing scheme which accounts for Chargaff's rules.

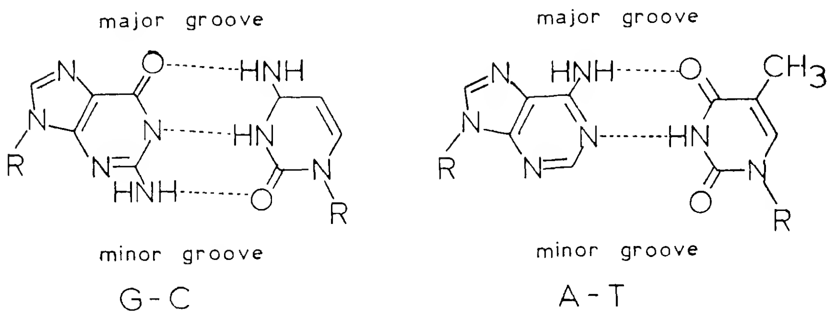

Figure 2. Watson-Crick Base Pairs

The individual DNA strands are composed of monomer nucleotide units which have been enzymatically joined to produce an alternating sugar-phosphate-sugar backbone, while the bases are stacked on top of one another (Figure 3). The D-deoxyribose sugar, which exists in the furanoside form, has two hydroxyl groups at the 3' and 5' position. In order to obtain maximum symmetry, the two complimentary strands are placed anitparallel. In other words, one strand has its sugar-phosphate chain directed 3'→5' while the other chain is directed 5'→3'. This aspect of the double helix was proven correct by Josse and coworkers using nearest neighbor analysis.[8]

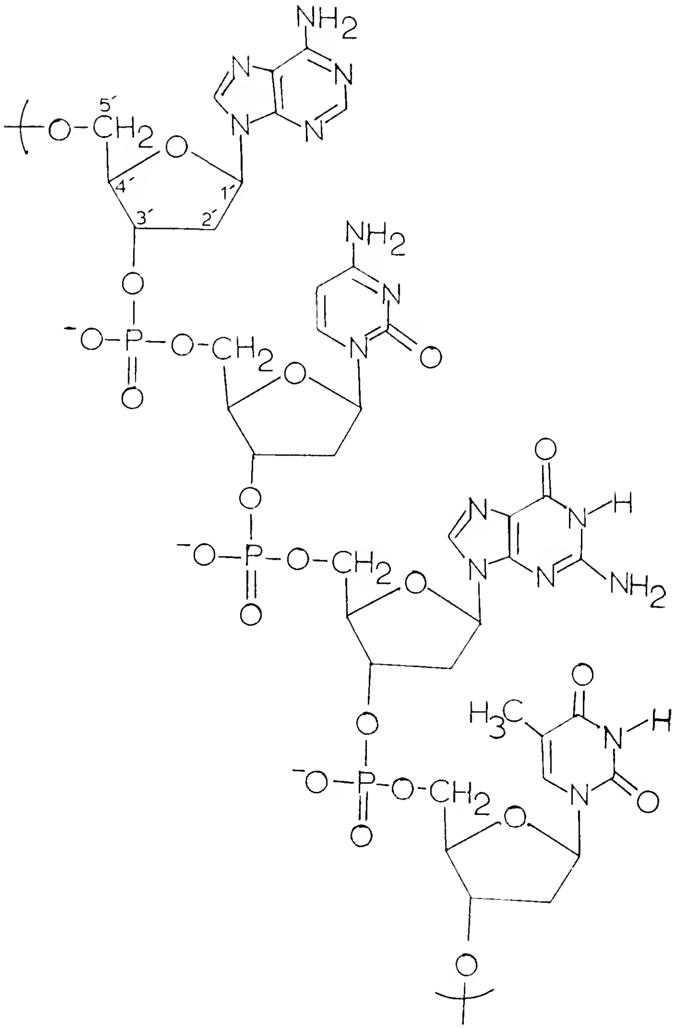

Figure 3. Structure of a Section of a DNA Chain

The phosphate groups are formally phosphate diesters. At neutral pH, the phosphates exist as monoanions and, due to this charged character, the oxygen atoms are not equivalent in that one lies parallel to the helical axis (axial) and the other lies perpendicular to it (equatorial).

Langridge and coworkers found from X-ray diffraction data that the double helix makes one complete turn every 34 angstroms.[9] In addition, there are ten base pairs in a pitch, or a translation of 3.4 angstroms between each base pair on the average. Since one turn of the double helix encompasses 360° of rotation, the model predicts that the average angle between successive base pairs is 36°. The planes of the base pairs are perpendicular to the helical axis.

As a consequence of the twist of the double helix, there exists two distinct grooves (i.e., the major and minor). Inspection of Figure 2 shows the positions of the major and minor grooves and, in addition, that (1) the third hydrogen bond of the G-C base pair is located in the minor groove, and (2) the methyl group of thymine is located in the major groove. These facts are important to the intercalation of small molecules with DNA.

All X-ray work on DNA has been done with fibers. Unlike X-ray analysis of small crystals, fibers do not produce enough definable data points so that a definite arrangement of the atoms can be made. Usually, molecular models are built and fitted to the available data. In this way,

models which are inconsistent with the data or are stereochemically unfeasible are ruled out. Eventually, this elimination of models yields at least one model which is consistent with the available X-ray data. Donohue has questioned this method of X-ray analysis and has suggested that it not be used.[10-12]

In the B form of DNA (where the base pairs are perpendicular to the helical axis and the pitch is 34 angstroms with 10 base pairs per turn), X-ray studies of the fiber cannot distinguish between a left- and a right-handed helix.[13] It is only because the A form of DNA (where the base pairs are at an angle of 15^o from perpendicular and the pitch is 28 angstroms with 11 base pairs per turn) can be established as a right-handed helix that it can be assumed that the B form is also. There have been at least eight structures proposed for nucleic acids, all varying in the angle of tilt of the base pairs from perpendicular and the pitch of the helix (i.e., A, B, C, P, P_2, J_1, J_2, and S).[14]

Different media from which the fibers of DNA are drawn for X-ray analysis yield slightly different structures for the same DNA molecule (i.e., Li^+, K^+, Na^+, or Mg^{2+} salts).[9] Above 80% relative humidity, X-ray data suggest the B, but below 80% relative humidity the data suggest the A form. In addition to dependence on salt and humidity, it has been shown that the A-T/G-C ratio of the DNA will cause a change in structure, suggesting that the secondary structure of DNA is a function of the primary sequence.[14] It is apparent

that DNA structure is a function of many variables and extrapolation of fiber structure to solution may not be justified. The necessity of using DNA in its fiber form for the X-ray analysis and then using these results to postulate a structure for DNA in solution, assumes that its molecular structure does not change upon solvation. In fact, Bram's studies using a low angle X-ray scattering technique on DNA in solution, supports the contention that fiber and solution structure of DNA are different.[15,16]

Physical Properties of DNA

It was pointed out earlier that DNA is a delicate molecule in terms of breakage due to shearing forces. However, there are a number of other precautions that must be observed when working with nucleic acids in solution. If a DNA solution is heated gradually and the absorption at the wavelength maximum for DNA is monitored (i.e., at 260 nm), a sigmoidal curve as shown in Figure 4 will be observed.[17,18] Similar behavior is also observed for the temperature dependence of the viscosity and molar ellipticity. The results are consistent with a molecular transformation, i.e., a helix-coil transition. The descriptive term, denaturation (and/or "melting out") of the native DNA structure is used to describe this phenomenon.

Hydrogen ion concentration also affects the structure of DNA. The viscosity-pH profile of a DNA solution is shown in Figure 5.[19] It is seen that at pH extremes of 4.5

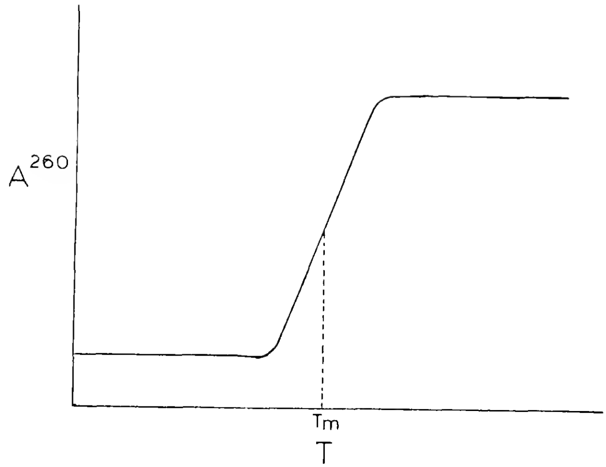

Figure 4. Absorption-Temperature Profile for DNA

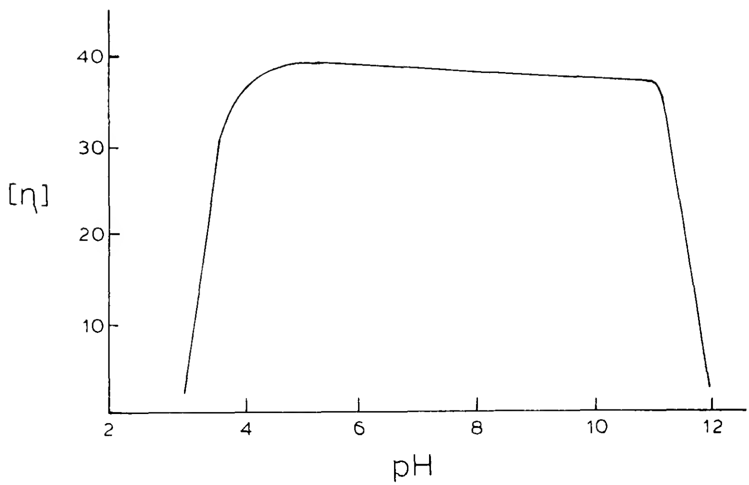

Figure 5. Intrinsic Viscosity-pH Profile for DNA

and 11.5, the viscosity of the solution starts to decrease rapidly, indicative of a "melting out" of the native DNA structure. It is for this reason that DNA solutions are always prepared in buffered solutions, usually in the pH range of 6 to 8. A titration curve of a DNA solution is presented in Figure 6.[20] Curve A represents a titration starting at pH 6.9 while curve B represents the back titration from pH 2.5 or 12.5 to neutral. Two observations may be made: 1) DNA has both acidic and basic titratable groups, and 2) the titration curves are not reversible.

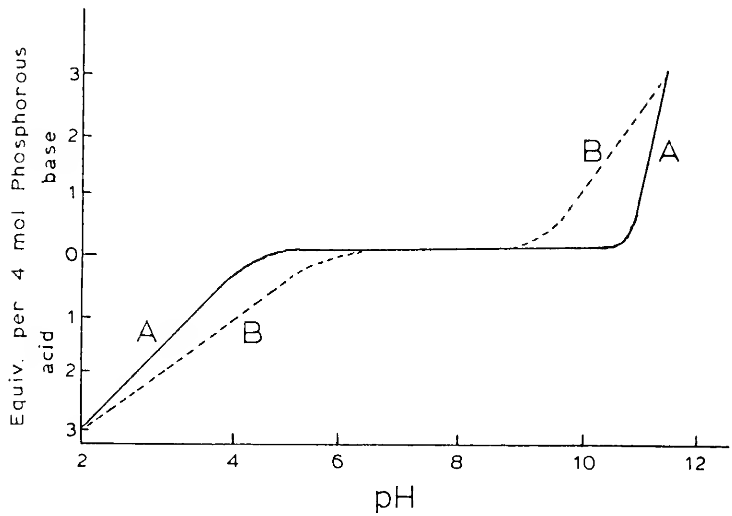

Figure 6. Acid-Base Titration Curve for DNA

The back titration reveals that weakly acidic and basic groups, not available in the first titration, are available in the second (denatured DNA).

In addition to temperature and pH, the DNA structure is also dependent on salt concentrations. Thomson et al. have shown that a DNA solution undergoes denaturation when the sodium chloride concentration is below 10^{-3} M or when the magnesium chloride concentration is below 10^{-5}M.[21] The helix-coil transition is again not reversible and, consequently, in preparing DNA solutions the ionic strength must be kept at a minimum of 1 mM.

The dielectric constant and hydrogen bonding capacity of the solution medium are also important in controlling the structure of DNA. Solvents such as formamide, DMF, or DMSO cause irreversible DNA denaturation. DNA, of course, is not soluble in pure organic solvents and these experiments are carried out by adding the organic solvent to an aqueous DNA solution.[22]

It is evident from the above studies that many types of forces may be important to the maintenance of the DNA helix. To gain insight into the mechanisms of the interactions of nucleic acids with other molecules and to understand the nature of the forces that influence the structure of DNA in solution, it is necessary to analyze these systems from a chemical standpoint. Unfortunately, macromolecules do not easily lend themselves to the classical chemical experimental approaches that are successful for small molecules. As a result, model systems often employing the monomer and oligomer units of nucleic acids (i.e., nucleosides and oligonucleotides) are used. A brief outline of some of the

more revealing studies in this regard is now presented with the intention of specifying the forces that control the structure of nucleic acid in solution.

Hydrogen Bonding Forces

While the geometrical constraints of colinear hydrogen bonds and hydrogen bonding lengths of 2.8 - 3.0 angstroms would allow for the formation of 29 possible base pairs connected by two or three hydrogen bonds, it has been found that even rather simple base derivatives exhibit surprising specificity in the hydrogen bonding schemes employed in practice.[23,24] In fact, only three different schemes have been found in the crystalline state. Calculations based on dipole-dipole interactions have shown that the Watson-Crick scheme is favored markedly for guanine-cytosine base pairing, but adenosine-uracil pairs can exist in three forms, two of them of approximately equal energy.[25] Indeed, two crystal structures have been found for substituted A-T base pairs. Cocrystals of 9-methyladenine and 1-methylthymine have been found to assume the Hoogsteen base pairing scheme (Figure 7a).[26,27] It was postulated by these authors that this structure was not seen in nucleic acids due to the fact that the electrostatic repulsion between strands was lower in the Watson-Crick base pairing scheme. This assertion was based on the fact that the two phosphodiester chains are further apart in the Watson-Crick than they are in the Hoogsteen scheme. Moreover, adenosine and 5-bromo-

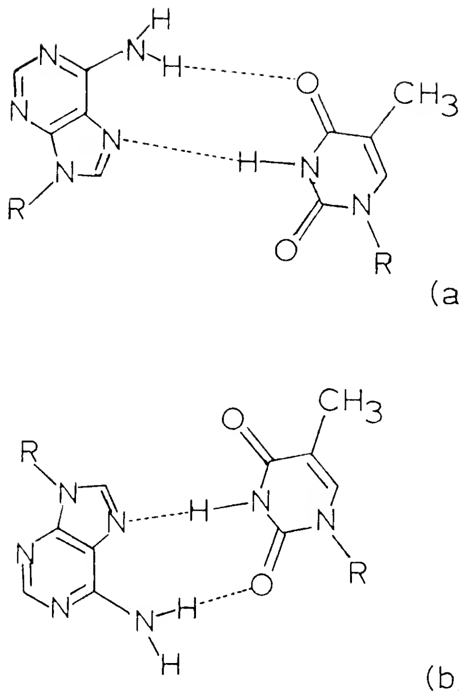

(a)

(b)

Figure 7. (a) Hoogsteen-Thymine Base Pair
(b) Anti-Hoogsteen Adenine-Thymine Base Pair

uridine have been found to assume the anti-Hoogsteen base pairs (Figure 7b).[28,29] On the other hand, single crystals of guanine and cytosine have yielded only the expected Watson-Crick base pairing scheme.[30,31] This may well be due to the fact that the Watson-Crick scheme (for G-C) has three hydrogen bonds while the others have only two.

Specific H-bonding has also been detected in aqueous solution. It was found that when a given nucleoside was covalently attached to an insoluble support and a mixture of the other three nucleosides was passed through this modified support, only the compliment to the covalently bound nuceo-

side was retarded.[32] In addition, elution of the column with aqueous urea instead of water abolished the association, thus strongly implicating hydrogen bonding as the force responsible for the binding of the complimentary nucleoside.

^{1}H nmr studies monitoring the downfield chemical shift of hydrogen bonded protons indicate that base pairing decreases as the hydrogen bonding ability of the solvents increases. Moreover, ^{1}H nmr studies in nonhydroxylic solvents showed that the base pairing is quite specific. For example, the chemical shift of the N-1 proton of guanine was downfield shifted only when the complement cytosine was added, with little effect being seen upon addition of other nucleosides.[33] A similar observation was also noted for the N-3 proton of uridine in the presence of adenine.[34] While these studies show that hydrogen bonding may be quite specific in nonhydroxylic solvents, it is hard to imagine that it plays a major role in stabilizing the double helical structure. In aqueous solution, the competition for the hydrogen bonding sites on the bases by water would minimize the importance of these forces. The answer to the question of the importance of hydrogen bonding in the aqueous environment lies in the realization that the double helix has a nonpolar interior region where the bases are located. The aqueous solvent is excluded from this region due to the hydrophobic nature of the bases, thus making this region ideal for the formation of hydrogen bonds.

Infrared spectroscopy studies monitoring the appearance of new absorption bands between 3500 cm^{-1} and 3000 cm^{-1} for the N-H stretching frequency also indicate specific hydrogen bonding between complementary bases.[35] For example, a mixture of 9-ethyladenine and 1-cyclohexyluracil exhibited two new bands at 3490 and 3330 cm^{-1} which were maximized when the components were mixed at a ratio of 1:1. Similar results have been obtained with derivatives of guanine and cytosine.[36]

Stacking Forces

In addition to the hydrogen bonding interactions between bases, hydrophobic forces are very important to maintaining the DNA double helix. The bases are essentially nonpolar molecules which tend to vertically stack in aqueous solution. This phenomenon is thought to be entropy driven since the associated bases are less hydrated than the individual bases.[37] Therefore, stacking causes the release of water from hydration. This can be represented by the formula below:

$$\text{Hydrophobe} \cdot XH_2O + \text{Hydrophobe} \cdot YH_2O \rightarrow$$
$$2\ \text{Hydrophobe} \cdot ZH_2O$$
$$Z < X+Y;\ \Delta S = +$$

Hydrogen bonding interactions are accentuated in organic solvents; however, DNA is denatured by these solvents. Therefore, it must be concluded that other forces are important to the double helix. Presumably, the major forces in maintaining the helix are hydrophobic interactions.

Determination of the osmotic coefficient for several purine and pyrimidine systems in aqueous media followed by calculation of activity coefficients by the Gibbs-Duhem equation show large deviation from ideality indicative of association.[37] Hydrogen bonding was ruled out since urea, which hydrogen bonds extensively in water, exhibits a much greater activity than the bases. Purines have been found to associate to a greater extent than pyrimidines; and, methylation of the bases increases the stacking interaction.

The stacking interaction was investigated by ^{1}H nmr based on the observation that as the concentration of purine increased, the chemical shift of the protons became increasingly upfield shifted.[38] From ^{1}H nmr theory on ring current anisotropy, illustrated in Figure 8, it is possible to predict that the association results from vertical stacking of the purine bases.[39]

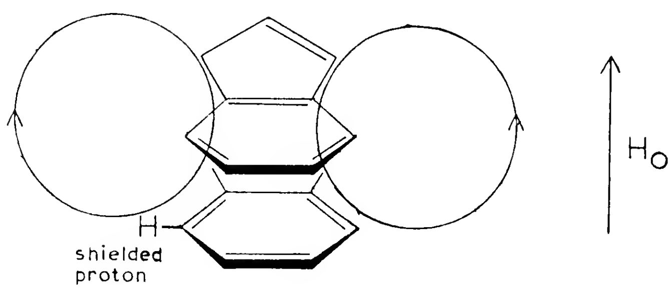

Figure 8. Shielding of the Aromatic Protons Caused by Vertical Stacking

From the magnitude of the ^{1}H nmr chemical shifts of the various protons of adenosine, it was noted that the six-membered ring of the purine experiences the greatest shielding followed by the five-membered ring.[40] Two models are proposed for the geometry of the stack and are shown in Figure 9.

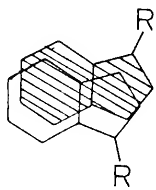

(a) Alternate

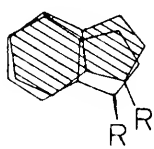

(b) Straight

Figure 9. Geometry of Nucleoside Stacks

If the purine nucleoside is substituted with an amino group in the 6 position (e.g., adenosine), it is found that the degree of stacking increases. Similarly, 5-bromouradine stacks to a greater extent than thymidine. From such comparisons, it is concluded that a hydrophobic force is not the sole factor in governing the stacking interaction.[37] Rather a correlation is found with the polarizability of

the bases. The conclusion by Hanlon that London dispersion forces are responsible for the stability of the DNA helix is in line with this concept.[41]

Investigations of dinucleoside phosphates has provided further information on the details of the stacking interactions. Chen and Nelson used ^{1}H nmr techniques to show that ApA exists in the 3'-anti-5'anti right-handed stack.[42] It should be noted that the Watson-Crick structure of DNA requires the bases to be in the anti conformation. Further, striking differences have been observed from one dinucleoside phosphate to another regarding their stacking ability.[43] It was found that UpU lost its ordered structure readily upon elevation of the temperature, while ApA's structure persisted. This was explained as being due to differing stacking interactions for the two dinucleoside phosphates.

Electrostatic Effects

The phosphate groups along the backbone of the DNA double helix are negatively charged at neutral pH. The charge repulsion between the two strands is the primary disruptive force of the double helix. It was previously stated that the DNA structure is not stable if the ionic strength is decreased below a minimum level. The reason is that the cations shield the anionic charge of the phosphate groups, thereby reducing the Coulombic repulsion between strands. In addition to the interstrand forces, intrastrand phosphate interactions are an important factor

in controlling DNA structure. The distance between adjacent phosphate groups along the same chain of the Watson-Crick double helix is roughly 7 angstroms. In concentrated salt solution the length of the DNA helix decreases as evidenced by a decrease in intrinsic viscosity of the DNA solution.[44] This decrease is due to the lowered repulsion between intra- and interstrand phosphates, allowing the helical molecule to contract.

Electronic Effects

That the nucleic acid bases interact with each other electronically is quite well known. The exciton theory unifies a number of experimental results and states that, for molecular crystals, energy is not absorbed by a single molecule but is distributed over many.[45-47] If the ordered polynucleotide is considered a one-dimensional crystal, the exciton theory is applicable.

As seen in Figure 10, the excited state energy levels of the bases are considered to be split to produce two new

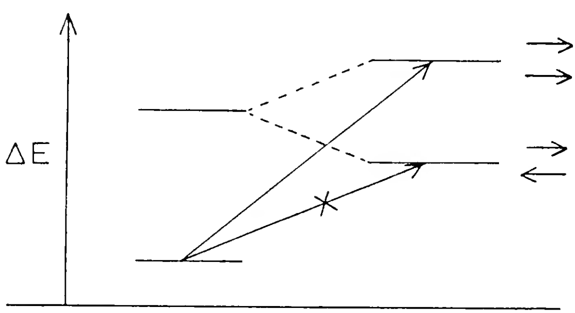

Figure 10. Exciton Splitting of Energy Levels

levels. The lower energy transition has the electronic vectors of the bases antiparallel, while the higher energy transition has these vectors parallel. Quantum mechanical selection rules forbid the transition to the lower excited level, so the transition seen is the one of higher energy than the original uncoupled transition. The absorption maximum is thus shifted toward the blue. Also seen is a hypochromic effect, with the intensity of the new transition being lower than that of the monomer. This fact is explained by the theory of intensity interchange of coupled transition momements and is illustrated in Figure 11.

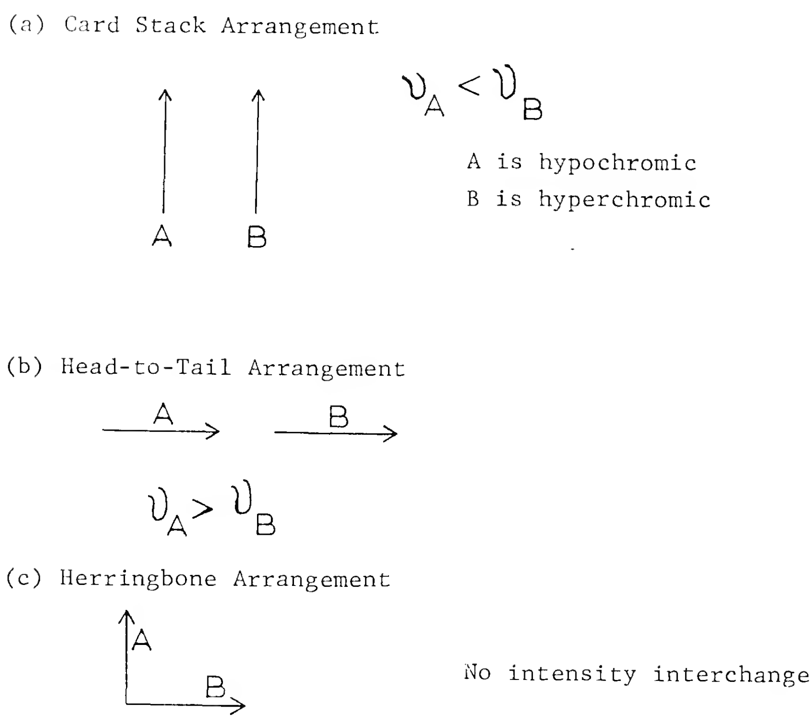

Figure 11. Intensity Interchange Between Two Interacting Transition Moments

If the transition moments are in a card stacked orientation as in the DNA molecule, the higher energy transition is hyperchromic, and the lower energy transition is hypochromic. The effects of the blue shift and hypochromism on the uv spectrum of oligoadenylic acid can be seen in Table 1.[48]

The technique of circular dichroism also demonstrates the theory to be correct.[49] Contrary to the situation in absorption spectroscopy, transitions to both the upper and lower states are allowed by pertinent selection rules. Thus, one sees both a red and blue shifted band as compared to the absorption maximum of the monomer. The signs of the CD bands, however, cannot be predicted without the consideration of more complicated quantum mechanical arguments.[50] It may be stated, however, that the two transitions are found to be opposite in sign, thus yielding the very distinctive double Cotton effect for the polynucleotide.

Dynamic Structure of Nucleic Acids

Several lines of evidence point toward a rather remarkable quality associated with the helical polynucleotides. It appears that the hydrogen bonded base pairs are in a continued state of flux with respect to their nonhydrogen-bonded "open" forms. The work of von Hippel and coworkers, utilizing tritium exchange have established a firm basis for the existence of the "open" forms of the nucleic

Table 1. The Effect of Increasing Length of the Polynucleotide $(Ap)_nA$ on the uv Absorption Spectrum

n	λmax	$\varepsilon_{max}/n+1$
0	260	15 000
1	257	13 600
2	257	12 600
3	257	11 300
4	257	11 300
5	257	10 800
300 (poly A)	256	9 000

acids.[51-53] Incubation of the nucleic acids in tritiated water and rapid separation of the labeled polynucleotide from radioactive solvent via gel filtration enabled these workers to show that the kinetics of exchange were much faster than for protein systems. Further, it can be shown that the observable exchange is taking place with protons involved in the base-base hydrogen bonding of the double helix. Three possible models were examined by McConnell and von Hippel.[52,53] These were (1) unstacking without hydrogen bond breakage, (2) hydrogen bond breakage without unstacking, and (3) hydrogen bond breakage with partial or complete unstacking and strand separation. By studying tritium exchange and pH studies, it was concluded that the "breathing model" (3) is correct. Kinetic studies of intercalation by Muller and Crothers and Gabbay et al. agree with this hypothesis.[54,55]

Genetic Control

The genetic code for all proteins of a particular organism is contained in the DNA of each cell, yet protein biosynthesis is a highly controlled operation (i.e., not all the proteins are made at once). This selective synthesis of protein requires a mechanism which is sensitive to the cell's needs and only allows the required section of DNA to be transcribed at any given period during the growth cycle. The regulatory mechanisms involved are still under intense study, but the general scheme has been pre-

sented by Jacob and Monod and will briefly be outlined for the lactose operon of *Escherichia coli*.[56] This operon is schematically represented in Figure 12.

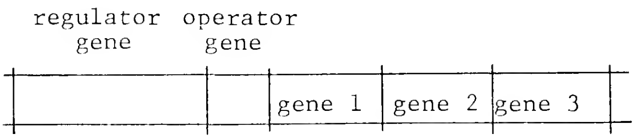

Figure 12. Schematic Representation of the Lactose Operon

It has been shown that the utilization of the sugar, lactose, by *E. coli* requires the synthesis of three proteins, β-galactosidase, β-galactoside permease, and galactoside transacetylase.[56] These proteins are necessary for the conversion of lactose into useable nutrients. The information for these proteins are coded by three genes that occur in a cluster on DNA. This cluster, in addition to a site called the operator and a gene for the regulating protein, is known as the operon, in this case, the lactose operon. The regulator gene codes for an repressor protein which has a specific affinity to the DNA sequence of its operator. When the repressor is bound to the operator, no transcription can take place. If, however, lactose is present, the sugar specifically binds with the repressor protein, rendering the protein incapable of binding to the operator, thus allowing the operon to be transcribed. When

the lactose in the cell is depleted, the free repressor reassociates with the operator and protein synthesis of the lactose operon ceases.

The above description of genetic control is by no means complete, yet the complexity can be appreciated. It is apparent that there are a number of specific nucleic acid-protein interactions of which the mechanisms are largely unknown. It is one of the purposes of this thesis to shed some light on this subject.

Peptide-Nucleic Acid Interactions

From the above discussion of control of genetic information, it is apparent that the experimentalist who wishes to determine the interaction mechanisms between nucleic acids and proteins is faced with the problem of dealing with at least two macromolecules. It is not in the realm of current technology to study the interactions of two large and complex macromolecules in detail. Therefore, a more practical approach to the problem is to utilize model systems. With a knowledge of the interaction mechanisms of small diamines, amino acid amides, and reporter molecules available, it is possible to study the specific interactions of oligopeptide amides with DNA and consider these systems as crude models for protein-nucleic acid systems.

The forces available to a protein molecule interacting with nucleic acid are: (1) electrostatic interactions

between charged amine groups of the protein and the phosphate anions, (2) hydrophobic forces involving intercalation of the aromatic amino acid residues as well as interactions with the apolar amino acid residues (e.g., alanine, valine, etc.), (3) hydrogen bonding interactions between functional groups on the purine and pyrimidine bases and available hydrogen bonding sites on proteins, (4) topological recognition of the surface structure of the nucleic acid (i.e., tertiary structure), and (5) electronic interactions between bases and intercalating amino acid moieties. The importance of these forces in providing specificity in the interaction of protein with DNA and RNA is currently a matter of conjecture. However, several recent studies employing small protein model systems (i.e., amino acids and peptides) with DNA systems have suggested that all of the forces could play important roles.

Electrostatic interactions are not expected to be specific, yet a number of studies done with oligolysine, polylysine, and polyarginine show that these molecules exhibit base pair specificity toward double stranded nucleic acid when the polymerization number is greater than four.[57,58] Polyarginine is specific for G-C rich regions of DNA, whereas polylysine is specific for A-T sites. However, to observe this specificity the ionic strength must be on the order of 1 M, indicating that electrostatic forces are not responsible for the specificity. Also, Shapiro et al. found that the A-T preference of polylysine increased as the pH

of the solution was increased from 7 to 10.[58] Since the extent of ionization of the ε-ammonium groups is expected to decrease, the increase in base pair specificity must be due to forces other than electrostatic interactions. The binding of these polybasic amino acids to DNA is known to be cooperative, thus, another explanation is that A-T and G-C rich regions of DNA have characteristic secondary and tertiary structures that facilitate the binding of the polylysine or polyarginine molecules and allow for a topographic recognition of DNA sequence.[59]

Hydrogen bonding interactions are known to be highly specific in nonhydroxylic solvents and/or in aqueous solution under conditions of water molecule exclusion as in the case of Watson-Crick base pairs. Formation of specific hydrogen bonds between protein amino acid side chains and the externally exposed hydrogen bond donors and acceptors of the DNA base pairs has been postulated by many researchers as a contributing element in the DNA-protein recognition process.[60,61] Although hydrogen bonding may strengthen the binding, such interactions probably do not contribute significantly to the recognition specificity for the following reasons: (i) the presence of hydrogen bond donors and acceptors at the DNA base pair sites and along the protein chain, (ii) the flexibility of both macromolecules may accomodate the formulation of numerous hydrogen bonding schemes, and (iii) the possible modification or exchange of such bonds by the intermediacy of water molecules. In

support of the latter contention is the observed high diffusion rate of the lactose repressor protein along the circular DNA of E. coli.[62]

Evidence for intercalation of aromatic amino acids exists with both double and single stranded nucleic acids. ^{1}H nmr studies using L-phenylalanine, L-tryptophan, and L-histidine with poly A indicate that these molecules cause a destacking of the adenine bases as evidenced by the down-field shift of the H-2 and H-8 protons of adenine in the complex.[63] The destacking of adenine in poly A is considered the result of intercalation of the aromatic ring of the amino acid. The relative magnitude of this interaction is tryptophan > phenylalanine > histidine.

Helene et al. have shown that tyramine, tyrosine, and tryptamine derivatives also intercalate and destack poly A, since it was found that the chemical shifts of aromatic protons of the former are upfield shifted in the poly A complex due to ring current anisotropy.[64-66] CD studies using DNA and poly A confirmed the possibility that intercalation causes a slight destacking of the bases of the nucleic acids, since the magnitude of the 280 nm peak is decreased in the nucleic acid-amino acid complex relative to the uncomplexed nucleic acid. Quenching of the fluorescence of these amino acid derivatives by nucleic acids was also taken as evidence for an intercalation model.

Brown, in a study of several dibasic peptide methyl esters, found that arginyltryptophan methyl ester has a

very large stabilizing effect on the Tm of DNA compared to other similarly charged dipeptide derivatives.[67] To account for his, he suggested the "bookmark" hypothesis whereby the aromatic rings of amino acids may behave as bookmarks and thus anchor the proteins to specific sequences of nucleic acids via an intercalation mode of binding.

In addition, work by Kapicak and Gabbay on model systems shown in Figure 13 has revealed that the extent of insertion

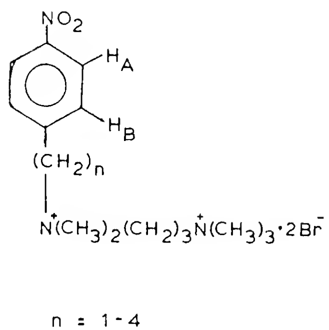

Figure 13. Reporter Molecule, I

of the aromatic ring between base pairs of DNA has profound effects on the tertiary structure of the latter, i.e., either shortening or lengthening of the helix.[68] For example, it is found that at n = 1, the nitrophenyl ring of the reporter molecule, I, is partially inserted between base pairs of DNA as evidenced by the lower viscosity of the DNA-reporter complex and by the lack of ^1H nmr signal broadening of the aromatic protons. Moreover, it is found

that the A protons of the aromatic ring of the reporter molecule, I, (n = 1) experience a greater upfield chemical shift than the B protons in the DNA-reporter complex which is consistent with the "wedge type partial insertion" model.[68] On the other hand, with n = 3 and 4 the aromatic cationic reporters cause enhanced viscosity of DNA solutions and the ^{1}H nmr signals of the aromatic protons are totally broadened and indistinguishable from baseline noise. Peptides containing the aromatic amino acids, tryptophan, phenylalanine, and tyrosine, exhibit effects identical with the aromatic reporter, where n = 1, i.e., partial insertion between base pairs of DNA leading to shortening of the DNA length.[69] Presumably, the single methylene group (CH_2) between the peptide backbone and the aromatic ring of tyrosine, tryptophan, and phenylalanine is not sufficient to allow for "full" insertion and lengthening of the helix.

Gabbay et al. have also presented evidence which indicates that L-lysyl-L-phenylalanine amide (L-lys-L-pheA) and the diastereometric L-lysyl-D-phenylalanine amide (L-lyl-D-pheA) interact in a stereospecific manner with salmon sperm DNA.[70] In particular, the ^{1}H nmr, viscometric, and flow dichroism data suggest that the aromatic ring of L-lys-L-pheA is partially inserted between base pairs of DNA whereas the aromatic ring of L-lys-D-pheA points outward toward the solvent. In order to account for this specificity it is necessary to conclude that the ε- and α-amino groups of the N-terminal L-lysyl residue interact in a stereo-

specific manner with DNA which dictates the positioning of the aromatic ring of the C-terminal phenylalanine residue of L-lys-L-pheA and L-lys-D-pheA. Since no significant differences in the binding of L and D-phenylalanine amide to DNA have been found by ^{1}H nmr studies, the specificity observed with L-lys-L-pheA and L-lys-D-pheA cannot be attributed to the chirality of the phenylalanine residue by itself.[69]

Statement of Problem I

In this thesis, the synthesis of oligopeptide amides containing an N-terminal L-lysine and L-phenylalanine were undertaken in order to determine the effect of the primary sequence and the stereochemistry of the α carbons of the peptides on the binding of the aromatic ring (used in this case as a probe) to DNA.

Anthracyclines

Adriamycin, daunorubicin, and carminomycin (shown in Figure 14) are glycosidic anthracycline antibiotics isolated of *Streptomyces peucetius* and are being used in the treatment of acute leukemia and solid tumors in man.[71-77] Both adriamycin and daunorubicin have been shown to inhibit nucleic acid synthesis in various cultured cell lines, while autoradiography and fluorescence quenching experiments show that daunorubicin concentrates in the nuclei of normal and tumor cells.[78-82] These results are consistent with selective binding of the drugs to chromatin.[83]

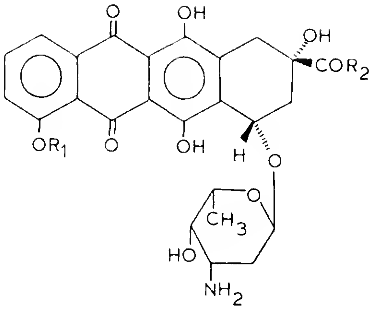

	R_1	R_2
adriamycin	CH_3	CH_2OH
daunorubicin	CH_3	CH_3
carminomycin	H	CH_3

Figure 14. The Anthracyclines

Cell cycle phase specificities of the antracyclines have been studied by several investigators and there appears to be conflicting data. For example, Silvestrini et al. found that daunorubicin caused significant inhibition of DNA and RNA synthesis in the G_1, S_1, and G_2 phases of the cell cycle in rat fibroblasts.[84] On the other hand, Tobey and Kim et al. found that the effects of daunorubicin are S-phase specific in HeLa cells.[85,86] Mizuno et al. observed a cytotoxic effect as a result of daunorubicin administration in all phases of the cell cycle.[87]

Substantial evidence exists which is indicative that the cytotoxicity of the anthracycline drugs is due to DNA template binding and concomitant inhibition of the replication and translation processes. However, there appears to be evidence for an alternate mechanism of action. Silvestrini et al. noted an antimitotic activity on cultured mouse cells

at levels of daunorubicin which are too low to effect nucleic acid synthesis.[84] In addition, it was demonstrated that the drug abruptly blocks mitosis when given only a few minutes before prophase. Gasalvez et al. found that the respiration of isolated mitochondria as well as that of intact tumor and normal cells is significantly inhibited by adriamycin and daunorubicin.[88] Similarily, Folkers and coworkers found that the anthracyclines inhibit NADH oxidase and respiratory enzymes which require coenzyme Q_{10}.[89] It has been suggested that adriamycin may cause changes in the cell surface based on the dramatic enhancement of concanavalin A induced agglutination of S180 cells caused by the drug.[90,91] Based on the observed induced resistance to vincristine and vinblastine in Ehrlich ascites tumor in the presence of adriamycin or daunorubicin, it has also been suggested that these drugs may act by interfering with the microtubule formation during mitosis.[92,93] It should be noted that in the above studies, it is not clear whether the observed activity of the anthracyclines is due to the drug itself or to one of the metabolites (e.g., the aglycone).

DNA-Anthracycline Binding

The interaction specificity of the anthracyclines with DNA is generally accepted to be by an intercalation mechanism. This conclusion is based on (1) the spectral changes induced in the DNA bound drug (i.e., red shift and hypochromism, induced circular dichroism, and fluorescence

quenching); (2) the enhanced viscosity of DNA solutions in the presence of drug; (3) flow dichroism data which indicate that the anthracycline ring system is in a plane perpendicular to the helix axis of DNA; (4) decrease in the buoyant density of the DNA-anthracylcine complexes;(5) unwinding of closed circular supercoiled DNA; and (6) the X-ray diffraction patterns of fibers of DNA-daunorubicin which are consistent with the intercalation model.[94-102] It should be noted that at an ionic strength in excess of 0.05 M and drug to DNA phosphate ratios less than 0.1, the intercalative mode of binding is predominant; however, at lower ionic strength and higher drug to DNA phosphate ratios, extensive external electrostatic binding is observed. The maximal binding by the intercalative mode has been shown to vary from one drug per 2 to 4 base pairs with an apparent binding constant of between 2×10^6 and 12×10^6 M^{-1}, depending on the ionic strength of the media.[94-97] The external mode of binding appears to saturate at one drug per base pair and is nearly abolished at ionic strengths greater than 0.2 M.[97]

Toxicity of the Anthracyclines

The anthracyclines unfortunately exhibit a deleterious effect on humans. The development of cardiopulmonary symptoms such as congestive heart failure have been observed in a number of patients who have received a total of 25 mg/kg or more of the drugs.[102-110] Work by Mhatre et al. and Herman et al., using adriamycin, daunorubicin, and N-acetyl-

daunorubicin, a biologically less toxic compound, showed that all three drugs are accumulated in heart and lung tissue soon after injection.[107,111] In addition, a rapid conversion of adriamycin and daunorubicin to the corresponding aglycones is found while comparatively little conversion of N-acetyldaunorubicin was detected. Thus, these workers concluded that the observed toxicity may be related to differences in the metabolism of the three compounds and the aglycone is the toxic agent. The observed long biological half-life of the anthracycline drugs, probably due to the water insolubility of the aglycone, leads to a cellular accumulation of the metabolite upon repeated injection.

Statement of Problem II

From the above studies, it appears as though the toxicity of the anthracyclines arises due to the aqueous insolubility of the aglycone leading to its accumulation in tissues. If this hypothesis is correct, an anthracycline drug which yields a water soluble aglycone upon hydrolysis should demonstrate decreased toxicity. However, such a drug must remain biologically active against leukemia and other tumors to be of medicinal importance.

The second part of this thesis includes the synthesis of anthacycline derivatives which could lead to water soluble aglycones upon glycosidic hydrolysis and the development of in vitro techniques useful to the rapid evaluation of such drugs.

CHAPTER II
PEPTIDES

The interactions of oligopeptide amides containing an N-terminal L-lysine and L-phenylalanine (shown in Figure 15) with DNA have been examined by pulsed Fourier transform ^{1}H nmr, viscosity, circular dichroism, equilibrium dialysis, and melting temperature (Tm of helix-coil transition) studies. The results are presented below.

<u>^{1}H nmr Studies</u>

The ^{1}H nmr studies conducted in this work monitor the change in (i) line width (i.e., $\Delta\nu_{1/2}$ (in Hz) = $\Delta\nu_{1/2}{}^{bound} - \Delta\nu_{1/2}{}^{free}$, where $\Delta\nu_{1/2}{}^{bound}$ and $\Delta\nu_{1/2}{}^{free}$ are the line broadenings in the presence and absence of DNA), (ii) spin-lattice or transverse relaxation times (T_1), and (iii) the upfield chemical shift (i.e., $\Delta\delta = \delta_{free} - \delta_{bound}$, where δ_{bound} and δ_{free} are the chemical shifts in the presence and absence of DNA) of the aromatic protons of the peptide. The change in chemical shifts is related to the proximity of the observed protons to the ring current of the DNA base pairs. The spin-lattice relaxation time (T_1) is dependent (among other things) upon the correlation time (T_c) and the mean residence time (T_m).[39,112,113] The ^{1}H nmr signal line broadening can be explained by several mechanisms: (i) slow

1 L-lys-L-pheA 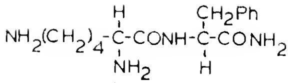

2 L-lys-D-pheA 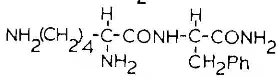

3 L-lys-L-phe-glyA 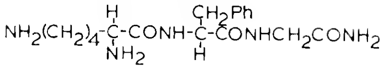

4 L-lys-gly-L-pheA 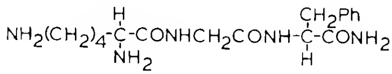

5 L-lys-L-phe-diMeA 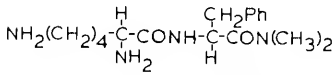

6 L-lys-L-phe-gly-glyA 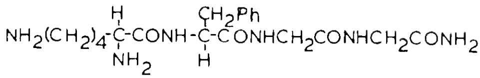

7 L-lys-L-phe-L-leu-glyA 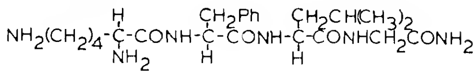

8 L-lys-L-phe-D-leu-glyA 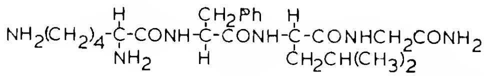

9 L-lys-L-phe-D-ala-L-leuA 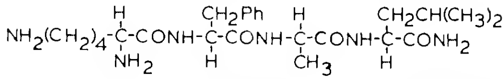

10 L-lys-L-phe-(gly-L-leu)$_2$A 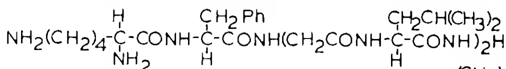

11 L-lys-L-phe-D-leu-L-leu-D-leuA 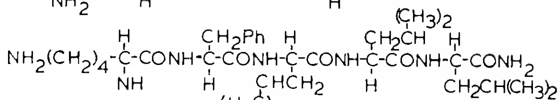

12 L-lys-L-phe-gly-L-leuA 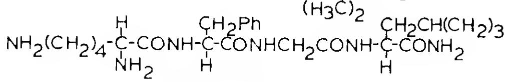

13 L-lys-L-phe-L-alaA 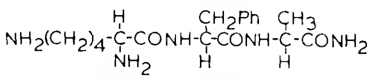

14 L-lys-L-phe-D-alaA 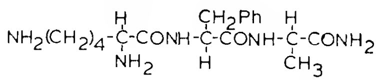

15 L-lys-L-phe-L-ala-L-valA 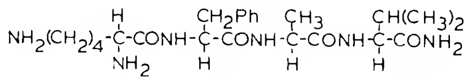

16 L-lys-L-phe-D-ala-L-valA 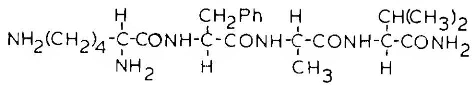

Figure 15. Structure of the Oligopeptide Amides

rate of tumbling of the observed proton, (ii) slow rate of exchange between nonidentical sites, (iii) large differences between the chemical shifts of the various protons observed (i.e., the ortho, meta, and para protons of the phenyl ring of phenylalanine), or (iv) a combination of the three mechanisms above. It should be noted that under the condition of the experiments (i.e., at a base pair/peptide ratio of 7.5 and 15) the peptides, 1-4, are almost fully bound to DNA (95%). This was determined quantitatively by equilibrium dialysis on the ^{1}H nmr samples themselves utilizing the fluorescamine assay technique described previously by Gabbay et al.[69]

The results of the above studies which are shown in Figures 16-19, Table 2, and Table 3 lead to the following observations.

(1) The upfield chemical shifts, $\Delta\delta$, experienced by the aromatic protons of the peptides upon binding to DNA depends on the primary structure and stereochemistry of the carbons of the amino acids contained therein. For example, the following order of decreasing upfield chemical shifts is observed (see Table 2): L-lys-L-pheA (1) > L-lys-L-phe-(N,N-dimethyl)A (5) > L-lys-L-phe(gly-L-leu)$_2$A (10) $\simeq$ L-lys-phe-glyA (3) $\simeq$ L-lys-L-phe-gly-glyA (6) $\simeq$ L-lys-L-phe-D-ala-L-leuA (9) $\simeq$ L-lys-L-phe-gly-L-leuA (12) $\simeq$ L-lys-L-phe-D-alaA (14) $\simeq$ L-lys-L-phe-D-ala-L-valA (16) $\simeq$ L-lys-L-phe-L-alaA (13) $\simeq$ L-lys-L-phe-D-leu-L-leu-D-leuA (11) $\simeq$ L-lys-gly-L-pheA (4) $\simeq$ L-lys-L-phe-L-ala-L-valA (15) $\simeq$

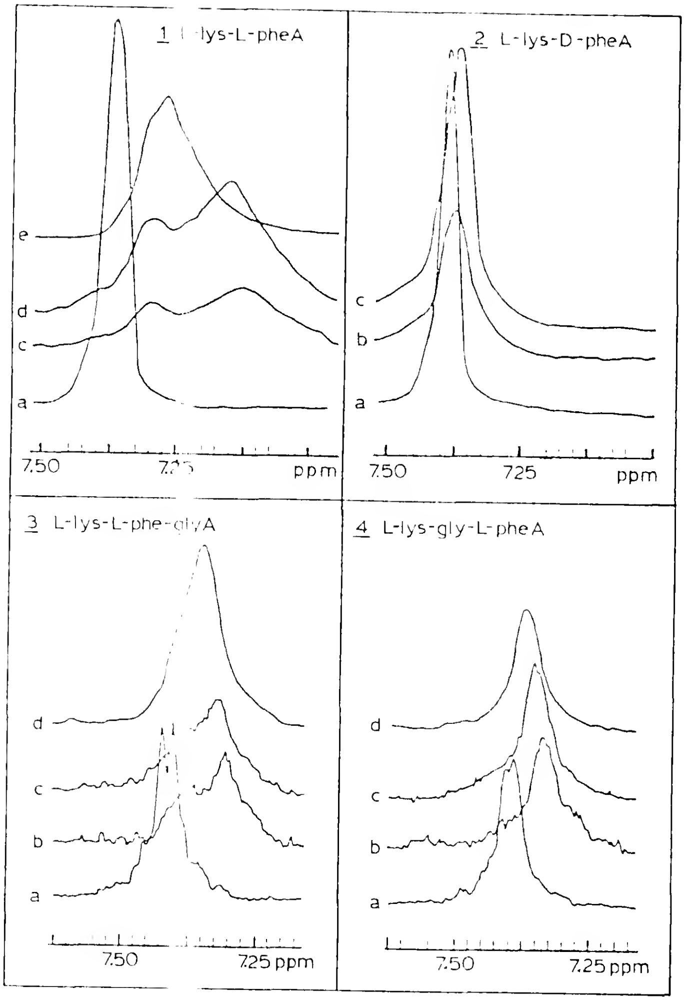

Figure 16. ^{1}H nmr Signal of the Aromatic Protons of Peptides 1-4 in the Presence and Absence of DNA. DNA base pair to peptide ratio is (a) 0, (b) 15.0, (c) 7.5, (d) 2.0, and (e) 1.0.

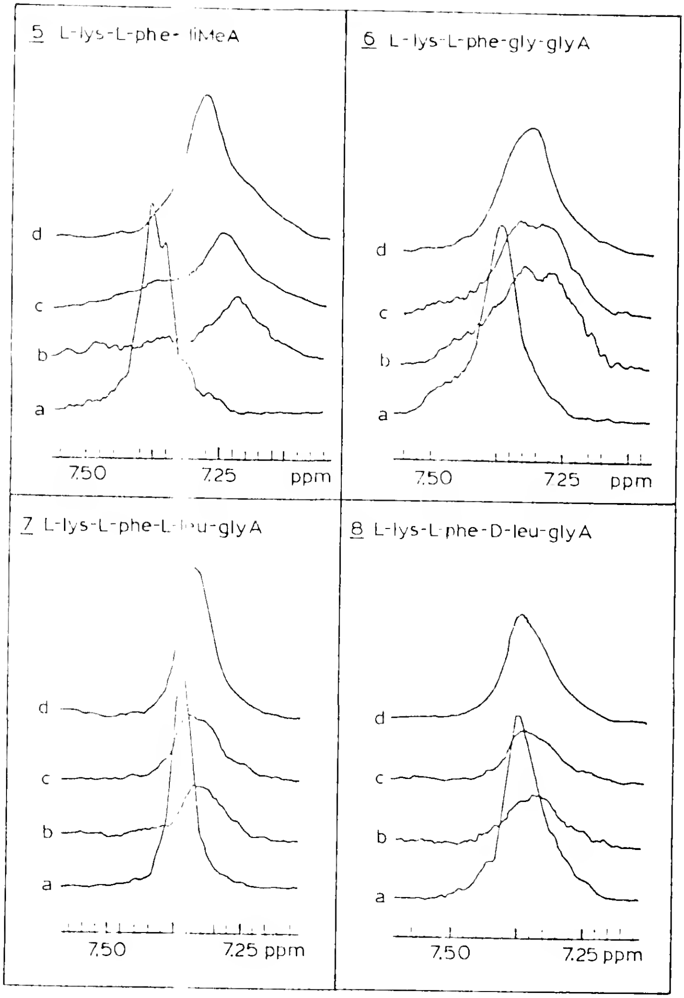

Figure 17. ^{1}H nmr Signal of the Aromatic Protons of Peptides 5-8 in the Presence and Absence of DNA. DNA base pair to peptide ratio is (a) 0, (b) 15.0, (c) 7.5, and (d) 2.0.

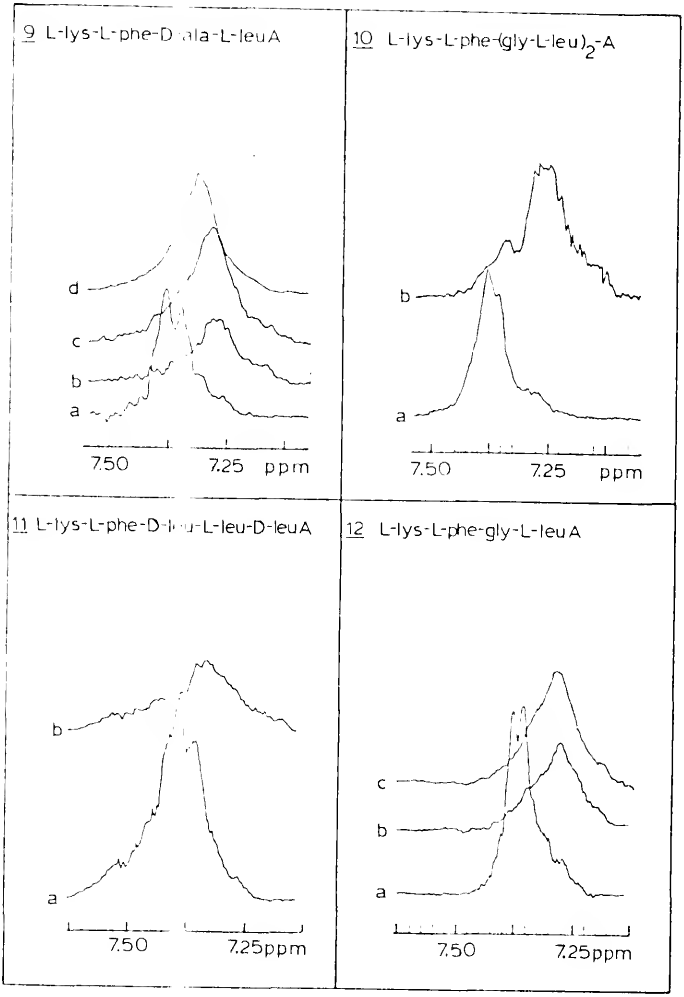

Figure 18. ^{1}H nmr Signal of the Aromatic Protons of Peptides 9-12 in the Presence and Absence of DNA. DNA base pair to peptide ratio is (a) 0, (b) 15.0, (c) 7.5, and (d) 2.0.

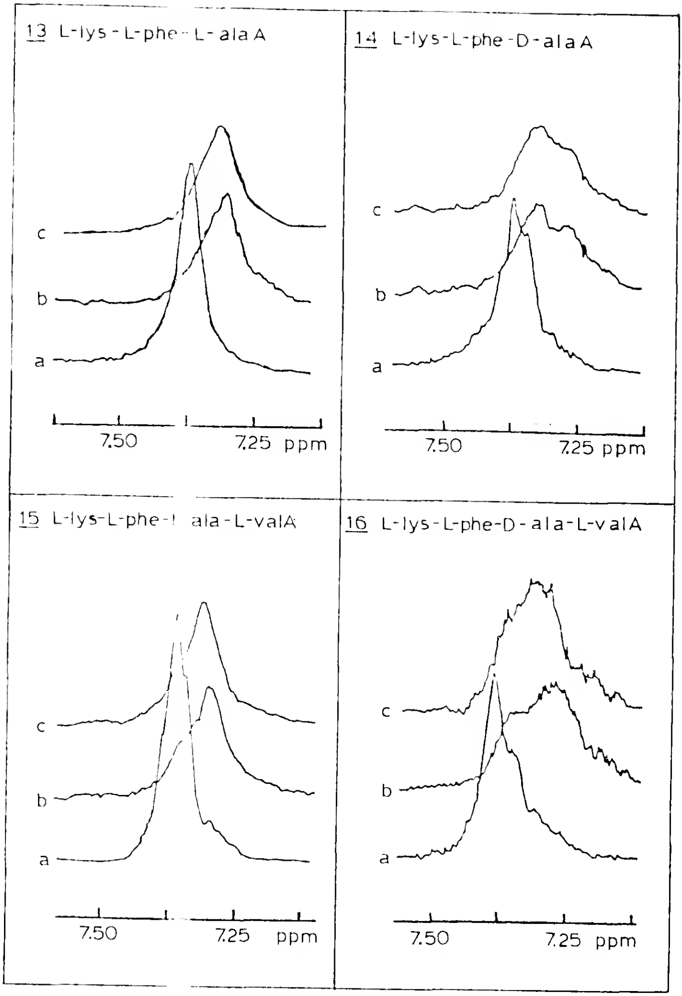

Figure 19. ^{1}H nmr Signal of the Aromatic Protons of Peptides 13-16 in the Presence and Absence of Sonicated Salmon Sperm DNA. DNA base pair to peptide ratio is (a) 0, (b) 15.0, and (c) 7.5.

Table 2. The Effect of DNA on the Upfield Chemical Shift (ΔS, in Hz) and Signal Line Broadening ($\Delta\nu_{1/2}$ in Hz) of the Aromatic Protons of Model Peptides.[a]

Peptide System	$\Delta\delta$ ($\Delta\nu_{1/2}$) in Hz[b]	
	DNA BP/Peptide	
	15.0	7.5
L-lys-L-pheA (1)	- -	23.5(25)
L-lys-D-pheA (2)	2.3(2)	2.2(2)
L-lys-L-phe-glyA (3)	11.0(10)	11.0(8)
L-lys-gly-L-pheA (4)	6.5(1)	6.0(1)
L-lys-L-phe-diMeA (5)	15.5(6)	13.0(6)
L-lys-L-phe-gly-glyA (6)	10.0(11)	8.0(7)
L-lys-L-phe-L-leu-glyA (7)	2.5(3)	2.5(3)
L-lys-L-phe-D-leu-glyA (8)	3.5(5)	3.0(4)
L-lys-L-phe-D-ala-L-leuA (9)	11.0(6)	10.0(5)
L-lys-L-phe-(gly-L-leu)$_2$A (10)	13.0(5)	- -
L-lys-L-phe-D-leu-L-leu-D-leuA (11)	6.5(7)	- -
L-lys-L-phe-gly-L-leuA (12)	11.0(9)	9.0(6)
L-lys-L-phe-L-alaA (13)	7.0(2)	6.0(3)

Table 2 - continued

Peptide System	$\Delta\delta$ $(\Delta\nu_{1/2})$ in Hz	
	DNA BP/Peptide	
	15.0	7.5
L-lys-L-phe-D-alaA (<u>14</u>)	10.(7)	7.5(5)
L-lys-L-phe-L-ala-L-valA (<u>15</u>)	5.5(2)	5.0(1)
L-lys-L-phe-D-ala-L-valA (<u>16</u>)	11.0(9)	8.5(6)

[a] Sonicated low molecular weight salmon sperm DNA was used at 75 mM P/l. PMR spectra were recorded on an XL-100 Varian Spectrometer using the Nicolet FT-accessory.

[b] The upfield chemical shift, $\Delta\delta$, ($\delta_{free}-\delta_{bound}$, where δ_{free} and δ_{bound} are the chemical shifts in the absence and presence of DNA), and the line broadening at half signal height, $\Delta\nu_{1/2} = (\Delta\nu_{1/2}{}^{bound} - \Delta\nu_{1/2}{}^{free})$, are measured at 34°C. It should be noted that the chemical shifts, S, are measured with respect to the internal standard, TSP, and are reproducible to within $\pm$ 0.2 Hz. The values of $\Delta\nu_{1/2}$ reported are not corrected for the viscosity effect of DNA solutions. The effect is small, e.g., TSP signal is found to have a $\Delta\nu_{1/2}$ of 2.5 $\pm$ 0.3 and 1.5 $\pm$ 0.2 Hz in the presence and absence of DNA.

Table 3. The Spin-Lattice Relaxation Time (T_1) of the Aromatic Protons of the Peptides in the Presence and Absence of DNA[a]

Peptide System	T_1 (sec)			
		Base Pair/Peptide		
	Free	7.5	3.6	2.4
L-lys-L-pheA (1)	2.02	0.57	0.62	0.61
L-lys-D-pheA (2)	2.02	0.66	0.71	0.72
L-lys-L-phe-L-alaA (13)	1.73	0.95	0.76	0.75
L-lys-L-phe-D-alaA (14)	1.17	0.59	0.71	0.76
L-lys-L-phe-L-ala-L-valA (15)	1.46	0.65	0.71	0.64
L-lys-L-phe-D-ala-L-valA (16)	1.14	0.50	0.54	0.54

[a]Sonicated low molecular weight salmon sperm DNA was used at 60-70 mM phosphate/liter in the presence of 1 mM EDTA in D_2O (pD = 7.0). The concentration of the peptide was varied from 4-15 mM. Spectra were recorded at 34°C using a Varian XL-100-15 spectrometer equipped with a Nicolet Technology FT accessory. It should be noted that the T_1 values are accurate to $\pm$ 10%. The T_1 value of the internal standard, TSP, is not affected by the presence of DNA ($T_1 \cong 3.4 \pm 0.2$).

L-lys-L-phe-D-leu-glyA (8) > L-lys-L-phe-L-leu-glyA (7) > L-lys-D-pheA (2).

(2) The extent of the ^1H nmr signal line broadening of the aromatic protons of DNA bound peptides is also found to depend on the primary sequence and chirality of the amino acids. For example, the following order of decreasing ^1H nmr line broadening is observed (see Table 2): L-lys-L-pheA (1) > L-lys-L-phe-gly-glyA (6) ≃ L-lys-L-phe-glyA (3) ≃ L-lys-L-phe-gly-L-leyA (12) ≃ L-lys-L-phe-D-ala-L-valA (16) > L-lys-L-phe-D-alaA (14) ≃ L-lys-L-phe-D-leu-L-leu-D-leyA (11) ≃ L-lys-L-phe-D-ala-L-leuA (9) ≃ L-lys-L-phe(dimethyl)A (5) ≃ L-lys-L-phe(gly-L-leu)$_2$A (10) ≃ L-lys-L-phe-D-leu-glyA (8) > L-lys-L--he-L-leu-glyA (7) ≃ L-lys-L-phe-L-alaA (13) ≃ L-lys-L-phe-L-ala-L-valA (15) ≃ L-lys-D-pheA (2) ≃ L-lys-gly-L-pheA (4).

(3) The spin lattice relaxation data (Table 3) suggest that the phenyl rings of all peptide amides in the DNA complexes experience restriction in tumbling to approximately the same degree. For example, the peptides (1, 2, and 3-16) exhibit similar T_1 values (for the aromatic protons) at various base pair/peptide ratios, although there are distinct differences in both the change in chemical shift (ΔS) and the signal line broadening ($\Delta\nu_{1/2}$). It should be noted that the effect of viscosity of the DNA solution on line broadening is found to be small (e.g., the signal line broadening of the internal standard, 2,2,3,3-d_4-3-trimethylsilylpropionate (TSP) is found to be 1.5 $\pm$ 0.2 and 2.5 $\pm$

0.3 Hz in the absence and presence of 70 mM DNA phosphate per liter, respectively). Also, the measured T_1 values are found not to be sensitive to dissolved oxygen in solution; however, considerable variations in T_1 values are obtained if paramagnetic impurities are present in the DNA. The work reported in this thesis was carried out with sonicated salmon sperm DNA which has been extensively dialyzed against EDTA.

Viscosity Studies

A number of investigators have shown that planar aromatic molecules such as proflavine, acridine orange, and ethidium bromide intercalate between base pairs in DNA. This process has been shown to increase the viscosity of DNA solutions and is presumably due to an increase in the length of the DNA molecule. The most definitive study to prove that the DNA length increases involves the determination of the intrinsic viscosity, $[\eta]$, of the solution. Intrinsic viscosity is defined by the equation,

$$[\eta] = \text{Limit}_{c \to 0} \frac{\eta_{sp}}{c}$$

where η_{sp} is the specific viscosity of solution and c is the concentration of the solute (e.g., DNA phosphate). However, these types of experiments are uninformative since the peptide-DNA complex dissociates at high dilution (probably due to the very low binding constant of the peptide to DNA) and the intrinsic viscosity of the complex approaches that of the DNA alone.

Thus, the effect of increasing concentrations of the oligopeptide amides on the relative specific viscosity, η_{sp}/η_{spo} (where η_{sp} and η_{spo} are the specific viscosities of DNA solutions in the presence and absence of peptides, respectively) at 2.6×10^{-4} M DNA phosphate/liter (in 10 mM 2-(N-morpholine) ethanesulfonate (MES), 5 mM Na^+, pH 6.2) was studied at 37°C using the low shear Zimm viscometer as modified by Pearce et al. (see experimental). Native salmon sperm DNA with a molecular weight of approximately 6×10^6 was used. Since the study was carried out at low concentrations of DNA, the relative values of η_{sp}/η_{spo} are close approximations of the relative values of the intrinsic viscosity of DNA-peptide complex to free DNA ($[\eta]/[\eta]_o$). The results of the viscometric titration studies, shown in Figures 20 - 22, indicate that the oligopeptide amides lower the specific viscosity of DNA. It should be noted that peptides 1, 14 and 16 decrease the viscosity to a greater extent than do the peptides 2, 13 and 15, respectively.

Circular Dichroism Studies

The interaction of the peptide amides with native salmon sperm DNA were studied by CD. However, there was little or no change in the trough at 245 nm or the peak at 275 nm in the CD of the DNA upon the addition of the peptides (Figures 23 - 25). Thus, there are no gross changes in the structure of the DNA that occur upon the binding of the peptides.

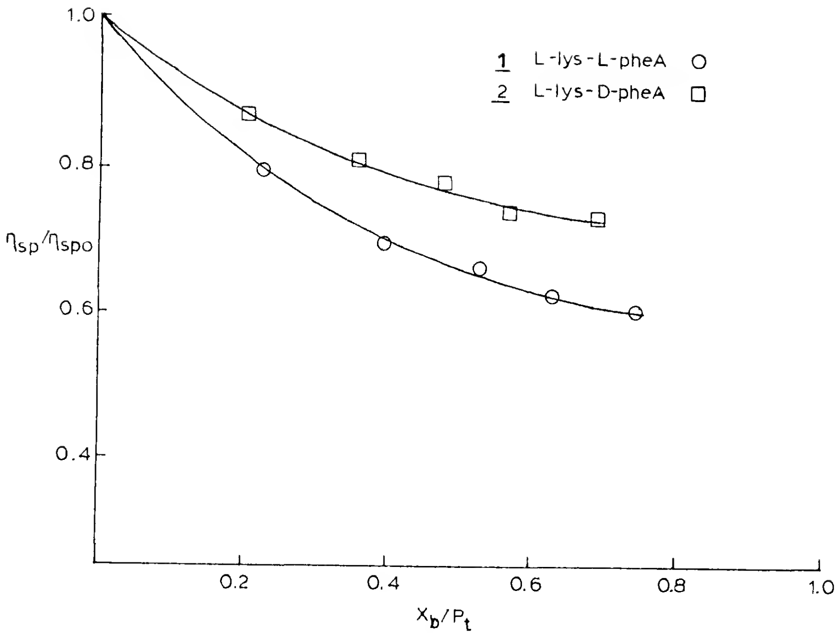

Figure 20. The Effect of Peptides 1 and 2 on the Relative Specific Viscosity of Salmon Sperm DNA

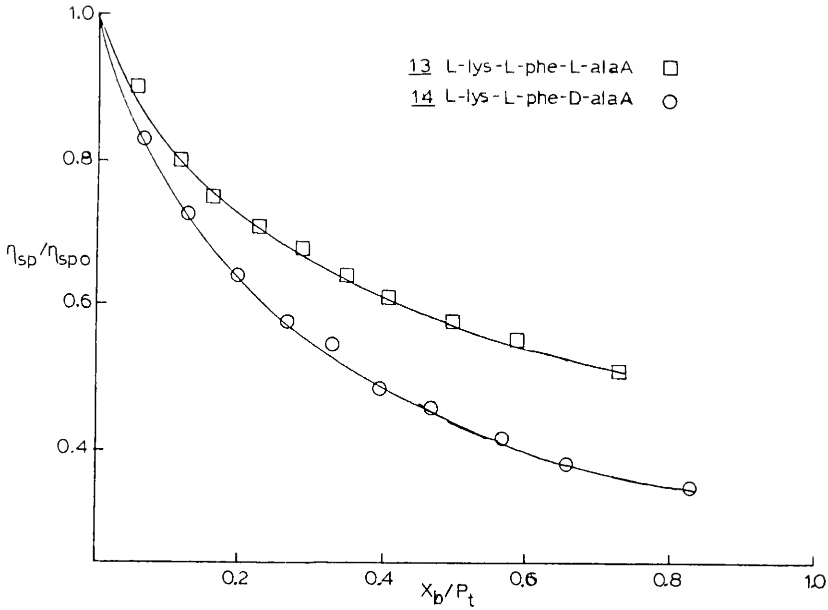

Figure 21. The Effect of Peptides 13 and 14 on the Relative Specific Viscosity of Salmon Sperm DNA

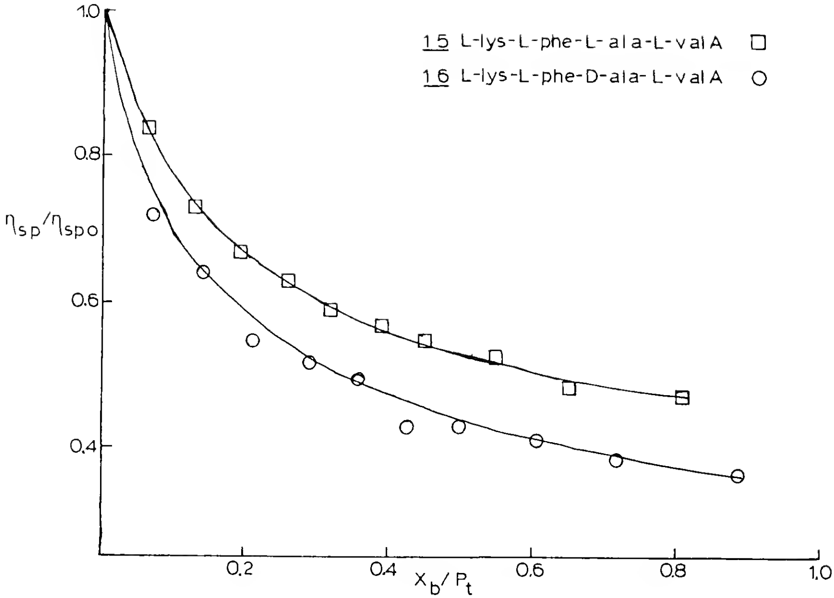

Figure 22. The Effect of Peptides 15 and 16 on the Relative Specific Viscosity of Salmon Sperm DNA

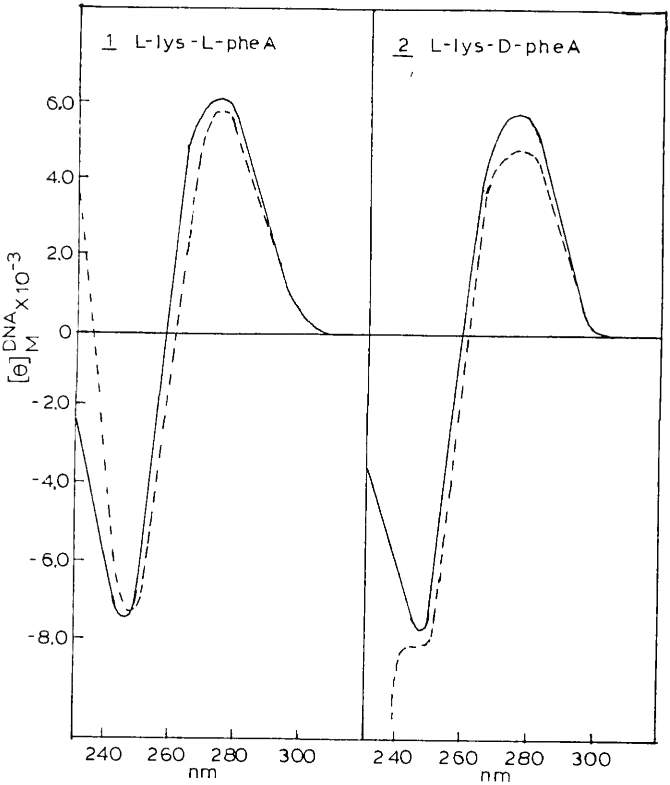

Figure 23. The Circular Dichroism Spectra of Salmon Sperm DNA in the Presence (----) and Absence (——) of Peptides 1 and 2

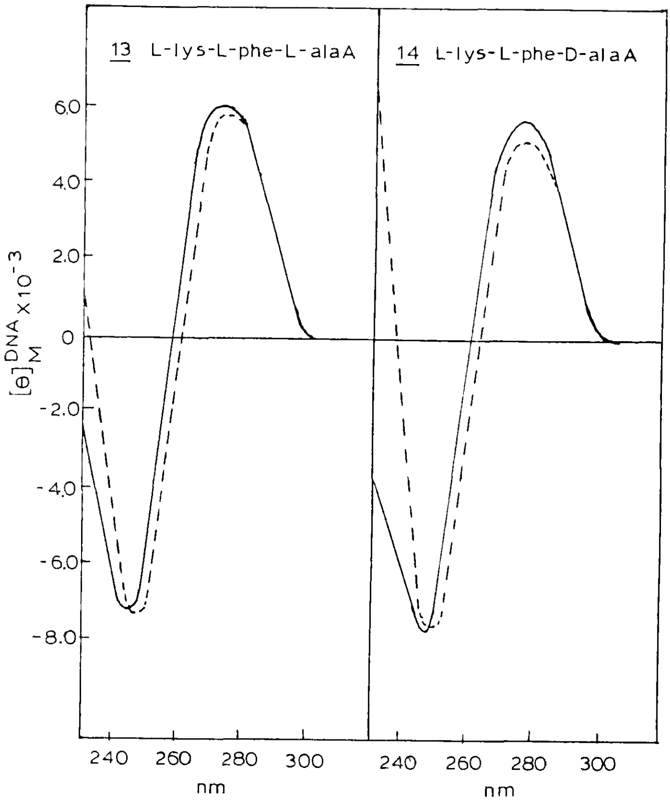

Figure 24. The Circular Dichroism Spectra of Salmon Sperm DNA in the Presence (- - -) and Absence (——) of Peptides 13 and 14

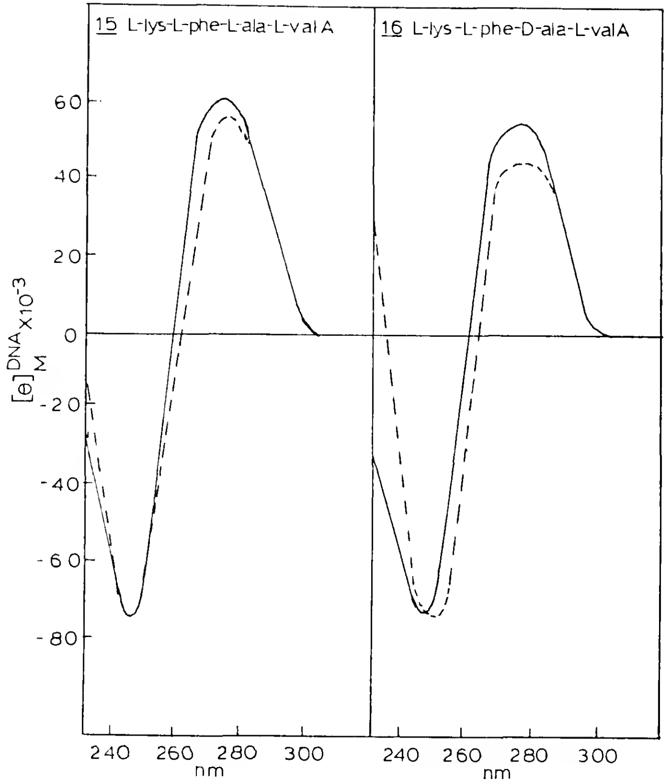

Figure 25. The Circular Dichroism Spectra of Salmon Sperm DNA in the Presence (- - -) and Absence (———) of Peptides <u>15</u> and <u>16</u>

Equilibrium Dialysis Studies

Direct binding studies of these peptide amides with native salmon sperm DNA were carried out using equilibrium dialysis. The quantitative analysis of the peptide concentration was accomplished via the fluorescamine reagent. The results of these studies are shown in Table 4. It should be noted that these studies were carried out in duplicate at a single peptide and DNA concentration (i.e., at 3.5×10^{-4} M DNA phosphate/liter and either 2.5×10^{-5} M or 5×10^{-5} M peptide) using 10 mM MES buffer (5 mM Na^{+}, pH 6.2). Attempts to carry out Scatchard-type binding studies in order to ascertain the maximum number of binding sites as well as the average binding constant have been unsuccessful. The most probable reason for this failure is due to the fact that the binding constants of the peptides to DNA are very low compared to systems such as proflavine, acridine orange, and ethidium bromide, where Scatchard plots have been successfully employed.[114] Thus, the apparent binding constant, K_a, was evaluated according to the equation,

$$K_a = \frac{R_b}{(P_t - R_b)R_f}$$

where R_f and R_b equal the concentration of free and bound peptide, respectively, and P_t is the total DNA phosphate concentration. This model assumes that each DNA phosphate group binds independently to a peptide molecule and that the maximum number of binding sites per DNA phosphate is one. Obviously, this may not be true; however, since the binding

Table 4. Apparent Binding Affinity (K_a) of the Peptides to Salmon Sperm DNA

Peptide System[a]	K_1	K_2
L-lys-L-pheA (1)	-	8.00×10^3
L-lys-D-pheA (2)	-	6.00×10^3
L-lys-L-phe-L-alaA (13)	4.67×10^2	1.06×10^3
L-lys-L-phe-D-alaA (14)	2.21×10^3	2.43×10^3
L-lys-L-phe-L-ala-L-valA (15)	1.38×10^3	1.73×10^3
L-lys-L-phe-D-ala-L-valA (16)	1.82×10^3	3.18×10^3

[a]Equilibrium dialysis was carried out with 3.5×10^{-4} M salmon sperm DNA in 10 mM MES (5 mM Na^+, pH 6.2) with a peptide concentration of either 2.5×10^{-5} (K_1) or 5×10^{-5} (K_2). The determinations were carried out in duplicate and were reproducible to $\pm$ 15%.

data from the interactions of peptides to the nucleic acids are always evaluated in the same manner, the differences in values of K_a shown in Table 4 do reflect the differences in strength of binding. This situation would especially be true if the total DNA phosphate, P_t, is present in large excess as compared to R_b. It should be noted that in all cases examined P_t/R_b is found to be greater than 30. It is noted that peptides 1, 14 and 16 bind more strongly to salmon sperm DNA than do peptides 2, 13 and 15, respectively (Table 4).

Melting Temperature Studies

The effect of the various peptide systems on the melting temperature, T_m, of the helix coil transition of the DNA was studied. The results (Table 5) indicate that the peptide amides stabilize the helix with respect to the random coil and that the transition exhibits monophasic melting behaviour. In addition, the data indicate that the least stabilization of the helix is obtained with peptides containing L-leucine.

The interpretation of these data is not clear because the helix-coil transition is complicated by the fact that it involves relative interactions of the peptide (P) with the helix (H) and the random coil (C). Nevertheless, the observa-

$$H + P \overset{K_H}{\rightleftarrows} H\cdot P \rightleftarrows C\cdot P \overset{K_C}{\rightleftarrows} C + P$$

tion that T_m is increased in the presence of the peptide system suggests that K_H is greater than K_C, although Gabbay and Kleinman have pointed out that only when the constants

Table 5. The Effect of Peptides on the ΔT_m of the Helix-Coil Transition of Salmon Sperm DNA ($\Delta T_m = T_m - T_{mo}$, where T_m and T_{mo} are the melting temperatures in the presence and absence of peptide).

Peptide System[a]	ΔT_m 100 μM	ΔT_m 200 μM
L-lys-L-pheA (1)	7.4	9.9
L-lys-D-pheA (2)	6.1	8.9
L-lys-L-phe-glyA (3)	6.6	9.8
L-lys-L-pheA(diMe) (5)	5.9	7.9
L-lys-L-phe-gly-glyA (6)	7.4	9.9
L-lys-L-phe-L-leu-glyA (7)	3.2	4.7
L-lys-L-phe-D-ala-L-leuA (9)	3.2	4.9
L-lys-L-phe(gly-L-leu)$_2$A (10)	4.1	5.9
L-lys-L-phe-D-leu-L-leu-D-leuA (11)	3.0	3.9
L-lys-L-phe-gly-L-leuA (12)	5.9	8.5
L-lys-L-phe-L-alaA (13)	3.7	5.6
L-lys-L-phe-D-alaA (14)	4.9	7.0

Table 5 - Continued

Peptide System[a]	ΔT_m	
	100 μM	200 μM
L-lys-L-phe-L-ala-L-valA (15)	6.1	7.9
L-lys-L-phe-D-ala-L-valA (16)	7.1	10.5

[a] T_m studies were carried out in 0.01 M MES buffer, pH 6.2, using 54 μM P/l of DNA and peptide concentrations of 100 and 200 μM.

K_H and K_C are directly determined is this conclusion warranted.[115]

Discussion

A great deal of interest in the past decade has centered around the recognition process between nucleic acids and protein systems. It is recognized that the interaction specificity between the two macromolecules is a problem of immense complexity and probably involves numerous types of forces operating at several sites along the nucleic acid and protein chains. In addition, recent studies on chromatin suggest that protein-DNA binding specificity is not only a dynamic process which is continually modified during the cell cycle, but may also involve specific protein aggregates-DNA recognition.[116-125]

The study presented here has taken a simplified approach to the above problem by studying the interaction specificities of small oligopeptide amides with DNA. Studies by Gabbay and coworkers have revealed that the nucleic acid helix may bind to small molecules via electrostatic, hydrogen bonding, and hydrophobic forces.[69,126-128] Hydrophobic-type interactions are of particular interest since at least three kinds have been noted, i.e., (1) intercalation between base pairs of DNA as exemplified by aromatic cations, (2) "partial" insertion or intercalation between base pairs demonstrated with sterically restricted aromatic ring containing compounds, and (3) external hydrophobic-type binding which is noted in

in the nucleic acid-steroidal amine complexes.[68-70,127,129,130]

In 1956, Wilkins proposed a model based on X-ray studies whereby basic proteins are wound in a helical fashion along the grooves of DNA.[131] The polypeptide chain appears to assume a slightly modified β-chain conformation with an approximate helical increment angle of 20^{o} per residue. This model has recently received added support from the observation that β-chains are not linear but rather helical in nature with dimensions similar to the DNA helix as evidenced by X-ray data of several proteins.[132]

In an attempt to provide experimental evidence for (or against) β-chain-DNA binding, the synthesis and study of interaction specificities of the oligopeptide amides were undertaken. Gabbay et al. have presented evidence that strongly suggests that L-lysine in the diastereomeric dipeptide amides, L-lys-L-pheA (1) and L-lys-D-pheA (2), binds stereospecifically to DNA and dictates the positioning of the aromatic ring of the C-terminal residue.[70] This conclusion is based on the following.

The ^{1}H nmr data (Table 2) indicate that the protons of the aromatic ring of L-lys-L-pheA (1) experience a large upfield chemical shift (23.5 Hz) and line broadening, whereas the aromatic protons of the diastereomeric peptide L-lys-D-pheA (2) is relatively unaffected upon binding to DNA. A model which assumes that the aromatic ring of (1) points into the helix (i.e., partial insertion between base-pairs of DNA) and the aromatic ring of (2) points outward toward

the solvent can best explain the data. The larger upfield chemical shift experienced by the aromatic protons of (1) as compared to (2) is indicative of closer contact to the DNA base-pairs and is due to ring current anisotropy.[39,66] On the other hand, the large ^{1}H nmr signal broadening of the aromatic protons of (1) ($\Delta\nu_{1/2}$ = 31 Hz) as compared to (2) ($\Delta\nu_{1/2}$ = 6.5 Hz) could be explained by several mechanisms: (i) slower tumbling rates of the aromatic ring of (1) in the DNA complex as compared to (2), (ii) slow exchange between various DNA binding sites for DNA-(1) as compared to DNA-(2) complex, (iii) larger differences in the chemical shifts are experienced by the ortho, meta and para protons of the aromatic protons of (1) in the DNA complex as compared to (2), and/or (iv) combination of all 3 mechanisms. In order to discriminate between the above alternatives, the spin lattice relaxation time (T_1) measurements were performed on the DNA-(1) and (2) complexes under conditions of total binding. Since (a) the value of T_1 is determined (among other things) by the correlation time (τ_c) and the mean residence time (τ_m) and (b) the observation that the T_1 values of the aromatic protons of (1) and (2) in the DNA complex are nearly identical ($T_1 \cong 0.65$ sec, Table 2) it is concluded that the tumbling rate ($1/\tau_c$) and the chemical exchange rate ($1/\tau_m$) of the aromatic protons of (1) and (2) in the DNA complex are very similar in magnitude.[39,112,113] Therefore, the large ^{1}H nmr signal line broadening observed for the aromatic protons of (1) in the DNA complex ($\Delta\nu_{1/2}$ = 31 Hz) can only be due to

large differences in the chemical shifts experienced by the ortho, meta, and para protons. The observation of two ^1H nmr signals for the aromatic protons of (1) in the presence of excess DNA (Figure 16) would result from the greater upfield chemical shift experienced by the meta and para protons than by the ortho protons as a consequence of ring current anisotropy of neighboring base pairs. The results of the T_1 studies of peptides 13 - 16 (Table 3) are consistent with this interpretation.

Since the magnitude of the ring current anisotropy experienced by the ortho, meta, and para protons of the aromatic ring of L-lys-L-pheA (1) depends on the geometry of the latter with respect to the base pairs in the DNA complex, large ^1H nmr signal line broadenings are observed. On the other hand, the ^1H nmr data of L-lys-D-pheA (2) indicate a small upfield chemical shift and absence of signal line broadening for the aromatic ring protons which is consistent with the interpretation that the aromatic ring of this peptide points outward into solution. Thus, the ^1H nmr techniques may be used to differentiate between and/or evaluate the extent of the "in" or "out" geometry of the aromatic ring of phenylalanine residues in the DNA-peptide complexes.

Figure 26 schematically illustrates the Wilkins model for peptide-DNA binding whereby the polypeptide chain assumes a helical β-sheet structure which is wrapped around the nucleic acid helix. It is noted that for polypeptides composed of L-amino acids, the side chains of the amino acid residues

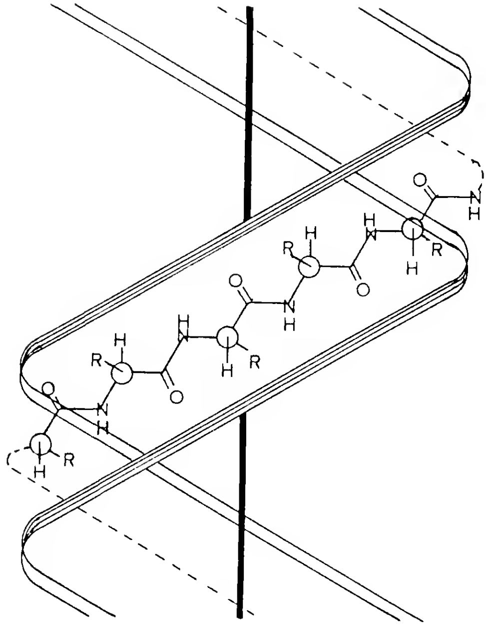

Figure 26. Schematic Representation of the Wilkins Model for Peptide-DNA Binding. The peptide shown is composed of only L-amino acids and the side chains alternately point into and out of the helix

would alternately point "into" and "out" of the helix. Polypeptides composed of alternating L- and D-amino acids can form two types of complexes with DNA, i.e., all side chains point into or out of the helix. The rationale for the synthesis of the oligopeptides amides, 1 - 16, now becomes a little clearer, i.e., the effect of chain elongation and chirality on the ^{1}H nmr of the aromatic protons of the phenylalanine residue may be used to provide experimental evidence for (or against) the Wilkins model. The initial starting point, the N-terminal L-lysine residue, is assumed to be anchored to the DNA in a sterospecific manner which would allow the side chain of the neighboring amino acid, as well as amino acids at the even-numbered positions, of the L-configuration to point into the helix. In addition, it is assumed that substitution of hydrophobic amino acids of the L and D configuration at the even- and odd-numbered positions, respectively, would allow close contact of the aromatic probe of L-phenylalanine with DNA base pairs if the former is present at an even-numbered position. On the other hand, it is reasoned that hydrophobic amino acids which are not in "register" with the aromatic probe would compete for the internal DNA site and, thus, weaken the interaction of the probe with the DNA base pairs.

If the above model is correct it should predict that the aromatic ring in L-lys-L-pheA (1), L-lys-L-phe-glyA (3), L-lys-L-phe-gly-glyA (6), L-lys-L-phe-D-leu-glyA (8), L-lys-L-phe-D-ala-L-leuA (9), L-lys-L-phe(gly-L-leu)$_2$A (10), L-lys-

L-phe-D-leu-L-leu-D-leuA (11), L-lys-L-phe-D-alaA (14), and L-lys-L-phe-D-ala-L-valA (16) is in close contact to the bases of DNA. Similarly, the model should predict a lesser contact between the aromatic ring "probe" and the DNA bases for the following peptides: L-lys-D-pheA (2), L-lys-gly-L-pheA (4), L-lys-L-phe-L-leu-glyA (7), L-lys-L-phe-L-alaA (13), and L-lys-L-phe-L-ala-L-valA (15). The ^{1}H nmr evidence (Table 2) is completely consistent with the above prediction except for two peptides. For example, large upfield chemical shifts, $\Delta\delta$ (indicative of close contact to the nucleic acid bases), and large signal line broadening, $\Delta\nu_{1/2}$ (indicative of the "in" geometry), are observed for the following peptide amides: 1, 3, 6, 9, 10, 12, 14, and 16; but not for 8 and 11. The small upfield chemical shift and signal line broadening for the aromatic proton signal of 2, 4, 7, 13, and 15 are accurately predicted.

The inaccurately predicted binding of the oligopeptide amides, 8 and 11, to DNA by the model may be due to steric factors which prohibit the simultaneous "internal" binding of the L-phe and D-leu side chains at the 2 and 3 positions of the peptide, respectively. In line with this explanation is the observation that substitution for the D-leu at the 3 position by an amino acid containing a small side chain (e.g., glycine or D-alanine) results in a peptide in which the aromatic ring probe is in closer contact with the DNA base pairs, e.g., the peptide amides, 6, 9, and 10.

It is tempting to suggest that protein-DNA interactions

are mediated via a single chain, helical peptide β-sheet structure especially since the primary structure of histones contains a statistically significant number of sequences in which basic and/or hydrophobic amino acids alternate with small hydrophylic amino acids, e.g. glycine and serine.[133]

CHAPTER III
ANTHRACYCLINES

The anthracycline drugs are some of the most important antitumor agents in use today. The biological activity seems to be a result of formation of a complex with chromatin DNA.[78-83] In vivo, anthracyclines inhibit both RNA and DNA synthesis, while, in vitro, DNA and RNA polymerases are inhibited.[80-83] However, the anthracyclines exhibit high toxicity in humans which is thought to be due to the accumulation and long biological half life of the hydrolytic product (i.e., the aglycone, see Figure 27) in heart

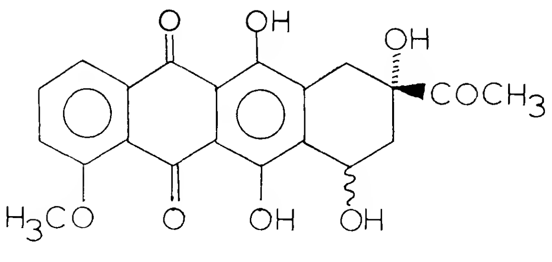

Figure 27. The Aglycone of Daunorubicin, Daunorubicinone

tissues.[107,111] In an attempt to overcome the toxicity, the synthesis of anthracycline analogs, which would lead not only

to water soluble aglycones (should glycosidic hydrolysis occur), but also to the retention of template binding properties, was undertaken.

Compounds which lead to water soluble aglycones have been synthesized by reaction of the 9-ketomethyl group of daunorubicin in such a way as to form an amine at the C-13 position. The analogs shown in Table 6 were studied by several in vitro techniques. In vivo activity against P-388 mouse lymphocytic tumor was also determined. The results of these studies are presented in this section.

Ultraviolet and Circular Dichroism Studies

Absorption and circular dichroism data on the anthracycines, 17-29, are given in Tables 7 and 8, respectively. The CD spectra of the anthracyclines, 17-29, indicate the presence of two electronic transitions above 300 nm, e.g., at 340 and 470 nm for daunorubicin, 16 (Figure 28). The allowed low energy transition ($\varepsilon \simeq 11\ 500$) at 470 nm is typical of the short axis transition of α-nitrogen or α-oxygen substituted 9, 10-anthraquinones.[134] The disallowed higher energy transition ($\varepsilon \simeq 2\ 000$) at 340 nm is typical of the long axis transition of unsubstituted and/or - alkyl-substituted 9, 10-anthraquinones. Consistent with this assignment is the observation that the 340 nm long axis transition (sensitive to β substituents) shows larger optical activity than the low-energy short axis transition at 470 nm. For example the values of the dichroic strength

Table 6. The Anthracycline Drugs Studied

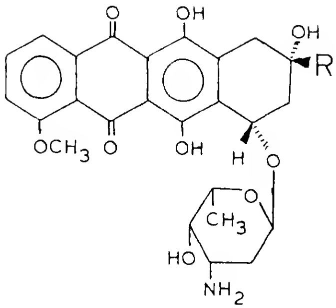

I

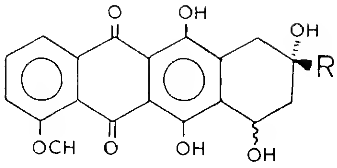

II

Compound[a]	NSC	Substitution
17 Adriamycin	123127	I; R = $COCH_2OH$
18 Daunorubicin	82151	I; R = $COCH_3$
19 D_9-NH_2	-	I; R = $\overset{*}{C}H(NH_2)CH_3$
20 D_9-MoMeA	257455	I; R = $\overset{*}{C}H(NHCH_3)CH_3$
21 D_9-PrA	-	I; R = $\overset{*}{C}H(NHC_3H_7)CH_3$
22 D_9-BuA	263673	I; R = $\overset{*}{C}H(NHC_4H_9)CH_3$
23 D_9-EolA	-	I; R = $\overset{*}{C}H(NHCH_2CH_2OH)CH_3$
24 D_9-PolA	266537	I; R = $\overset{*}{C}H(NH(CH_2)_3OH)CH_3$
25 D_9-GlyA	-	I; R = $\overset{*}{C}H(NHCH_2CONH_2)CH_3$
26 D_9-Gly-L-LeuA	277454	I; R = $\overset{*}{C}H(NHCH_2CONHCH(CH_2CH(CH_3)_2)$-$CONH_2)CH_3$
27 D_9-Gly-L-PheA	-	I; R = $\overset{*}{C}H(NHCH_2CONHCH(CH_2\phi)CONH_2)$-$CH_3$

Table 6 - Continued

Compound	NSC	Substitution
28 A_9-MoMeA	-	II; R = $\overset{*}{C}H(NHCH_3)CH_3$
29 A_9-BuA	277453	II; R = $CH(NHC_4H_9)CH_3$

[a]The compounds (19 - 29) may in fact be a mixture of two diastereomers (R and S configuration at C*) which cannot be separated.

Table 7. Absorption and Hypochromicity Data on the Anthracycline Drugs.

Compound[a]	Free λ_{max}	Free ε_{max}	Free λ_{max}	Free ε_{max}	DNA complex λ_{max}	DNA complex ε_{max}	DNA complex H
Adriamycin (17)	476	11500	495	11500	505	6930	31
Daunorubicin (18)	477	11500	495	11200	506	6830	33
D_9-NH_2 (19)	475	11500	494	11500	500	8570	28
D_9-MoMeA (20)	477	11500	495	11500	506	7030	33
D_9-PrA (21)	478	11500	493	11500	503	7990	30
D_9-BuA (22)	475	11500	495	11300	504	6940	30
D_9-EolA (23)	476	11500	494	11500	501	7670	25
D_9-PolA (24)	475	11500	493	11500	503	7560	29
D_9-GlyA (25)	475	11500	496	11600	504	7420	25
D_9-Gly-L-LeuA (26)	475	11500	497	11500	503	8990	23
D_9-Gly-L-PheA (27)	473	11500	493	11500	502	8430	27
A_9-MoMeA (28)	476	11500	495	11600	503	7500	22
A_9-BuA (29)	478	11500	493	11500	500	7920	22

[a]Measurements were carried out in 2 mM PIPES buffer (21 mM Na^+; pH 7.8) using the Cary 15 spectrophotometer at 25°C using salmon sperm DNA.

Table 8. Molar Ellipticity of the Anthracycline Drugs.

	Free				DNA complex			
Compound[a]	λ_1	$[\theta]_1 x 10^{-3}$	λ_2	$[\theta]_2 x 10^{-3}$	λ_1	$[\theta]_1 x 10^{-3}$	λ_2	$[\theta]_2 x 10^{-3}$
Adriamycin (17)	345	6.7	470	3.1	381	6.7	492	4.4
Daunorubicin (18)	346	8.4	468	4.2	378	8.2	490	6.1
D_9-NH_2 (19)	342	3.0	455	2.0	370	4.0	485	2.7
D_9-MoMeA (20)	343	4.8	470	3.0	380	5.4	495	3.5
D_9-PrA (21)	355	1.6	468	5.8	382	3.4	503	6.4
D_9-BuA (22)	344	5.4	465	3.6	380	6.4	497	4.6
D_9-EolA (23)	348	3.4	463	2.2	387	4.5	501	3.0
D_9-PolA (24)	343	4.3	468	2.5	380	4.6	492	3.1
D_9-GlyA (25)	345	4.0	458	3.2	375	5.7	492	3.5
D_9-Gly-L-LeuA (26)	345	4.3	455	5.5	375	7.4	495	4.9
D_9-Gly-L-PheA (27)	345	5.8	460	5.8	378	8.4	490	4.9
A_9-MoMeA (28)	345	4.8	460	2.7	380	5.1	493	3.0
A_9-BuA (29)	342	2.8	460	1.2	380	2.8	495	1.8

[a]Measurements were carried out in a 10 cm cell with 10 μM of drug in the presence and absence of salmon sperm DNA in 2 mM PIPES buffer (21 mM Na^+; pH 7.8) on a Jasco J-20 spectropolarimeter at 25°C.

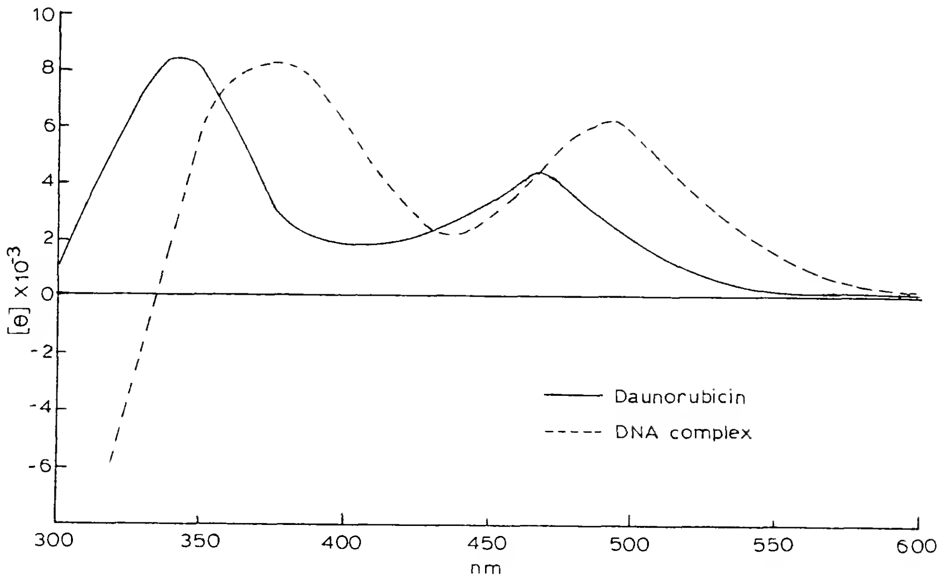

Figure 28. The Circular Dichroism Spectra of Daunorubicin in the Presence and Absence of Salmon Sperm DNA

$\Delta\varepsilon_i/\varepsilon_i$ (where $\Delta\varepsilon_i$ is the difference in the molar extinction coefficients for the left and right cicular polarized light, and ε_i is the molar extinction coefficient of the i th transition), are found to be 1.5×10^{-3} and 1.2×10^{-4} for the long and short axis transitions, respectively. Since the asymmetry in the anthracycline systems resides at the β position of the 9, 10-anthraquinone ring and the long axis transition is strongly affected by β substitution as compared to the short axis transition, the above assignments are reasonable.

Large hypochromic effects on the short and long axis transition of the anthracyclines, 17-29, are observed in the presence of excess salmon sperm DNA. It is noted that hydrolysis of the amino sugar moiety to form the aglycone (compounds 28 and 29) lowers the hypochromic effect observed for the anthracycline transition (320-600 nm) upon binding to DNA. For example, the following order of decreasing hypochromism, H, is observed: daunorubicin (18) > adriamycin (17) = D_9-MoMeA (20) > D_9-BuA (22) = D_9-PrA (21) > D_9-NH_2 (19) = D_9-PolA (24) > D_9-Gly-PheA (27) > D_9-EolA (23) = D_9-GlyA (25) > D_9-Gly-LeuA (26) > A_9-MoMeA (28) = A_9-BuA (29). It should be noted that the absorption studies were carried out under conditions of total binding to DNA and at a base pair to drug ratio of 10. In all cases, the absorption spectra of the DNA bound anthracyclines reach a limiting value at a base pair to drug ratio greater than 3 under these conditions (2 mM PIPES; 21 mM Na^+; pH 7.8).

A large red shift in the circular dichroism of the short and long axis transitions of the anthracyclines, 17-29, is observed upon binding to DNA. For example, the peak at 470 nm (short axis transition) is red shifted by approximately 20-35 nm for compounds 17-19. The extent of the red shift of the peak at 340 nm (long axis transition) of 17-19 in the presence of DNA, however, is found to depend on the anthracycline structure, i.e., the values decrease as follows: D_9-EolA (23) > A_9-BuA (29) > D_9-MoMeA (20) = D_9-PolA (24) > Adriamycin (17) = D_9-BuA (22) > A_9-MoMeA (28) > D_9-GlypheA (27) > Daunorubicin (18) > D_9-GlyA (25) = D_9-GlyleuA (26) > D_9-NH_2 (19) > D_9-PrA (21). Similarly, the molar ellipticity, $[\theta]$, for the long axis transition at 340 nm is observed to remain unchanged or decrease for daunorubicin (18), adriamycin (17), and A_9-BuA (29) while it increases for the other drugs, 19-28, upon addition of DNA. It should be noted that the circular dichroism studies were carried out under conditions of total binding to DNA and at a base pair to drug ratio of 10. In summary, the absorption and circular dichroism spectra indicate that the aglycones, 28 and 29, exhibit both lower hypochromicity and induced CD compared to the other semisynthetic derivatives, 19-27, and the naturally occuring drugs, 17 and 18, with DNA.

Binding Studies

The binding of the anthracycline drugs to salmon sperm

DNA was studied by spectral titration techniques. It should be noted that the more direct equilibrium dialysis method has been found to be unsatisfactory due to the strong binding of the anthracyclines to the membrane.

The effect of increasing concentration of salmon sperm DNA on the absorption of the anthracycline drugs, 17-29 (7×10^{-5} M), at 480 nm was studied in 2 mM PIPES buffer (pH 7.8) at two ionic strengths (i.e., 51 mM and 201 mM Na^+) in a 10 cm cell which was thermostated at 25^oC. The spectral data were analyzed by the Scatchard technique according to the following equation:

$$\frac{\bar{n}}{D_f} = K_a n_{max} - K_a \bar{n}$$

where $\bar{n}$ is the number of moles of drug bound per mole of DNA phosphate, D_f is the concentration of free drug, K_a is the apparent binding constant, and n_{max} is the maximum number of binding sites per DNA phosphate.[114] A plot of $\bar{n}/D_f$ versus $\bar{n}$ gives the values of n_{max} (X-axis intercept) and K_a (negative slope). The values of D_f and D_b were calculated from the spectrophotometric data in a manner similar to that described by Hyman and Davidson utilizing the determined values of ε_f^{480} and ε_b^{480}, the extinction coefficients of the free and DNA-bound anthracylcines, respectively. The results of the binding isotherms are summarized in Table 9.. It should be noted that the data was analyzed using the least squares method for fitting a straight line and the correlation coefficient was calculated. The minimum

Table 9. Binding Isotherm Data for the Anthracycline Drugs.

Compound[a]	PIPES (51 mM)		PIPES (201 mM)	
	$K_a x10^{-6}$	n_{max}	$K_a x10^{-6}$	n_{max}
Adriamycin (17)	13.3	0.11	10.0	0.10
Daunorubicin (18)	10.7	0.15	7.3	0.08
D_9-NH_2 (19)	1.6	0.21	1.4	0.19
D_9-MoMeA (20)	7.9	0.13	4.6	0.11
D_9-PrA (21)	7.0	0.15	5.6	0.15
D_9-BuA (22)	9.5	0.11	3.2	0.08
D_9-EolA (23)	4.8	0.16	1.9	0.15
D_9-PolA (24)	5.3	0.11	1.8	0.09
D_9-GlyA (25)	3.1	0.18	1.8	0.18
D_9-Gly-L-LeuA (26)	2.3	0.19	1.2	0.18
D_9-Gly-L-PheA (27)	3.7	0.18	2.6	0.18
A_9-MoMeA (28)	4.4	0.11	3.5	0.11
A_9-MoBuA (29)	2.0	0.09	0.8	0.07

[a]Measurements were carried out on a Cary 15 spectrophotometer at 480 nm with salmon sperm DNA in 2 mM PIPES buffer (pH 7.8) in a 10 cm cell at 25°C. The correlation coefficients of the data are greater than 0.95 in all cases.

acceptable limits of this analysis were taken to be four points within the binding range of 5 to 95% and a correlation coefficient of not less than 0.95. The most striking observation which can be seen in Table 9 is the greatly reduced binding affinity of the aglycones, 28 and 29, as compared to the unhydrolyzed drugs, 20 and 22.

Distribution Coefficients

The determination of the distribution coefficients of the anthracycline drugs 17-29, in an n-octanol/water system (2 mM PIPES; 21 mM Na^+; pH 7.8) was determined spectrophotometrically. Such studies provide a comparative estimate of the potential in vivo cell membrane permeability of the newly synthesized derivatives. From Table 10, it is evident that addition of another positive charge increases the hydrophilic character of the molecule (e.g., compound 19 versus 18) while addition of a hydrophobic amine increases the lipophilicity (e.g., compound 22 versus 18). Hydrolysis of the drugs to the aglycones greatly enhances the hydrophobicity of the analog as compared to the parent molecule (i.e., 28 and 29 versus 20 and 22, respectively). It should be noted that each study was determined in triplicate and the values did not vary by more than ± 15%.

Inhibition of DNA-Template Activity

The effect of the anthracyclines (17-29) on the DNA-dependent E. coli RNA polymerase is summarized in Table 11.

Table 10. Distribution Coefficients of the Anthracyclines.

Compound[a]	D
Adriamycin (17)	0.48
Daunorubicin (18)	2.76
D_9-NH_2 (19)	1.05
D_9-MoMeA (20)	0.31
D_9-PrA (21)	1.12
D_9-BuA (22)	4.28
D_9-EolA (23)	0.861
D_9-PolA (24)	0.841
D_9-GlyA (25)	0.251
D_9-GlyLeuA (26)	2.32
D_9-GlyPheA (27)	4.98
A_9-MoMeA (28)	2.24
A_9-BuA (29)	23.3

[a]The distribution coefficient D (concentration in octanol/ concentration of the drug in 2 mM PIPES buffer, 21 mM Na^+; pH 7.8) was determined by spectrophotometric analysis of the drug concentration in both solvent systems with a Gilford 240 spectrometer.

Table 11. Relative Inhibition of RNA Polymerase by the Anthracyclines.

Compound[a]	% Enzymatic Activity
Control	100
Adriamycin (17)	9
Daunorubicin (18)	9
D_9-NH_2 (19)	12
D_9-MoMeA (20)	10
D_9-PrA (21)	14
D_9-BuA (22)	13
D_9-EolA (23)	19
D_9-PolA (24)	10
D_9-GlyA (25)	36
D_9-GlyLeuA (26)	36
D_9-GlyPheA (27)	46
A_9-MoMeA (28)	73
A_9-BuA (29)	49

[a]The *E. coli* RNA polymerase catalyzed incorporation of (5-^{3}H)UMP was carried out according to published procedures utilizing 0.12 mM calf thymus DNA as the template and 0.12 mM of the anthracyclines. The correlation coefficients of the data are greater than 0.95 in all cases.

The extent of the inhibition is determined from the rate of incorporation of 5-^3H UMP into RNA. The rate plots for daunorubicin (18), D_9-PrA (21), D_9-EolA (23) and the control (absence of drug) are shown in Figure 29. It is noted that the aglycones (28 and 29) inhibit the polymerase activity although to a much lesser extent than the corresponding parent compounds in which the amino sugar moiety is still attached, that is, D_9-MoMeA (20) and D_9-BuA (22). In addition, the derivatives with peptide amides, 25-27, show less inhibition than the analogs with less bulky side chains, 17-24.

Kinetics of Dissociation

The effect of increasing ionic strength on the dissociation of the DNA-drug complexes was studied by stop-flow techniques utilizing sodium dodecyl sulfate (SDS) according to previously published methods. The reactions are found to be first order to at least 2.5 half-lives with respect to the DNA-drug complexes. In addition, increasing the concentration of SDS (0.1-1%) and/or the concentration of DNA (base pair/drug = 3-30) has minimal effect on the observed first-order rate constant, that is, the value of k remains constant to $\pm$ 5%. The data are consistent with the following mechanism whereby the first-order rate constant, k, of the dissociation process in the rate-controlling step and the bimolecular sequestering process, k_2, is diffusion controlled.

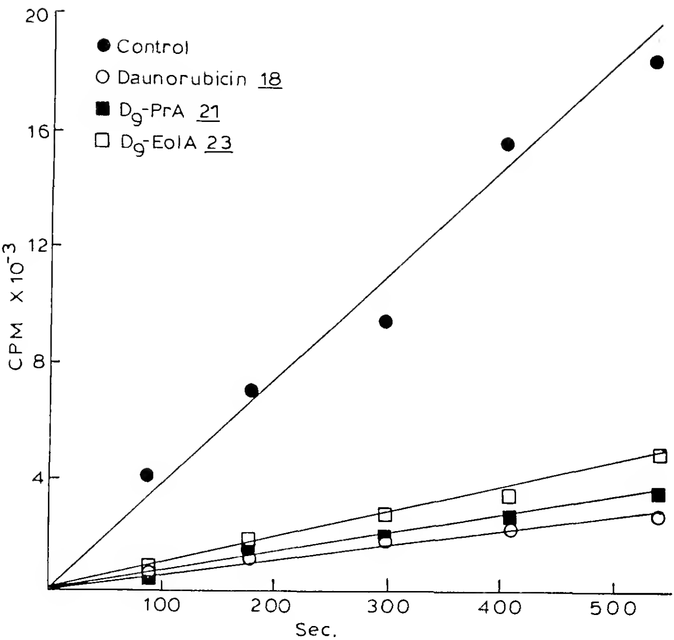

Figure 29. The Effect of the Anthracyclines 18, 21, and 23 on the Incorporation of [5-^{3}H]UMP into RNA by DNA-Dependent *E. coli* RNA Polymerase

$$\text{DNA-D} \xrightarrow{k} \text{DNA+D}$$

$$\text{SDS+D} \xrightarrow{k_2} \text{SDS-D}$$

The results of the dissociation of the anthracycline drugs from salmon sperm DNA in 2 mM PIPES buffer (pH 7.8) at various ionic strengths are given in Table 12. The kinetics of dissociation were measured at 480 nm using 0.6% SDS. It is noted that the rate of dissociation of the DNA-D_9-BuA is found to be considerably slower than the rate observed for the corresponding DNA-A_9-BuA complex. In addition, the rates of dissociation of the anthracyclines 17-29 from DNA complexes increase with increasing ionic strength.

Hydrolytic Stability of the Anthracyclines

It is commonly accepted that the anthracyclines, e.g., daunorubicin, are stable in neutral aqueous media, even under reflux conditions.[83] The rate of glycosidic hydrolysis of daunorubicin 18, adriamycin 17, and the daunorubicin analogs, D_9-MoMeA (20), D_9-BuA (22), and D_9-PolA (24) were determined by a technique based on the detection of nanomole quantities of daunoseamine (see Figure 30) (in 10 mM phosphate buffer; 150 mM Na^+; pH 7.5). The method utilizes the highly sensitive fluoropa reagent for the detection of sterically unhindered primary amines which was recently described by Roth and Hanpai and Benson et al.[135,136] It is observed that the intact anthracyclines (i.e., 17, 18, 20, 22, and 24) do not react with the reagent. However, the hydrolytic product, daunoseamine, rapidly reacts with fluoropa to yield a highly fluorescent adduct.[137]

Table 12. Rate of Dissociation of the DNA-Drug Complexes.

Salmon Sperm DNA Complex[a]	21 mM Na^+		51 mM Na^+		201 mM Na^+	
	k (sec^{-1})	Rel. Rate	k (sec^{-1})	Rel. Rate	k (sec^{-1})	Rel. Rate
Adriamycin (17)	0.29	0.91	0.41	0.98	0.55	0.81
Daunorubicin (18)	0.32	1.00	0.42	1.00	0.68	1.00
D_9-NH_2 (19)	0.46	1.44	0.73	1.74	1.74	2.56
D_9-MoMeA (20)	0.45	1.41	1.00	2.38	2.28	3.35
D_9-PrA (21)	0.13	0.41	0.24	0.57	0.51	0.75
D_9-BuA (22)	0.41	1.28	0.42	1.00	0.29	0.43
D_9-EolA (23)	0.11	0.34	0.29	0.69	0.42	0.62
D_9-PolA (28)	0.57	1.78	1.22	2.90	2.92	4.29
D_9-GlyA (25)	0.55	1.72	1.04	2.48	4.54	6.68
D_9-GlyLeuA (26)	0.54	1.69	0.80	1.90	1.03	1.51
D_9-GlyPheA (27)	0.61	1.91	2.14	5.10	3.43	5.07
A_9-BuA (29)	14.5	45.3	12.5	29.8	-	-

[a]Kinetics of dissociation were measured with a Durrum-Gibson stop-flow instrument at 480 nm using 0.6% SDS at 15°C in 2 mM PIPES buffer, pH 7.8. The correlation coefficients of the data are greater than 0.97 in all cases.

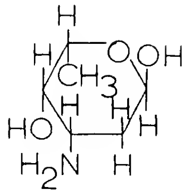

Figure 30. The Amino Sugar of the Anthracyclines, Daunosamine

The data were fitted to a straight line by the least squares method and correlation coefficients were calculated. The following equations were employed in the analysis of the rates:

$$-\frac{dC}{dt} = \frac{dD}{dt} = kC$$

$$\ln \frac{C_o}{C_t} = \ln \frac{C_o}{C_o - D_t} = kt$$

where C_o is the initial concentration of the anthracycline. C_t and D_t are the concentration at time t of the unhydrolyzed anthracycline and free daunoseamine, respectively.

The results of the temperature-dependent hydrolysis of the anthracyclines are summarized in Table 13. It is noted that the glycosidic hydrolysis of the drug is enhanced with increasing temperature and is quite rapid at 70^{o}C and pH 7.5. On the other hand, the hydrolytic rate (with one exception,

Table 13. Temperature Dependence of the Rate of Hydrolysis of the Glycosidic Bond of the Anthracyclines at pH 7.5 and 9.7.

	$k\ (sec^{-1})x10^6$; ($t_{1/2}$; hrs)					
	pH 7.5				pH 9.7	
Anthracycline[a]	37°	50°	60°	70°	50°	60°
Adriamycin (<u>17</u>)	1.53(126)	7.33(26)	22.9(8.4)	48.5(4.0)	29.6(6.5)	32.0(6.0)
Daunorubicin (<u>18</u>)	1.15(168)	2.75(70)	6.38(30)	18.7(10.3)	21.0(9.2)	18.1(11)
D_9-MoMeA (<u>20</u>)	1.66(116)	8.76(22)	27.4(7.0)	64.2(3.0)	31.7(6.1)	30.8(6.3)
D_9-BuA (<u>22</u>)	2.39(81)	16.7(11)	93.9(2.1)	243(0.8)	14.2(14)	10.0(19)
D_9-PolA (<u>24</u>)	3.78(51)	16.7(11)	68.4(2.8)	117(1.65)	41.8(4.6)	34.3(5.6)

[a]Kinetic studies were carried out in 50 mM phosphate buffer, pH 7.5, 200 mM Na^+ and 50 mM borate buffer, pH 9.7, 200 mM Na^+. The correlation coefficients of the data are greater than 0.98 in all cases.

i.e., adriamycin) exhibits a negative temperature dependence at pH 9.7.

From the data in Table 13, the values of the enthalpy, $\Delta H^{\ddagger}$, and entropy, $\Delta S^{\ddagger}$, of activation for the hydrolysis of the anthracyclines at pH 7.5 were calculated and shown in Table 14. It is noted that the hydrolysis has a positive enthalpy of activation and with one exception a highly negative entropy of activation. The exception, D_9-BuA (22), exhibits a positive value for both the enthalpy and entropy of activation suggesting that the mechanism of hydrolysis of 22 may be different from that of 17, 18, 20, and 24. The effect of pH on the rate of hydrolysis of the anthracyclines was studied at 50°C (Table 15). The results indicate that the rate of glycosidic hydrolysis is enhanced at higher pH.

Because of the possible catalytic role for the C-6 phenolic proton of the anthracyclines, the pK_a of the latter was determined at 25° and 50°C in 25 mM borax buffers according to Bates and Bower.[138] The results indicate that daunorubicin has a pK_a of 10.1 ± 0.05 and 9.7 ± 0.1 at 25° and 50°C. respectively.

It should be noted that in addition to the aglycone and daunoseamine, it was found that at 70°C and at pH 7.5 a third product of hydrolysis of daunorubicin (18) was formed. This product has been shown to be the totally aromatic aglycone system (II) shown in Figure 31 and accounts for approximately half of the total aglycone formed after 14 hours of incubation as shown by thin layer chromatography

Table 14. Enthalpy ($\Delta H^{\neq}$) and Entropy ($\Delta S^{\neq}$) of Activation for the Hydrolysis of the Anthracyclines at pH 7.5

Compound[a]	$\Delta H^{\neq}$ (kcal)	$\Delta S^{\neq}$ (e.u.)
Adriamycin (17)	19.9	-21.0
Daunorubicin (18)	15.6	-34.0
D_9-MoMeA (20)	21.2	-14.5
D_9-BuA (22)	29.0	+ 8.1
D_9-PolA (24)	22.3	-11.7

[a]The activation parameters were obtained from a van Hoff plot (ln k/T vs. 1/T) of the data at pH 7.5 shown in Table 13. The correlation coefficients of the data are greater than 0.95 in all cases.

Table 15. Effect of pH on the Rate of Hydrolysis of the Glycosidic Bond of the Anthracyclines at 50°C.

	$k\ (sec^{-1})\times10^{6}$; ($t_{1/2}$; hrs)		
Anthracycline[a]	pH 5.7	pH 7.5	pH 9.7
Adriamycin (17)	1.04(185)	7.33(26)	29.6(6.5)
Daunorubicin (18)	1.44(133)	2.75(70)	21.0(9.2)
D_9-MoMeA (20)	1.67(115)	8.76(22)	31.7(6.1)
D_9-BuA (22)	7.87(24.5)	16.7(11)	14.2(13.6)
D_9-PolA (24)	1.69(114)	16.7(11)	41.8(4.6)

[a]Buffers used: pH 5.7 - 10 mM MES, 200 mM Na^{+}; pH 7.5 - 50 mM phosphate buffer, 200 mM Na^{+}; and pH 9.7 - 50 mM borate buffer, 200 mM Na^{+}. The correlation coefficients of the data are greater than 0.98 with the exception of 18, 20, and 24 at pH 5.7 and 22 at pH 9.7 where the correlation is greater than 0.95.

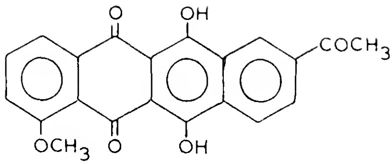

Figure 31. The Totally Aromatic Aglycone, II

(silica gel, $CHCl_3$). The assignment of structure is based on results of both ^1H nmr and mass spectroscopy studies.

^1H nmr studies of the totally aromatic aglycone (II) in $CDCl_3$ show no protons above δ 7 ppm with the exception of a singlet at δ 4.12 ppm for the methoxy protons (A) and a singlet at δ 2.77 ppm for the 9-ketomethyl protons (B). It should be noted that daunorubicinone shows two complicated multiplets centered at δ 2.2 ppm and δ 3.0 ppm. Moreover, high resolution mass spectroscopy of this material showed a base peak at 362.0804 which is well within acceptable tolerance for the calculated molecular mass of 362.0789 ($C_{21}H_{14}O_6$).

Biological Activity

Preliminary screening results obtained by the Drug Research and Development Branch of the National Cancer Institute on selected anthracyclines in the treatment of

mouse P-388 lymphocytic leukemia are shown in Tables 16 and 17. T/C is the mean survival of treated/control animals in percent. The values of T/C for daunorubicin in 5 separate determinations varies by $\pm$ 10%. It is noted that the toxic dose (i.e., the daily dose at which the onset of drug toxicity is observed, i.e., T/C = 100) and the optimal dose of the newly synthesized analogs are considerably higher than that for daunorubicin (18) and adriamycin (17).

Discussion

The anthracyclines, daunorubicin and adriamycin, undergo rapid in vivo hydrolysis of the glycosidic bond, leading to highly insoluble aglycones (see introduction section). Herman and coworkers have suggested that the observed cardiotoxicity of the anthracyclines is due to the accumulation of the insoluble aglycone in the heart tissues.[107,111] The synthesis of the derivatives 19-27 was undertaken in order to overcome the latter problem. For example, if in vivo hydrolysis of the glycosidic bond in D_9-MoMeA (20) occurs, the resulting aglycone, A_9-MoMeA (28), would still retain aqueous solubility and DNA binding properties. The results of the in vitro studies indeed show that the water-soluble aglycones, A_9-MoMeA (28) and A_9-BuA (29), are bound strongly to DNA. However, it is noted that the inhibitory activity of 28 and 29 on the DNA-dependent RNA polymerase is diminished and the dissociation rate of the DNA complex is substantially enhanced as a result of excision of the amino sugar moiety (Table 11). It appears that the role of

Table 16. Biological Activity of the Anthracyclines against Mouse Lymphocytic Leukemia.

Compound[a]	Toxic Dose mg/kg	Optimal Dose mg/kg	T/C
Adriamycin (17)	3.0	1.0	204
Daunorubicin (18)	2.0	0.83 - 1.0	175
D_9-MoMeA (20)	16.0	8.0	160
D_9-BuA (22)	10.0	5.0	190
D_9-PolA (24)	32.0	16.0	201

[a]All tests were carried out by A. D. Little Laboratories (NCI contractor) using CDF_1 male mice bearing i. p. implanted P-388 lymphocytic leukemia (10^6 cells). Aqueous drug solutions were administered daily (days 1 - 9) via the intraperitoneal route.

Table 17. Biological Activity of the Anthracyclines against Mouse Lymphocytic Leukemia.

Compound[a]	Toxic Dose mg/kg	Optimal Dose mg/kg	T/C
Daunorubicin (18)	32	16.0	135
D_9-GlyLeuA (26)	128	64	131
A_9-BuA (29)	>128	128	111

[a]All tests were carried out by A. D. Little Laboratories (NCI contractor) using CDF_1 female mice bearing i. p. implanted P-388 lymphocytic leukemia (10^6 cells). Aqueous drug solutions were administered daily (days 1 - 9) via the intraperitoneal route.

the amino sugar moiety of the anthracyclines is important in conferring a specific electrostatic and hydrogen bonding interaction in the DNA complex as has previously been postulated by Pigram and coworkers.[102]

The data obtained via in vitro studies indicate that the peptide daunorubicin derivatives (25-27) exhibit a lower binding affinity to DNA than daunorubicin. It was hoped that hydrogen bonding between the peptide and the nucleic acid would increase the binding affinity. The fact that such is not the case indicates either the hydrogen bond acceptors and donors are not in the proper geometry, or unfavorable steric effect of the peptide side chain.

On the other hand, in vitro data for the simple alkylated amino derivatives of daunorubicin (19-24) indicate that the binding properties to DNA are similar to those of highly active antitumor agents, daunorubicin and adriamycin. For example, (i) high binding affinity to DNA (Table 9), (ii) high template inhibitory activity (Table 11), and (ii) low rates of dissociation of the DNA complexes (Table 12) are observed. However, the results of the biological activity of those compounds are somewhat disappointing. It is noted, for example, that the observed T/C values in the treatment of P-388 mouse leukemia are found to be lower than that for adriamycin in all cases and only slightly higher than that for daunorubicin in the cases of D_9-BuA (22) and D_9-PolA (24). Moreover, it is noted that the optimal dose for all of the newly synthesized anthracyclines which

have been tested is considerably higher than that of 17 and 18. The observed lower in vivo activities of 20, 22, 24, and 26 are probably due to (i) low lipid solubility (especially for compound 20 where the observed distribution coefficient, D, is 0.3) and/or (ii) the observed higher hydrolytic susceptibility of the glycosidic bond as compared to daunorubicin, 18.

The results of the temperature dependent kinetic studies on glycosidic hydrolysis (Table 13) indicate the following order of increasing sensitivity: daunorubicin (18) < D_9-GlyA (25) < D_9-GlyLeuA (26) < adriamycin (17) < D_9-MoMeA (20) < D_9-BuA (22) ≈ D_9-PolA (24). It is noted that the rate of hydrolysis is lower at 60^oC than at 50^oC at pH 9.7. Since the pK_a of the anthracylcines is approximately 9.7 at 50^oC and decreases with increasing temperature, these results are consistent with the C-6 hydroxyl group playing a catalytic role in the hydrolysis.

There are two general routes for the hydrolysis of the glycosidic bond of the anthracyclines, i.e., either A or B cleavage (Figure 32). Glycosidic linkage is known to undergo acid catalyzed hydrolysis at the B position, however such bonds are stable under basic conditions.[139] It is, therefore, unlikely that a similar mechanism is involved for the anthracyclines since the rate is observed to decrease at lower pH (i.e., in the range of 5.7-9.7 (Table 15). Figure 33 shows one possible working mechanism involving an Sn1 A-cleavage and the intermediacy of a 2^o benzylic

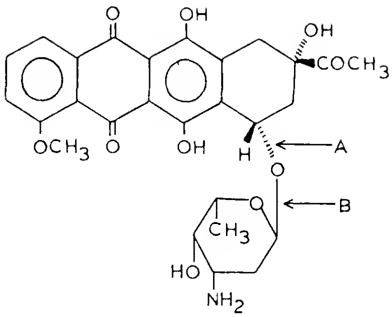

Figure 32. Positions of A and B Cleavage of the Anthracycline Glycosidic Bond

carbonium ion. The C-6 hydroxyl group is tentatively assigned the role of a general acid catalyst. Further studies are in progress to shed further insight on the mechanism of the hydrolytic reaction.[140]

There appears to be a high degree of correlation between the observed hypochromicity, H (Table 7), and the apparent binding constant, K_a (Table 9), of the anthracyclines with DNA. This finding is consistent with an intercalation mode of binding of the aglycone ring between base pairs of DNA and such aromatic stacking interaction leads to intensity interchange between neighboring chromophores.[45-47] Since the intensity interchange parameter is strongly dependent on distance (as well as orientation) between the interacting transition moments, comparative hypochromism

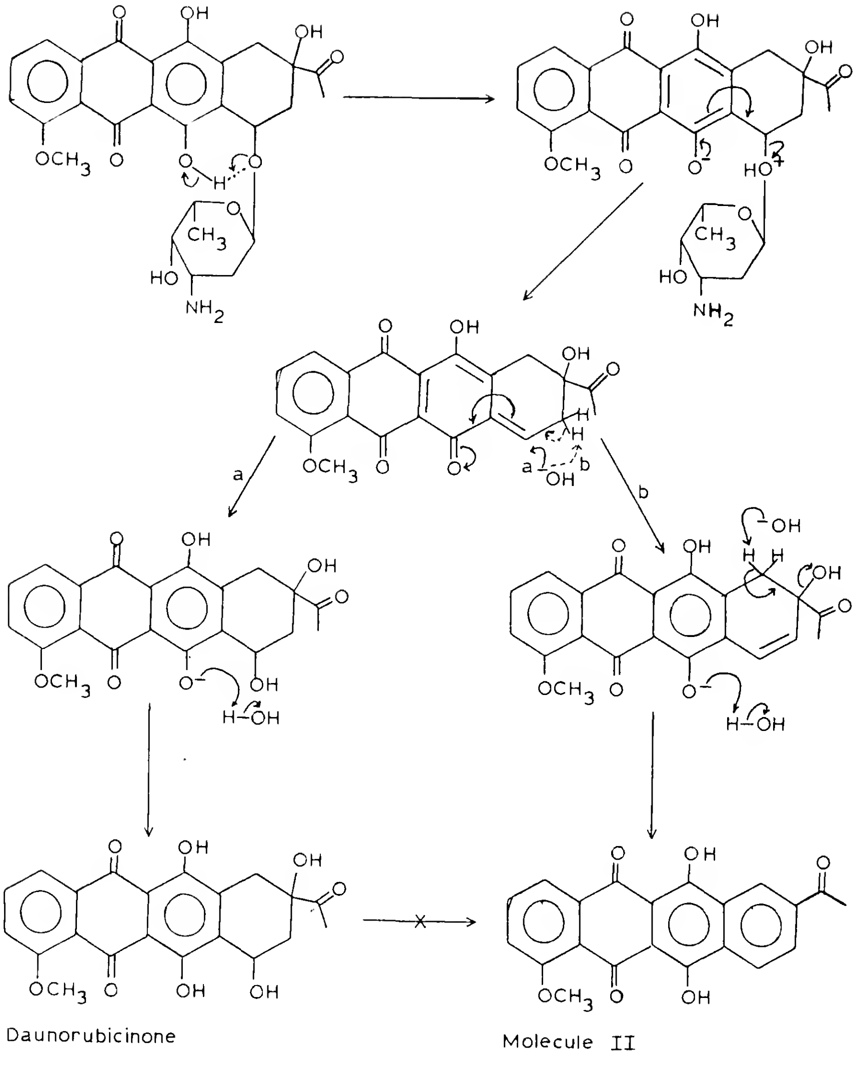

Figure 33. Possible Mechanism for the Glycosidic Hydrolysis of the Anthracycline

data may reveal the extent of formation of "intimate complexes" of the drug with DNA base pairs. Thus, hypochromicty is a quick, simple method of determining comparative binding affinities of newly synthesized analogs with DNA.

Muller and Crothers have shown (through extensive studies of the interaction specificities of actinomycin D and its derivative with DNA) that the extent of in vitro inhibition of template activity is inversely proportional to the rate of dissociation of drug-nucleic acid complexes.[54] A similar finding is observed for the anthracyclines studied in this thesis, that is, the observed dissociation rate constant of the DNA-drug complex (Table 12) is inversely proportional to the extent of polymerase activity (Table 11). Extension of the results of the two techniques to in vivo systems is not readily possible due to the problems associated with pharmacodynamics (such as glycosidic hydrolysis), cellular permeability, and biological half-life.

CHAPTER IV
EXPERIMENTAL

Analyses were performed by Atlantic Microlab, Inc., Atlanta, Georgia. ^{1}H nmr spectra were recorded on either a Varian A-60A or a Varian XL-100-15 spectrometer at $34^{o}C$. The Varian XL-100-15 employs a Nicolet Technology Corp. Fourier transform accessory. Chemical shifts determined in deuterium oxide were measured relative to the internal standard 2,2,3,3-d_4-3-trimethylsilylpropionate (TSP), whereas chemical shifts determined in organic solvents were measured relative to the internal standard trimethylsilane (TMS). Circular dichroism measurements were recorded on a Jasco J-20 spectropolarimeter and molar elliplicities, [θ], were measured relative to the elliplicity of a standard D-camphor sulfonic acid solution (Durrum Instrument Co.). Ultraviolet and visible absorption measurements were recorded on either a Cary 15 or Gilford 240 spectrophotometer. Quantitative assay for peptide concentration was made using fluorescamine according to previously described procedures.[69] Quantitative determination of daunoseamine concentration was made with fluoropa reagent in the same manner.[135,136] Both assays used a Earrand ratio fluorimeter with primary and secondary filters designed for excitation at 390 nm and emission at 490 nm. Melting points were taken on either

a Mel-Temp or a Thomas Hoover apparatus and the measurements are uncorrected. Viscosity measurements were performed with a low shear Zimm viscometer (Beckman Instrument Co.). Stop-flow kinetics were measured with a Durrum-Gibson apparatus (Durrum Instrument Co.) thermostated with a Lauda K-2/R constant temperature circulator. Radioactivity was counted on a LS-133 liquid scintillation counter (Beckman Instrument Co.).

All amino acid derivatives used in the synthesis of the peptides were purchased from Sigma Chemical Corp. and used without further purification. The anthracyclines, daunorubicin and adriamycin, were generously supplied by Dr. Georges Jolles (Rhone-Paulenc, France) and Dr. H. Wood (Drug Development Branch, NCI). Salmon sperm DNA was purchased from Worthington Biochemical Corp. All solutions containing DNA, peptide systems, and anthracycline drugs were prepared in buffers made with deionized water.

Synthesis

Peptides 1-12 and A_9-MoMeA were synthesized, characterized, and graciously supplied by Drs. K. Sanford, L. Kapicak, P. D. Adawadkar, and W. D. Wilson.

Preparation of L-lysyl-L-phenylalanyl-L-alanine amide hydrochloride, 13

The peptide systems were synthesized by the general method of Anderson et al.[141] To a three necked flask containing 30 ml of freshly distilled tetrahydrofuran (THF), 3.0 mmol (1.24 g) of dicarbobenzoxy-(CBZ)-L-lysine (Sigma

Chem.) was added. The solution was protected against moisture by the use of a calcium chloride drying tube and a constant flow of nitrogen through the flask. The solution was cooled to -10^{o}C in an acetone/ice bath and 3.0 mmol of triethylamine added. To this solution 1.1 mmol of isobutylchloroformate (Aldrich Chem.) was added and allowed to stir for 10 minutes. A precooled (-10^{o}C) solution of L-phenylalanine ethyl ester hydrochloride (Sigma Chem.; 0.69 g; 3.0 mmol) in 5 ml THF, and 3.0 mmol of triethylamine was added followed by stirring of the reaction mixture at -10^{o}C for one hour. After this time the bath was removed and the solvent evaporated by a stream of nitrogen. The resulting solid was disolved in ethyl acetate which was then extracted three times with 1 M HCl, saturated sodium bicarbonate, and deionized water. The organic phase was dried over magnesium sulfate, filtered, and the solvent evaporated. The solid obtained was recrystallized from ethyl acetate/hexane to yield 1.29 g (2.4 mmol) of di-CBZ-L-lysyl-L-phenylalanine ethyl ester (79% yield).

The ester was hydrolyzed in 30 ml ethanol containing 4.8 ml 1 M NaOH for one hour at room temperature and the pH adjusted with 6 M HCl. Excess water was added and the di-CBZ-L-lysyl-L-phenylalanine extracted with ethyl acetate. The solvent was dried over magnesium sulfate, evaporated, and the resulting solid recrystallized from ethyl acetate/hexane to yield 1.07 g (2.1 mmol, 86% yield). ^{1}H nmr in $CDCl_3$ showed a broad 6 H multiplet at δ 1.3 ppm, a broad 3

H multiplet at δ 3.0 ppm, and 4 H singlet at δ 4.1 ppm, a broad 1 H singlet at δ 6.1 ppm, a 5 H singlet at δ 7.1 ppm, and a 10 H singlet at δ 7.3 ppm.

The protected di-CBZ-tripeptide amide, di-CBZ-L-lysyl-L-phenylalanyl-L-alanine amide, was synthesized from 1.0 mmol (0.518 g) of di-CBZ-L-lysyl-L-phenylalanine, 2.2 mmol triethylamine (total), 1.1 mmol isobutylchloroformate, and 1.0 mmol (0.113 g) of L-alanine amide hydrochloride (Sigma Chem.). Workup and recrystallization from ethyl acetate yielded 0.98 mmol (0.564 g, 98% yield) of product. This solid was dissolved in 50 ml of methanol and 100 mg of 10% Pd/C and 10 drops of glacial acetic acid added. The mixture was hydrogenated in a Paar shaker under 2 atmospheres of hydrogen for 4 hours. The catalyst was removed by filtration, the solvent evaporated, and the residue dissolved in deionized water. This solution was passed through a column containing an ion exchange resin (Amberlite CG-400, bromide form). The effluent was collected and lypholized to give after recrystallization from ethanol/diethyl ether 0.58 mmol (0.28 g, 58% yield) of L-lysyl-L-phenylalanyl-L-alanine amide dihydrobromide, (m.p. 155-159°C). ^{1}H nmr in D_2O showed a doublet at δ 1.3 ppm and a broad multiplet at δ 1.5 ppm accounting for 9 H, a broad 5 H multiplet at δ 3.0 ppm, a 2 H multiplet at δ 4.1 ppm, and a 5 H singlet at δ 7.3 ppm. Anal. calculated for $C_{18}H_{31}Br_2O_3N_5 \cdot 1\ H_2O$: C, 39.79; H, 6.12. Found: C, 39.46; H, 5.90.

Preparation of L-lysyl-L-phenylalanyl-D-alanine amide dihydrobromide, 14

The tripeptide amide, A, was synthesized in the same manner as compound 1; however, D-alanine amide had to be prepared first. To a solution of CBZ-D-alanine (5.3 mmol; 1.12 g) in THF at -10^{o}C, 5.5 mmol of triethylamine and 6.5 mmol of isobutylchloroformate were added and ammonia gas bubbled through for 10 minutes. The solvent was evaporated, the solid dissolved in ethyl acetate and washed with 1 M HCl, saturated sodium bicarbonate, water, and the organic layer was dried over $MgSO_4$. The residual solid after evaporation of the organic solvent was recrystallized from ethyl acetate/hexane (2.6 mmol, 0.59 g, 49% yield). ^{1}H nmr in $CDCl_3$ showed a 3 H doublet at δ 1.4 ppm, a 1 H broad peak at δ 1.8 ppm, a 1 H quartet at δ 4.2 ppm, a 2 H singlet at δ 5.1 ppm, and a 5 H singlet at δ 7.3 ppm.

The protected alanine amide was then hydrogenated and passed through an ion exchange column (Amberlite CG-400, bromide form) giving after recrystalization from ethanol/diethyl ether, 2.3 mmol (0.358 g) of D-alanine amide hydrobromide (87% yield). ^{1}H nmr in D_2O showed a 3 H doublet at δ 1.3 ppm, and a 1 H quartet at δ 4.2 ppm.

The protected tripeptide amide, di-CBZ-L-lysyl-L-phenylalanyl-D-alanine amide, was prepared by reacting 1.0 mmol (0.518 g) of di-CBZ-L-lysyl-L-phenylalanine with 1.1 mmol of triethylamine and 1.1 mmol of isobutylchloroformate at -10^{o}C followed by the addition of 1.0 mmol (0.570 g) of D-alanine and 1.1 mmol of triethylamine. Workup and crystallization

from ethyl acetate/hexane yielded 0.99 mmol (0.57 g, 99% yield) of product. Hydrogenolysis of this solid in a Paar shaker followed by ion exchnage and recrystallization from ethanol/diethyl ether yielded 0.74 mmol (0.36 g, 74% yield) of L-lysyl-L-phenylalanyl-D-alanine amide dihydrobromide, 2 (m.p. 146-149^{o}C). ^{1}H nmr in D_2O showed a 3 H doublet at δ 1.0 ppm, a 6 H broad multiplet at δ 1.6 ppm, a 3 H multiplet at δ 3.0 ppm, a 2 H multiplet at δ 4.1 ppm, and a 5 H singlet δ 7.3 ppm. Anal. calculated for $C_{18}H_{31}Br_2O_3N_5 \cdot 1H_2O$: C. 39.79; H, 6.12. Found: C, 39.99; H, 6.24.

Preparation of L-lysyl-L-phenylalanyl-L-alanyl-L-valine amide dihydrobromide, 15

The protected dipeptide, CBZ-L-alanyl-L-valine methyl ester was first synthesized by reaction of CBZ-L-alanine (Sigma Chem.) (3.19 mmol, 0.67 g) with 3.2 mmol of triethylamine and 3.3 mmol of isobutylchloroformate at -10^{o}C followed by 3.0 mmol (0.503 g) of L-valine methyl ester (Sigma Chem.). Workup and recrystallization yielded 1.7 mmol (0.575 g) of product (57% yield). This was then hydrogenated in a Paar shaker and isolated as the acetate of L-alanyl-L-valine methyl ester (1.2 mmol, 0.316 g, 81% yield). ^{1}H nmr in $CDCl_3$ showed a 6 H doublet of doublets at δ 0.9 ppm, a 3 H doublet at δ 1.4 ppm, a 3 H singlet at δ 2.1 ppm, a 3 H singlet at δ 3.7 ppm, and a broad, 3 H singlet at δ 5.0 ppm.

At -10^{o}C, di-CBZ-L-lysyl-L-phenylalanine (1.0 mmol, 0.51 g) was reacted with 1.1 mmol of triethylamine and 1.1 mmol of isobutylchloroformate followed by 1.0 mmol (0.262 g) of L-alanyl-L-valine methyl ester acetate. The reaction

yielded after workup and recrystallization from ethyl acetate/diethyl ether, 0.684 mmol (0.48 g) of the protected tetrapeptide. Ammonolysis of the ester was accomplished in 30 ml of methanol, saturated with ammonia gas (at -10°C) in a sealed glass tube for 3 days at room temperature. The solvent was then evaporated and the solid residue recrystallized from ethanol/water to yield di-CBZ-L-lysyl-L-phenylalanyl-L-valine amide (0.486 mmol, 0.33 g, 71% yield). This was then hydrogenated in a Paar shaker and passed through an ion exchange column to give 0.289 mmol (0.165 g) of the tetrapeptide amide, 3 (m.p. 148-152°C, 59% yield). ^{1}H nmr in D_2O showed a broad 6 H doublet at δ 0.9 ppm, a 9 H broad multiplet at δ 1.5 ppm, a 5 H broad multiplet at δ 3.0 ppm, a 4 H multiplet at δ 3.9 ppm, and a 5 H singlet at δ 7.3 ppm. Anal. calculated for C H Br O N : C, 44.24; H, 6.45. Found: C, 44.27; H, 6.51.

Preparation of L-lysyl-L-phenylalanyl-D-alanyl-L-valine amide dihydrobromide, 16

This tetrapeptide was synthesized with the same sequence of reaction that was used for the preparation of 3. CBZ-D-alanine (3.19 mmol, 0.67 g) was coupled with L-valine methyl ester hydrochloride (3.19 mmol, 0.503 g) which after workup and recrystallization from ethyl acetate/hexane yielded 1.7 mmol (0.575 g) of the protected dipeptide. ^{1}H nmr in $CDCl_3$ showed a 6 H doublet of doublets at δ 0.9 ppm, a 3 H doublet at δ 1.4 ppm, a 1 H multiplet at δ 2.1 ppm, a 3 H singlet at δ 3.7 ppm, a 2 H multiplet at δ 4.4 ppm, and 2 H singlet at δ 5.1 ppm, a 1 H broad doublet at δ 5.7 ppm, a 1 H broad doublet at δ 6.9 ppm, and a 5 H singlet at δ 7.3 ppm.

The CBZ-D-analyl-L-valine methyl ester was then hydrogenated and isolated as D-alanyl-L-valine methyl ester acetate (1.25 mmol, 0.328 g, 84% yield). Ci-CBZ-L-lysyl-L-phenylalanine (1.0 mmol, 0.518 g) was then coupled to 1.0 mmol (0.262 g) of D-analyl-L-valine methyl ester acetate by the mixed anhydride method yielding 0.78 mmol (0.55 g) of the protected tetrapeptide after workup and recrystallization from ethyl acetate/hexane (78% yield). Ammonolysis of the ester was carried out in 30 ml of methanol saturated with ammonia (at $10^{o}C$) and placed in a sealed tube at room temperature for 3 days. The solvent was then evaporated and the solid recrystallized from ethanol/water to yield 0.71 mmol (0.48 g) of di-CBZ-L-lysyl-L-phenylalanyl-D-analyl-L-valine amide (90% yield). Hydrogenolysis was carried out followed by ion exchange to form the bromide, <u>4</u> (0.52 mmol, 0.31 g, 73% yield). ^{1}H nmr in D_2O showed a 9 H multiplet at δ 1.0 ppm, a 6 H broad multiplet at δ 1.5 ppm, a 3 H broad multiplet at δ 3.0 ppm, a 4 H multiplet at δ 4.0 ppm, and a 5 H singlet at δ 7.3 ppm, (m.p. 159-163^{o}C). <u>Anal</u>. calculated for $C_{24}H_{42}Br_2O_4N_6 \cdot 1H_2O$: C, 43.00; H, 6.59. Found: C, 43.11; H, 6.60.

<u>Preparation of D_9-NH_2, 19</u>

To 10 ml of methanol, 28 mg (0.05 mmol) of daunorubicin·HCl (<u>18</u>) was added along with 100 mg (1.9 mmol) of ammonium chloride and 0.2 ml of 0.25 <u>M</u> NaOH in methanol. The resulting solution was refluxed for 30 min., cooled to room temperature and 1 ml of freshly prepared 0.1 <u>M</u> $NaCNBH_3$ (Aldrich

Chem.) in methanol was added. The reaction was allowed to continue overnight and then was quenched with 50 ml of $CHCl_3$ and 10 ml of pH 10.4 aqueous borate buffer. The aqueous layer was extracted 3 times with $CHCl_3$, and the organic phase was subsequently washed with water, separated, dried over Na_2SO_4, and evaporated under a stream of nitrogen. The resulting solid was dissolved in 10 ml of methanol. The solution was cooled in an ice bath, 0.1 ml of 1 M HCl was added, and the solvent evaporated under a nitrogen stream. The resulting solid was recrystallized twice from methanol/ethyl acetate to yield 12 mg (0.02 mmol) of D_9-NH_2, 19 (40%, m.p. 186-188°C). ^1H nmr in $CDCl_3$ showed three complex multiplets at δ 1.30, 1.73, and 3.08 ppm, a singlet at δ 4.09 ppm, two broad singlets at δ 2.57 and 5.51 ppm, two doublets at δ 7.38 and 8.06 ppm, and a triplet at δ 7.78 ppm. Anal. calculated for $C_{27}H_{34}Cl_2O_9N_2$: C, 53.92; H, 5.70. Found: C, 54.16; H, 5.79.

Preparation of D_9-MoMeA, 20

Daunorubicin·HCl (466 mg, 0.825 mmol) was dissolved in 20 ml of methanol containing 1.35 g (20 mmol) of methylamine hydrochloride, 8 ml of 0.25 M NaOH, and 1.6 ml of freshly prepared 1 M $NaCNBH_3$ in methanol. The reaction was allowed to continue overnight and then was quenched with 50 ml of $CHCl_3$ and 50 ml of pH 10.4 aqueous borate buffer. The aqueous layer was extracted 3 times with $CHCl_3$, and the organic phase was subsequently washed with water, separated, dried over Na_2SO_4, and evaporated under a stream of nitrogen.

The resulting solid was dissolved in 30 ml of methanol. The solution was cooled in an ice bath, adjusted to pH 5 with 1 M HCl and the solvent evaporated under a nitrogen stream. The resulting solid was recrystallized twice from methanol/ethyl acetate to yield 253 mg (0.41 mmol) of D_9-MoMeA (50%, m.p. 179-182^oC). ^1H nmr in $CDCl_3$ showed a triplet at δ 0.98 ppm, two complex multiplets at δ 1.26 and 2.57 ppm, a singlet at δ 4.06 ppm, two broad singlets at δ 5.28 and 5.52 ppm, two doublets at δ 7.37 and 8.07 ppm, and a triplet at δ 7.78 ppm. Anal. calculated for $C_{28}H_{36}Cl_2O_9N_2 \cdot 2H_2O$: C, 51.62; H, 6.18. Found: C, 51.39; H, 5.59.

Preparation of D_9-PrA, 21

Daunorubicin·HCl (188 mg; 0.33 mmol) was dissolved in 10 ml of methanol containing 200 mg (3.3 mmol) of propylamine. The resulting solution was refluxed for 30 min., cooled to room temperature and 0.67 ml of freshly prepared 1 M $NaCNBH_3$ in methanol was added. The reaction was allowed to continue overnight and then was quenched with 50 ml of $CHCl_3$ and 30 ml of water. The aqueous layer was extracted 3 times with $CHCl_3$, and the organic phase was subsequently washed with water, separated, dried over Na_2SO_4, and evaporated under a stream of nitrogen. The resulting solid was dissolved in 20 ml of methanol, cooled in an ice bath, and 0.67 ml of 1 M HCl was added, and the solvent was evaporated under a stream of nitrogen. The solid was recrystallized twice from methanol/ethyl acetate to yield 70 mg (0.11 mmol) of D_9-PrA, 21 (33%, m.p. 176-180^oC). ^1H nmr in $CDCl_3$ shows a triplet

at 0.94 ppm, two complex multiplets at δ 1.26 and 2.58 ppm, a singlet at δ 4.06 ppm, two broad singlets at δ 5.27 and 5.51 ppm, two doublets at δ 7.38 and 8.08 ppm, and a triplet at δ 7.77 ppm. Anal. calculated for $C_{30}H_{40}Cl_2O_9N_2 \cdot 3H_2O$: C, 51.65; H, 6.64. Found: C, 51.64; H, 6.52.

Preparation of D_9-BuA, 22

To 15 ml of methanol, 0.275 mg (2.5 mmol) of butylamine hydrochloride, 56 mg (0.1 mmol) of daunorubicin·HCl, and 2 ml of 0.25 M NaOH were added. The solution was stirred at room temperature for 2 hours and 2 ml of freshly prepared 0.1 M $NaCNBH_3$ in methanol was added. The reaction was allowed to continue for 24 hours, and then was quenched with 20 ml of $CHCl_3$ and 20 ml of pH 10.4 aqueous borate buffer. The aqueous layer was extracted 3 times with $CHCl_3$, and the organic phase was subsequently washed with water, separated, dried over Na_2SO_4, and evaporated under a nitrogen stream. The resulting solid was dissolved in 10 ml of methanol, cooled in an ice bath, 0.2 ml of 1 M HCl was added, and the solvent was evaporated under a stream of nitrogen. The resulting solid was recrystallized twice with methanol/ethyl acetate to yield 45 mg (0.067 mmol) of D_9-BuA (67%, m.p. 160-162°C). ^1H nmr in $CDCl_3$ showed a triplet at δ 0.94 ppm, two complex multiplets at δ 1.29 and 2.52 ppm, a singlet at δ 4.08 ppm, two broad multiplets at δ 5.26 and 5.50 ppm, two doublets at δ 7.39 and 8.07 ppm, and a triplet at δ 7.76 ppm. Anal. calculated for $C_{31}H_{42}Cl_2O_9N_2 \cdot H_2O$: C, 55.11; H, 6.56. Found: C, 55.44; H, 6.31.

Preparation of D_9-EolA, 23

Daunorubicin·HCl (188 mg, 0.33 mmol) was dissolved in 10 ml of methanol containing 200 mg (3.3 mmol) of ethanolamine. The mixture was refluxed for 30 min., cooled to room temperature, and 0.67 ml of freshly prepared 1 M $NaCNBH_3$ in methanol was added. The reaction was allowed to continue overnight and then was quenched with 50 ml of $CHCl_3$ and 30 ml of water. The aqueous layer was extracted 3 times with $CHCl_3$ and the organic phase was subsequently washed with water, separated, dried over Na_2SO_4, and evaporated under a stream of nitrogen. The resulting solid was dissolved in 25 ml of methanol, cooled in an ice bath, 0.67 ml of 1 M HCl was added, and the solvent was evaporated under a nitrogen stream. The resulting solid was recrystallized twice from methanol/ethyl acetate to yield 134 mg (0.21 mmol) of D_9-EolA (63%, m.p. 177-179^oC). ^1H nmr in $CDCl_3$ shows two complex multiplets at δ 1.28 and 2.55 ppm, a singlet at δ 4.06 ppm, two broad singlets at δ 5.27 and 5.51 ppm, two doublets at δ 7.38 and 8.08 ppm, and a triplet at δ 7.77 ppm. Anal. calculated for $C_{29}H_{38}Cl_2O_{10}N_2$: C, 53.96; H, 5.93. Found: C, 53.75; H, 5.95.

Preparation of D_9-PolA, 24

To 20 ml of methanol, 2.4 g (22 mmol) of 3-amino-i-propanol hydrochloride was added, the pH was adjusted to 8.0 with 0.25 M NaOH, 451 mg (0.8 mmol) of daunorubicin·HCl and 1.6 ml of freshly prepared 1 M $NaCNBH_3$ in methanol was added. The reaction was allowed to continue for 24 hours, and then

quenched with 50 ml of $CHCl_3$ and 20 ml of pH 10.4 aqueous borate buffer. The aqueous phase was extracted 3 times with $CHCl_3$ and the organic phase was subsequently washed with water, separated, dried over Na_2SO_4, and evaporated under a stream of nitrogen. The resulting solid was dissolved in 50 ml of methanol, cooled in an ice bath, 1.6 ml of 1 M HCl was added, and the solvent evaporated under a nitrogen stream. The resulting solid was recrystallized twice from methanol/ethyl acetate to yield 201 mg (0.3 mmol) of D_9-PolA (38%, m.p. 174-176^{o}C). ^{1}H nmr in $CDCl_3$ showed three complex multiplets at δ 1.29, 1.74, and 2.59 ppm, a singlet at δ 4.10 ppm, two broad singlets at δ 5.29 and 5.52 ppm, two doublets at δ 7.37 and 8.05 ppm, and a triplet at δ 7.76 ppm. Anal. calculated for $C_{30}H_{40}Cl_2O_{10}N_2$: C, 54.61; H, 5.96. Found: C, 54.71; H, 5.97.

Preparation of D_9-GlyA, 25

To 10 ml of methanol, 56 mg (0.1 mmol) of daunorubicin·HCl was added along with 220 mg (2 mmol) of glycinamide and 0.8 ml of 0.25 M NaOH in methanol. Sufficient amount of H_2O was added for dissolution of the glycinamide together with 2 ml of freshly prepared 0.1 M $NaCNBH_3$. The reaction was allowed to continue overnight and then quenched with 50 ml of $CHCl_3$ and 20 ml of pH 10.4 aqueous borate buffer. The aqueous layer was extracted 3 times with $CHCl_3$ and the organic phase was subsequently washed with water, separated, dried over Na_2SO_4, and evaporated under a stream of nitrogen. The resulting solid was dissolved in 10 ml of methanol. The

solution was cooled in an ice bath, 0.2 ml of 1 M HCl was added, and the solvent evaporated under a nitrogen stream. The resulting solid was recrystallized twice with methanol/ethyl acetate to yield 15 mg (0.023 mmol) of D_9-GlyA (23%, m.p. 179-183^oC). ^1H nmr in $CDCl_3$ showed four complex multiplets at δ 1.31, 1.76, 2.61, and 3.42 ppm, a singlet at δ 4.07 ppm, two broad singlets at δ 5.26 and 5.53 ppm, two doublets at δ 7.38 and 8.08 ppm, and a triplet at δ 7.78 ppm. Anal. calculated for $C_{29}H_{37}Cl_2O_{10}N_3$: C, 52.89; H, 5.66. Found: C, 52.64; H, 5.64.

Preparation of D_9-Gly-L-LeuA, 26

To 10 ml of methanol, 113 mg (0.2 mmol) of daunorubicin·HCl was added along with 0.9 g (4 mmol) of gly-L-leuA hydrochloride and 1.6 ml of 0.25 M NaOH in methanol. Freshly prepared 0.1 M $NaCNBH_3$ (4 ml) was added to the solution. The reaction was allowed to continue overnight and then quenched with 50 ml of $CHCl_3$ and 20 ml of pH 10.4 aqueous borate buffer. The aqueous layer was extracted 3 times with $CHCl_3$ and the organic phase was subsequently washed with water, separated, dried over Na_2SO_4, and evaporated under a stream of nitrogen. The resulting solid was dissolved in 15 ml of methanol. The solution was cooled in an ice bath, 0.4 ml of 1 M HCl was added, and the solvent was evaporated under a nitrogen stream. The resulting solid was recrystallized twice with methanol/ethyl acetate to yield 52 mg (0.066 mmol) of D_9-Gly-L-LeuA, 25 (33%, m.p. 166-170^oC). ^1H nmr in $CDCl_3$ showed five multiplets at δ 0.95, 1.28, 1.69, 2.58,

and 3.44 ppm, a singlet at δ 4.09 ppm, two broad singlets at δ 5.27 and 5.51 ppm, two doublets at δ 7.38 and 8.06 ppm, and a triplet at δ 7.78 ppm. Anal. calculated for $C_{35}H_{48}$-$Cl_2O_{11}N_4 \cdot H_2O$: C, 53.24; H, 6.38. Found: C, 53.42; H, 6.11.

Preparation of D_9-Gly-L-PheA, 27

To 10 ml of methanol, 113 mg (0.2 mmol) of daunorubicin·HCl was added along with 1.1 g (4 mmol) of gly-L-pheA·HCl and 1.6 ml of 0.25 M NaOH in methanol. Freshly prepared 0.1 M $NaCNBH_3$ (4 ml) was added to the solution. The reaction was allowed to continue overnight and then quenched with 50 ml of $CHCl_3$ and 20 ml of pH 10.4 aqueous borate buffer. The aqueous layer was extracted 3 times with $CHCl_3$ and the organic phase was subsequently washed with water, separated, dried over Na_2SO_4, and evaporated under a nitrogen stream. The resulting solid was dissolved in 15 ml of methanol. The solution was cooled in an ice bath, 0.4 ml of 1 M HCl was added, and the solvent evaporated under a nitrogen stream. The resulting solid was recrystallized twice from methanol/ethyl acetate to yield 34 mg (0.041 mmol) of D_9-Gly-L-PheA, 27 (21%, m.p. 166-170°C). ^1H nmr in $CDCl_3$ showed five multiplets at δ 0.88, 1.30, 1.66, 2.47, and 3.28 ppm, two singlets at δ 7.39 and 8.09 ppm, and a triplet at δ 7.80 ppm. Anal. calculated for $C_{38}H_{46}Cl_2O_{11}N_4 \cdot H_2O$: C, 55.41; H, 5.87. Found: C, 55.16; H, 5.62.

Preparation of A_9-BuA, 29

D_9-BuA, 22 (20 mg, 0.03 mmol) was dissolved in 10 ml

of 1 M HCl and warmed on a steam bath for 15 min. The solution was adjusted to pH 8 with 1 M NaOH and the product was extracted with $CHCl_3$. The organic solvent was dried over Na_2SO_4 and removed on a rotary evaporator. The solid was dissolved in methanol, 1 ml of 1 M HCl added, and the solvent evaporated. The resulting solid was recrystallized twice from ethanol/diethylether to yield 10 mg (0.02 mmol) of A_9-BuA, 29 (68%, m.p. 177-179°C). ^1H nmr in $CDCl_3$ showed a triplet at δ 0.94 ppm, two multiplets at δ 1.24 and 2.44 ppm, a singlet at δ 4.08 ppm, broad singlets at δ 7.36 and 8.06 ppm, and a triplet at δ 7.76 ppm. Anal. calculated for $C_{25}H_{30}Cl\ O_7N$: C, 61.04; H, 6.15. Found: C, 60.78; H, 6.09.

Preparation of the Totally Aromatic Aglycone, II

Daunorubicin HCl, 18 (4.5 mg) was dissolved in 10 ml of methanol and the volume of the solution brought up to 25 ml with 2 mM phosphate buffer (200 mM Na^+, pH 7.5). In a second flask, 3.2 mg of daunorubicinone was dissolved in the same manner. Both solutions were incubated at 70°C for 14 hrs and extracted with $CHCl_3$. Silica gel chromatrography using 4% methanol in $CHCl_3$ showed that the daunorubicin had been hydrolyzed to a mixture of the aromatic aglycone, II, and daunorubicinone in a ratio of approximately 1:1. However the daunorubicinone was found to be stable under these conditions.

The aromatic aglycone, II, was purified by thick layer silica gel chromatography and was eluted with $CHCl_3$. The desired product was extracted from the chromatography support with a mixture of 5 ml of 1 M HCl and 50 ml of $CHCl_3$. The organic layer was dried with Na_2SO_4, filtered, and evaporated.

^1H nmr of the product showed four singlets at δ 2.77, δ 4.12, δ 15.20, and δ 15.64 ppm, and four multiplets at δ 7.41, δ 7.64, δ 7.81, and δ 9.05 ppm. Mass Spec calculated for $C_{21}H_{14}O_6$: 362.0789. Found: 362.0804 (100%).

Analytical Methods

^1H nmr Experiments

The nucleic acid used in the ^1H nmr studies was sonicated salmon sperm DNA prepared and supplied by Dr. P. D. Adawadkar. A stock solution of the latter was prepared by dissolving 72.4 mg of the DNA in 2.41 ml of D_2O containing 0.2% TSP (internal standard) to give a solution that was 72 mM phosphate/liter (3.3 mM Na^+, 1 mM phosphate buffer pD 7.3) of each peptide (0.1 M) were made in D_2O (0.2% TSP) and aliquouts of the latter were added to 5 mm nmr tubes containing 0.5 ml of the DNA stock solution. The concentration of the peptides was varied from 2 to 70 mM.

^1H nmr spectra of the peptides and the DNA-peptide com-

plexes (at different base pair to peptide ratios) were taken on a Varian XL-100-15 spectrometer at $34^{o}C$. The spin-lattice relaxation times, T_1, were measured by the inversion recovery method with a Nicolet Technology Corp. FT accessory.[142] Pulse widths of 64 (180^{o}) and 32 sec. (90^{o}) were used, and 10 scans were accumulated for each delay time, t. Twenty seconds was taken as the infinite delay time and 16 K transform was used. A typical series of partially relaxed Fourier transorm ^{1}H nmr spectra at various delay times, t, are shown in Figure 34. The T_1 value for the observed protons is the time, t, when $I_{\infty} - I_t$ (where I_{∞} and I_t are the peak intensities at delay times of infinity and t, respectively) has fallen to $(I_{\infty}-I_o)/e$, where I_o is the peak intensity at t = 0. In order to achieve accurate I_o values, log $(I_{\infty}-I_t)$ versus t was plotted to obtain a straight line from which the T_1 value may be obtained.

Chemical shifts (in Hz) from the internal standard, TSP, are reported. It is found that the chemical shifts and T_1 values are reproducible to $\pm$ 0.2 Hz and $\pm$ 10%, respectively.

Viscometric Apparatus and Measurements

A Beckman rotating cyclinder viscometer was used as supplied except that the rotors allowing for different shear stresses were prepared in a manner similar to that of Zimm and Crothers.[143] The instrument was modified so that the timing of the rotation of the cyclinder is based on the reflection of light from a thin styrofoam strip of width slightly less than the internal diameter of the rotor and a

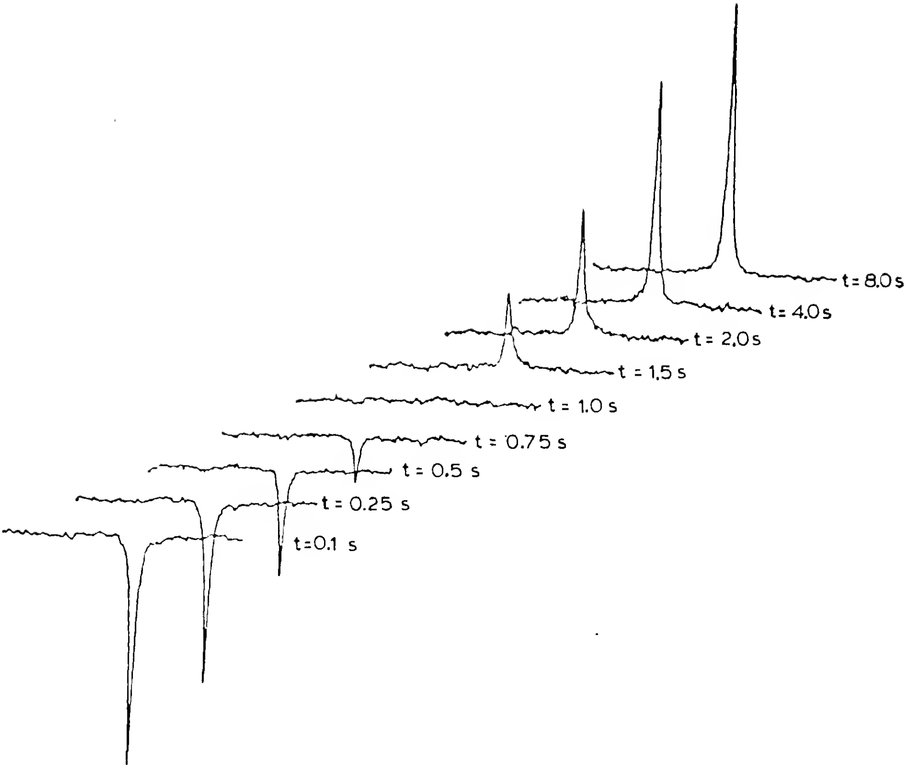

Figure 34. Typical Partially Relaxed Fourier Transform ^1H nmr Spectra

length approximately two-thirds of that of the rotor.[144] The styrofoam, with one side painted black, is placed in the rotor during viscosity measurements and differentially reflects light from the unpainted side into a phototransistor. The signal thus generated at the phototransistor is processed by the circuit illustrated in Figure 35.

When light falls on the phototransistor (Q_1; MRD 450) current flows resulting in a voltage drop at the collector. This creates the base current required to saturate the PNP transistor (Q_2; 2 N 5142) and causes the collector voltage of Q_2 to be approximately the voltage of the battery used (V_i; 6 V). This is then followed by a voltage divider so that the signal may be attenuated to a suitable level for recording. R_1, R_2, R_3, and R_4 are standard 1/2 watt, $\pm$ 5% resistors of values 5.1 K, 1.0 K, 62 K, and 10 K, respectively. The output voltage (V_o) is approximately 1 mV.

The electronic apparatus was constructed such that it could be enclosed in a small piece of 1/4" diameter heat-shrunk tubing. This was mounted on the stator support with the phototransistor against the glass of the stator as shown in Figure 36. A standard 15 watt light bulb was placed on a ring stand behind the phototransistor to provide enough light for the measurements.

A salmon sperm DNA solution (3×10^{-4} P/l) was pipeted into the viscometer which was thermostated at 37.5°C with a Haake constant-temperature circulator. The rotor was placed into the viscometer and the height of the rotor

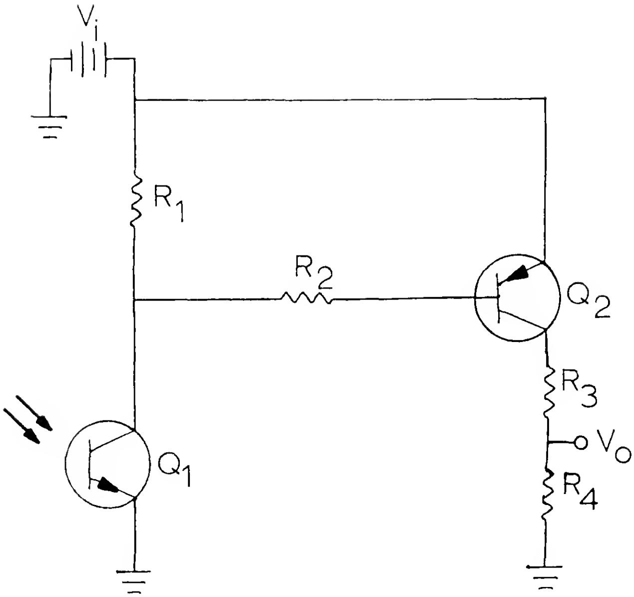

Figure 35. Schematic of the Photoelectric Timing Device. R_1, R_2, R_3, and R_4 are standard 1/2 watt, ± 5% resistors of values 5.1K, 1.0K, 62K, and 10Ω, respectively. Q_1 is a MRD 450 Phototransistor and Q_2 is a 2N5142 PNP transistor. The battery is a standard 6v lantern battery. The recorder is connected between V_o and the system ground.

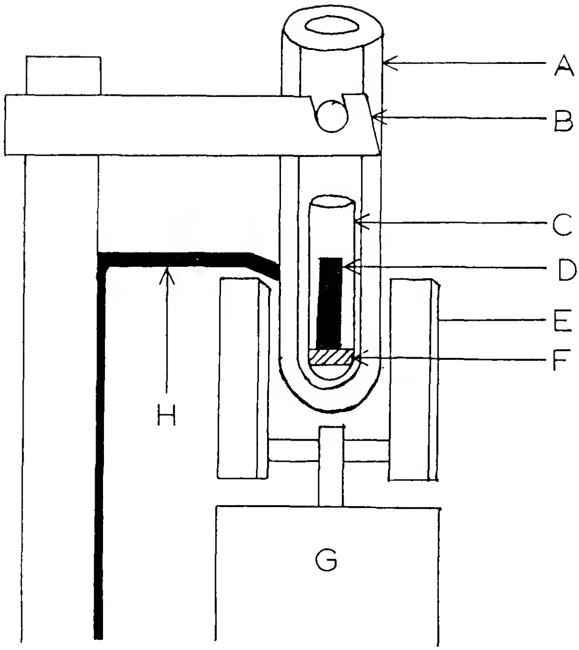

Figure 36. Diagram of the Viscometer with the Photoelectric Device in Place. Components in the figure are A, water jacketed stator; B, stator support; C, rotor; D, reflector; E, rotating magnet assembly; F, metal pellet; G. motor; H, photoelectric device as attached to the stator support.

adjusted with respect to an etched line on the stator. The total volume of the solution in the viscometer was 2.5 ml. A total of 100 rotations was counted with the photoelectric device and the length of chart paper measured. This was divided by the measured length required for 100 rotations in buffer to obtain the relative viscosity (η_{rel}) of the DNA solution. The calculation of the specific viscosity (η_{sp}) is straightforward (i.e., $\eta_{sp} = \eta_{rel}{}^{-1}$). To the DNA solution, aliquots of a 0.01 M peptide solution were added and after mixing the viscosity of the solution was determined.

Melting Temperature (Tm) Measurements

Tm measurements were run in 1 ml quartz cuvettes thermostated with a Haake constant-temperature circulator equipped with a constant speed motor to provide a heating rate of 0.71°C/min. A Gilford 240 spectrophotometer equipped with automatic recording accessories was used and the temperature of the cell compartment was measured directly with an iron-constantan thermocouple connected to a chart recorder which had been standardized at 0° and 100°C.

The experiment consisted of 0.8 ml of a 6.75 x 10^{-5} M salmon sperm DNA P/l in 10 mM MES buffer (pH 6.2) and 10 or 20 μl of a 0.01 M solution of peptide. The volume of the solution was adjusted to 1 ml with 10 mM MES buffer (pH 6.2). The solutions were placed in the thermostated compartment of the spectrophotometer with a buffer blank and allowed to equilibrate at 45°C for 10 minutes. Initial absorption was

recorded and the temperature programmer was initiated. The temperature and absorption were recorded continuously throughout the procedure.

Circular Dichroism Measurements

CD spectra of salmon sperm DNA and peptide solutions were taken in a 1 cm cell at DNA and peptide concentration of 2.4×10^{-4} M P/1 and 2.0×10^{-4} M, respectively, in 10 mM MES buffer (pH 6.2). Spectra were recorded between 220 nm and 320 nm using a Jasco J-20 spectropolarimeter at ambient temperature. CD spectra of the anthracycline in the presence and absence of salmon sperm DNA were recorded between 300 nm and 600 nm. A 10 cm cell was filled with a 2×10^{-6} M solution of the anthracycline in 2 mM PIPES buffer (21 mM Na^+, pH 7.8) and titrated with a 6×10^{-3} M DNA P/1 solution containing 2×10^{-6} M of the anthracycline until saturation was obtained.

Equilibrium Dialysis of Peptides

Equilibrium dialysis studies of the binding of the peptides to salmon sperm DNA was carried out using Visking dialysis tubing (26/100 ft. NOJAX castings) which was cut into 20 cm strips. The membranes were cleaned by boiling in 50% aqueous ethanol containing 5×10^{-3} M EDTA and 5×10^{-2} M $NaHCO_3$ for 1 hour and repeated 3 times. The membranes were then boiled in deionized H_2O for 5 hours and this was repeated 6 times. The clean membranes were stored in deionized H_2O containing 2% $CHCl_3$.

The dialysis experiments were conducted in a pair of

plexiglass blocks with 10 shallow cylindrical depressions cut into each (3 x 0.25 nm). A clear membrane was placed between the cells to form 2 chambers. Each half of the plexiglass block, prior to placement of the membrane, was lightly coated with silicone grease to prevent leakage. The blocks were fastened together with 12 screws and 4 C-clamps. To one side of the membrane 0.2 ml of 3.5×10^{-4} M of salmon sperm DNA P/1 in 10 mM MES buffer (pH 6.2; 5 nM Na^+) was added. To the other side of the membrane 0.2 ml of a peptide solution (either 2.5×10^{-4} or 5×10^{-5} M) in the same buffer was added. The top of the cells was sealed with a strip of lightly greased parafilm. Equilibrium was allowed to take place for 48 hrs. at 4°C. Blank determinations showed that the absorption at 260 nm was never greater than 0.030 across the membrane from the DNA solution. The concentration of peptide on both sides of the membrane was determined with the fluorescamine reagent as described by Gabbay et al.[69]

Absorption Studies

Absorption spectra (320-600 nm) of the anthracycline (in the presence and absence of excess salmon sperm DNA) were recorded on a Cary 15 spectrophotometer using a thermostated cell compartment at 25°C in a 10 cm cell. A 7×10^{-6} M solution of the drug in 2 nM PIPES buffer (21 mM Na^+, pH 7.8) was added to the cell and the spectra taken. This was then titrated with a 6×10^{-3} M salmon sperm DNA P/1 solution which also contained 7×10^{-6} M drug until saturation is obtained.

Hypochromicity, H, is defined by the equation:

$$H = 100(1-f_b/f_f),$$

where f_b and f_f are the oscillator strengths of the DNA bound and free drug. Quantum mechanical calculations show that the oscillator strength, f, is proportional to the area of the absorption spectrum by the formula,

$$f = 4.32 \times 10^{-9} \int \varepsilon \, d\bar{\nu}$$

where ε is the extinction coefficient of the molecule at wave number $\bar{\nu}$.[145] Thus, the spectra were replotted (absorption vs. wave number) and the area under the curve determined for the free and bound anthracycline, A_f and A_b, respectively, and the hypochromicity calculated as follows:

$$H = 100\ (1-A_b/A_f).$$

Binding Studies of the Anthracyclines

The apparent binding constant, K_a, and maximum number of binding sites per DNA phosphate, n_{max}, were determined by spectral titration in a 10 cm thermostated cell in a Cary 15 at 25°C. A 7×10^{-6} M solution of the anthracycline in 2 mM PIPES buffer (pH 7.8; either 51 or 201 mM Na^+) was added to the cell and the absorption at 480 nm determined. Aliquots of 6×10^{-3} M salmon sperm DNA P/l and 7×10^{-6} M drug in the same buffer were added. After each addition the absorption at 480 nm was recorded. This procedure was continued until no change in the absorption at 480 nm is observed. The parameters necessary to make a Scatchard plot, $\bar{n}$ and $\bar{n}/R_f$, are calculated by the following equations:

$$\bar{n} = \frac{D(A_o-A_n)}{(A_o-A_s)P_t}$$

$$\frac{\bar{n}}{R_f} = \frac{\bar{n}}{D-\bar{n}\ P_t}$$

where D is the total drug concentration, A_o, A_s, and A_n are the initial absorption, at saturation, and for a given alliquot of DNA solution added, respectively; n, and P_t is the total concentration of DNA added. The data were then plotted and least squares analysis performed. All calculations were carried out on either a Digital PDP-8E computer or a Texas Instruments SR-56 programmable calculator.

Distribution Coefficient of the Anthracyclines

A 1.2 x 10^{-4} M solution of the anthracycline (1 ml) in 2 mM PIPES buffer (pH 7.8, 21 mM Na^+) was vigorously shaken with 1 ml of n-octanol for 2 minutes at 25°C. After separation of the layers, the absorption at 480 nm of each was determined on a Gilford 240 spectrophotometer at ambient temperature. The distribution coefficient was calculated as the ratio of the absorption in octanol to the absorption in buffer.

RNA Polymerase Assay of the Anthracycline Template Inhibition

The kinetics of DNA-dependent *E. coli* RNA polymerase (Sigma Chem.) reactions were followed by the incorporation of [5-^{3}H] UMP (ICN) into TCA insoluble RNA according to the procedure of Preston et al.[146] The final reaction contained the following: 50 mM tris buffer, pH 7.8, 4 mM $MgCl_2$, 1 mM $mMCl_2$, 5 mM β-mercaptoethanol, 0.4 mM of nucleotide triphosphates ATP, GTP, CTP, AND UTP, 150 mM KCl, 0.12 mM calf thymus DNA P/1 0.12 mM anthracycline, 4.2% ethanol, and 4

Sigma units/ml of enzyme. All components in the above mixture were brought to 37°C and the reaction was initiated by addition of the polymerase. Samples of 100 μl were withdrawn at different intervals and immediately placed into a test tube containing 2 ml of 10% TCA at 0°C. The tube was shaken and allowed to incubate for 30 min. The mixture was then filtered through a Whatman GF/C fiber disks which had been prewashed with 5 ml of 10% TCA solution. Each disk was then washed 3 times with 5-10 ml of TCA, 3 times with 5-10 ml of an ether-ethanol solution (2:1), and 3 times with 5-10 ml of ether, dried at 80°C, placed in scintillation vials containing 5 ml of toluene, 0.4% 2,5-diphenyloxazole, 0.01% 1,4-di[2-(5-phenyloxazolyl)] benzene, and counted for 20 min in a Beckman LS-133 liquid scintillation counter.

<u>Rate of Dissociation of the Anthracyclines DNA Complex</u>

A solution which was 4 x 10^{-6} M anthracycline and 8 x 10^{-5} M salmon sperm DNA P/1 was prepared in 2 mM PIPES buffer (pH 7.8, either 21, 51, or 201 mM Na^{+}). Solutions of sodium dodecylsulfate (SDS) (0.6% concentration) were made in the same buffer and at 21, 51, and 201 mM Na^{+}. The rate of dissociation was determined by mixing the two solutions at 15°C in a Durrum-Gibson stop-flow apparatus (Durrum Instrument Corp.) thermostated with a Lauda K-2/R constant-temperature circulator.

<u>Hydrolysis of the Glycosidic Linkage of the Anthracyclines</u>

A 5 x 10^{-5} M solution of the anthracycline was prepared in the appropriate buffer and the concentration of daunose-

amine was determined as a function of time as follows.[137] A solution of o-phthalaldehyde (floropa), 2 ml of β-mercapto-ethanol and 0.4 M borate buffer (pH 9.7) was continuously passed through a flow through fluorescence cell in a Farrand ratio fluorometer connected to a Texas Instruments integrating recorder. A sample of the reaction mixture was injected into the buffer stream and the concentration of daunoseamine was determined from the area of the fluorescence peak by comparison to a standard curve. The data were calculated and plotted according to first order kinetics by a Digital PDP-8E computer. Least squares analysis was also performed.

pK_a of Daunorubicin

Spectra of daunorubicin at pH 6.5 and 12 showed that the transition at 480 nm had an extinction coefficient of 11500 and 3000 at pH 6.5 and 12, respectively. Solutions of daunorubicin (7×10^{-5} M) were made in 25 mM borax buffers at various pH, i.e., 9.2-10.8. Ten different borax buffers were prepared according to Bates and Bower.[138] Upon equilibration at either 25° or 50°C, the pH was determined with a Ratiometer Model 26 pH meter which had been standardized at the appropriate temperature with 0.1 molal borax buffer and a saturated $Ca(OH)_2$ solution according to the procedure of Bates.[147] The absorption of each solution was determined at 480 nm on a Gilford 240 spectrophotometer equipped with a thermostated cell compartment at either 25° or 50°C. The pK_a was then determined from a second derivative plot of absorption vs. pH.

REFERENCES

1. Watson, J. D., and Crick, F. H. C. (1953) Nature, 171, 737.

2. Watson, J. D. and Crick, F. H. C. (1953) Nature, 171, 964.

3. Watson, J. D. (1970) Molecular Biology of the Gene, N.Y., N.Y., W. A. Benjamin, Inc.

4. McBurney, M. W. and Whitmore, G. F. (1972) Biochem. Biophys. Res. Comm., 46, 898.

5. Josse, J. and Eigner, J. (1966) Ann. Rev. Biochem., 35, 789.

6. Emanuel, C. F. and Chailsoff, I. L. (1953) J. Biol. Chem., 203, 167.

7. Chargaff, E. and Lipschlitz, R. (1953) J. Am. Chem. Soc., 75, 3658.

8. Josse, J., Kaiser, A. D., and Kornberg, A. (1961) J. Biol. Chem., 236, 864.

9. Langridge, R., Wilson, H. R., Hooper, C. W., Wilkins, M. H. F., and Hamilton, L. P.(1960) J. Mol. Biol., 2, 19.

10. Donohue, J. (1969) Science, 165, 1091.

11. Donohue, J. (1970) Science, 167, 1700.

12. Donohue, J. (1971) J. Mol. Biol., 59, 381.

13. Davies, D. R. (1967) Ann Rev. Biochem., 36, 321.

14. Brams, S. (1972) Biochem. Biophys. Res. Comm., 48, 1088.

15. Brams, S. (1971) J. Mol Biol., 58, 277.

16. Brams, S. (1971) Nature New Biol., 233, 161.

17. Arnott, J., Fuller, W., Hodgson, A., and Prutton, I., (1968) Nature, 220, 561.

18. Doty, P. Boedtker, H., Fresco, J., Haselkorn, R., and Litt, M. (1959) Proc. Natl. Acad. Sci. U.S., 45, 482.

19. Mathieson, A. R. and Matty, S. (1957) J. Polymer Sci., 23, 747.

20. Gulland, J. M., Jordon, D. O., and Taylor, H. F. W. (1947) J. Chem. Soc., 1131.

21. Thomson, J. F., Carttar, M. S., and Tourtellotte, W. W. (1954) Radiation Res., 1, 165.

22. Helmkamp, G. K. and Ts'O, P. O. P. (1961) J. Am. Chem. Soc., 82, 138.

23. Donohue, J. (1956) Proc. Natl. Acad. Sci. U.S., 42, 60.

24. Donohue, J. (1960) J. Mol. Biol., 2, 263.

25. Nash, H. A. and Bradley, D. F. (1966) J. Chem. Phys., 45, 1380.

26. Hoogsteen, K. (1959) Acta Cryst., 12, 822.

27. Hoogsteen, K. (1963) Acta Cryst., 16, 907.

28. Haschemeyer, A. E. V. and Sobell, H. M. (1963) Proc. Natl. Acad. Sci. U.S., 50, 782.

29. Haschemeyer, A. E. V. and Sobell, H. M. (1965) Acta Cryst., 18, 525.

30. O'Brien, E. J. (1963) J. Mol. Biol., 7, 107.

31. O'Brien, E. J. (1966) J. Mol. Biol., 22, 377.

32. Tuppy, H. T. and Kuechler, E. K. (1964) Biophys. Biochem. Acta, 80, 669.

33. Katz, L., Tomaita, K., and Rich, A. (1965) J. Mol. Biol., 13, 340.

34. Katz, L. and Penman, S. (1965) J. Mol Biol., 15, 220.

35. Hamlin, R. M., Lord, R. C., and Ruh, A. (1965) Science, 148, 1734.

36. Fritzsche, H. (1971) Experientia, 27, 507.

37. Ts'O, P. O. P. (1968) Molecular Associations in Biology, Pulman, B., Editor, New York, N. Y., Academic Press.

38. Chan, S. I., Schweizer, M. P., Ts'O, P. O. P., and Helmkamp, G. K. (1964) J. Am. Chem. Soc., 86, 4182.

39. Pople, J. A., Schneider, W. G., and Bernstein, H. J. (1959) High Resolution Nuclear Magnetic Resonance, New York, N. Y., McGraw-Hill Book Co.

40. Broom, A. D., Schweizer, M. P., and Ts'O, P. O. P. (1967) J. Am. Chem. Soc., 89, 3612.

41. Hanlon, S. (1966) Biochem. Biophys. Res. Comm., 23, 861.

42. Chan, S. I. and Nelson, J. A. (1969) J. Am. Chem. Soc., 91, 168.

43. Tinoco, I., Jr., Davis, R. C., Jaskunas, S. R. (1968) Molecular Association in Biology, Pullman, B., Editor, New York, N. Y., Academic Press.

44. Cohen, G. and Eisenberg, H. (1969) Biopolymers, 35, 251.

45. Tinoco, I., Jr. (1960) J. Am. Chem. Soc., 82, 4745.

46. Tinoco, I., Jr. (1961) J. Chem. Phys., 34, 1067.

47. Devoe, H. and Tinoco, I., Jr. (1962) J. Mol. Biol., 4, 518.

48. Leng, M. and Felsenfeld, G. (1964) J. Mol. Biol., 15, 455.

49. Cantor, C. R. and Warshaw, M. M. (1970) Biopolymers, 9, 1059.

50. Tinoco, I., Jr. (1964) J. Am. Chem. Soc., 86, 297.

51. Printz, M. P. and von Hippel, P. H. (1965) Proc. Natl. Acad. Sci. U.S., 53, 363.

52. McConell, B. and von Hippel, P. H. (1970) J. Mol. Biol., 50, 297.

53. McConell, B. and von Hippel, P. H. (1970) J. Mol. Biol., 50, 317.

54. Muller, W. and Crothers, D. (1968) J. Mol. Biol., 35, 251.

55. Gabbay, E. J., DeStafano, R., and Baxter, C. S. (1973) Biochem. Biophys. Res. Comm., 51, 1083.

56. Jacob, J. and Monad, J. (1961) J. Mol. Biol., 3, 318.

57. Leng, M. and Felsenfeld, G. (1966) Proc. Natl. Acad. Sci. U.S., 56, 1325.

58. Shapiro, T., Leng, M., and Felsenfeld, G. (1969) Biochemistry, 8, 3219.

59. Raukas, E. (1965) Biokhimiya, 30, 1122.

60. Feugelman, M., Langridge, R., Sieds, W., Stokes, A., Wilson, H., Hooper, C., Wilkins, M., Barclay, R., and Hamilton, L. (1955) Nature, 175, 834.

61. Sobell, H. M., Jain, S. C., Sakore, P. D., and Nordman, C. E. (1971) Nature New Biol., 231, 200.

62. Richter, P. H. and Eigen, M. (1974) Biophys. Chem., 2, 255.

63. Raska, M. and Mandel, M. (1971) Proc. Natl. Acad. Sci. U.S., 68, 1190.

64. Helene, C., Montenay-Garestier, T., nad Dimicoli, J. L. (1971) Biophys. Biochem. Acta, 254, 349.

65. Helene, C., Dimicoli, J. L., and Brun, F. (1971) Biochemistry, 10, 3802.

66. Jardetsky, O. and Jardetsky, C. D., (1962) Methods Biochem. Anal., 9, 235.

67. Brown, P. E. (1970) Biophys. Biochem. Acta, 213, 282.

68. Kapicak, L. and Gabbay, E. J. (1975) J. Am. Chem. Soc., 9, 403.

69. Gabbay, E. J., Sanford, K., Baxter, C. S., and Kapicak, L. (1973) Biochemistry, 12, 4021.

70. Gabbay, E. J., Adawadkar, P. D., and Wilson, W. D. (1976) Biochemistry, 15, 146.

71. Ghione, M. (1975) Cancer Chemotherapy Reports, Part 3, 6, 83.

72. Arcamone, F., Franceschi, G., Orezzi, P., and Renco, S. (1968) Tet. Lett., 30, 3349.

73. Arcamone, F., Casinelli, G., Franceschi, G., Orezzi, P., and Modelli, R. (1968) Tet. Lett., 30, 3353.

74. Anguili, R., Arcamone, F., Foresti, E., Isaacs, N. W., Kennard, O., Motherwell, W. D. S., Riva di Sanseverino, L., and Wampler, D. L. (1971) Nature New Biol., 234, 78.

75. DiMarco, A., Gaetani, N., Orezzi, P., Scarpinato, B., Silverstrini, R., Soldatai, M., Dasdia, T., and Valentine, L. (1964) Nature, 201, 706.

76. Tan, C., Tasaka, H. Yu, L., Murphey, M. L., and Karnofoky, D. A. (1967) Cancer, 20, 333.

77. Boiron, M., Jacquillar, C., Weil, M., Tanzer, J., Levy, D., Sultan, G., and Bernard, J. (1969) Lancet, 1969, 330.

78. Theologides, A., Yarbro, J. W., and Kennedy, E. J. (1968) Cancer, 21, 16.

79. Rusconi, A. and DiMarco, A. (1969) Cancer Res., 29, 1507.

80. Meriwether, W. D. and Bachur, N. R. (1972) Cancer Res., 32, 1137.

81. Dano, K., Frederiksen, S., and Hellung-Larsen, P. (1972) Cancer Res., 32, 1307.

82. Silverstrini, R., Lenaz, L., DiFronzo, G., and Sanfilippo, O. (1973) Cancer Res., 33, 2954.

83. Bernard, J., Paul, R., Boirou, M., Jacquillat, C., and Maral, R. (1969) Rubiomycin, New York, N. Y., Springer Verlag.

84. Silverstrini, R., DiMarco, A., and Dasdia, T. (1970) Cancer Res., 30, 966.

85. Tobey, R. A. (1972) Cancer Res., 32, 2720.

86. Kim, S. H. and Kim, J. H. (1972) Cancer Res., 32, 323.

87. Mizuno, N. S., Zakis, B., and Decker, R. W. (1975) Cancer Res., 35, 1542.

88. Gasalvez, M., Blanco, M., Hunter, J., Miko, M., and Chance, B. (1974) Europ. J. Cancer, 10, 567.

89. Iwamoto, Y., Hausen, I. L., Porter, T. H., and Folkers, K. (1974) Biochem. Biophys. Res. Comm., 58, 633.

90. Murphree, S. A. Hwang, K. M., and Sartorelli, A. C. (1974) Pharmacologist, 16, 209.

91. Hwang, K. M., Murphree, S. A., and Sartorelli, A. C. (1974) Cancer Res., 34, 3396.

92. Dano, K. (1972) Cancer Chemotherapy Reports, Part 1, 56, 701.

93. Hasholt, L. and Dano, K. (1974) Hereditas, 77, 303.

94. DiMarco, A. (1975) Cancer Chemotherarpy Reports, Part 3, 6, 91.

95. DiMarco, A. (1975) Antineoplastic and Immunosuppressive Agents, Part II, Sartorelli, A. C. and Jones, D. C., Editors, New York, N. Y., Springer Verlag.

96. DiMarco, A. and Arcamone, F. (1975) Arzneim-Forsch., 25, 368.

97. Gabbay, E. J., Grier, D., Fingerle, R. E., Riemer, R., Levy, R., Pearce, S. W., and Wilson, W. D. (1976) Biochemistry, 15, 2062.

98. Dall'acqua, F., Terbojevich, M., Marciani, S., Vedaldi, D., and Rodighiero, G. (1974) Il. Farmaco, Ed. Sci., 29, 682.

99. Kersten, W., Kersten, H., and Szybalski, E. (1966) Biochemistry, 5, 236.

100. Lerman, L. S. (1961) J. Mol. Biol., 3, 18.

101. Waring, M. J. (1970) J. Mol. Biol., 54, 247.

102. Pigram, W. J., Fuller, W., and Hamilton, L. D. (1972) Nature New Biol., 235, 17.

103. Smith, B. (1969) Brit. Heart J., 31, 607.

104. Raskin, M. M., Rajurkar, M. G., and Altman, D. H. (1973) Am. J. Roetgenol., 118, 68.

105. Buja, I. M., Ferrans, V. J., Mayer, R. J., Roberts, W. C., and Henderson, E. S. (1973) Cancer, 26, 771.

106. Halazun, J. F., Wagner, H. R., Gaeta, J. F., and Sinks, L. F. (1974) Cancer, 27, 545.

107. Mhatre, R., Herman, E., Huidobro, A., and Wavavdekar, V. (1971) J. Pharmacol. and Exptl. Therapy, 178, 216.

108. Cargill, C., Bachmann, E., Zhinden, G. (1974) J. Natl. Cancer Inst., 53, 481.

109. Macrez, C., Maneffe-Lebrequillat, C., Weil, M. (1967) Pathol. Biol., 15, 949.

110. Minnow, R. A., Benjamin, R. S., and Gottlieb, J. A. (1975) Cancer Chemotherapy Reports, Part 3, 6, 195.

111. Herman, E., Mhatre, R., Lee, I. P., Vick, J., and Wavavdekar, V. S. (1971) Pharmacology, 6, 230.

112. Mildvan, A. S., and Cohn, M. (1970) Adv. Enzymol. Relat. Areas Md. Biol., 33, 1.

113. Dewek, R. A. (1973) Nuclear Magnetic Resonance in Biochemistry, Oxford, Clarendon Press.

114. Scatchard, G. (1949) Ann. N. Y. Acad. Sci., 51, 660.

115. Gabbay, E. J., and Kleinman, R. (1970) Biochem. J., 117, 247.

116. Gilmour, R. S., and Paul, J. (1970) FEBS Lett., 9, 242.

117. Kleinsmith, L. J., Heidema, J., and Carroll, A. (1970) Nature, 226, 1025.

118. Spelsberg, T. C., and Hnilica, L. S. (1970) Biochem. J., 120, 435.

119. Stein, G. S., and Farber, J. (1972) Proc. Natl. Acad. Sci. U. S., 69, 2918.

120. D'Anna, J. A., and Isenberg, I. (1974) Biochemistry, 13, 4992.

121. Kornberg, R. D. (1974) Science, 184, 868.

122. Kornberg, R. D., and Thomas, J. O. (1974) Science, 184, 865.

123. Olins, A. L., and Olins, D. E. (1974) Science, 183, 330.

124. Stein, G. S., Spelsberg, T. C., and Kleinsmith, L. J. (1974) Science, 183, 817.

125. van Holde, K. E., Sahasrabuddhe, C. G., and Shaw, B. R. (1974) Biochem. Biophys. Res. Comm., 70, 1365.

126. Gabbay, E. J., Glaser, R., and Gaffney, B. L. (1970) Ann. N. Y. Acad. Sci., 171, 810.

127. Gabbay, E. J., and Glaser, R. (1970) Biochemistry, 10, 1665.

128. Gabbay, E. J., Sanford, K. and Baxter, C. S. (1972) Biochemistry, 11, 3429.

129. Serman, L. S. (1961) J. Mol. Biol., 3, 18.

130. Mahler, H. R., Goutarel, R., Khuong-Huu, G., and Ho, M. T. (1966) Biochemistry, 5, 1966.

131. Wilkins, M. H. F. (1956) Cold Spring Harbor Symp. Quant. Biol., 21, 75.

132. Chothia, C. (1973) J. Mol. Biol., 75, 295.

133. Delange, R. J., and Smith, E. L. (1972) Acc. Chem. Res., 5, 368.

134. Sidman, J. W. (1956) J. Am. Chem. Soc., 78, 4567.

135. Roth, M., and Hampai, A. (1973) J. Chromatog., 83, 353.

136. Benson, J. R., and Hare, P. E. (1975) Proc. Natl. Acad. Sci. U. S., 72, 619.

137. Adkins, M., and Gabbay, E. J., unpublished results.

138. Bates, R. G., and Bower, U. E. (1956) Anal. Chem., 28, 1322.

139. Capon, B. (1971) Organic Reaction Mechanisms, 1971, New York, N. Y., Interscience Publishers.

140. Adkins, M., Vinson, T., O'Brien, D., and Gabbay, E. J., work in progress.

141. Anderson, G. W., Zimmerman, J. E., and Callahan, F. M. (1967) J. Am. Chem. Soc., 89, 5012.

142. Levy, G. C., and Nelson, G. L. (1972) Carbon-13 Nuclear Magnetic Resonance for Organic Chemists, New York, N. Y., Wiley-Interscience.

143. Zimm, B. H., and Crothers, D. M. (1962) Proc. Natl. Acad. Sci. U. S., 48, 905.

144. Pearce, S. W., Griggs, B. G., O'Brien, F., and Wilson, W. D. (1976) Chemical Instrumentation, 7, 33.

145. Sandorfy, C. (1964) Electronic Spectra and Quantum Chemistry, Englewood Cliffs, N. J., Prentice-Hall, Inc.

146. Preston, J. F., Stark, H. S., and Kimbrough, J. W. (1975) Lloydia, 38, 153.

147. Bates, R. G. (1962) J. Research N. B. S., 66A, 179.

BIOGRAPHICAL SKETCH

Stevens White Pearce

1948	Born August 7, in Annapolis, MD.
1966	Graduated from Seminole High School, Sanford, FL.
1966 - 67	Attended Seminole Junior College, Sanford, FL.
1967	A. A. Degree, Seminole Junior College, Sanford, FL.
1968	Attended University of Georgia, Athens, GA.
1968 - 70	Attended University of West Florida, Pensacola, FL., majored in biology.
1970	B. S. Degree, University of West Florida, Pensacola, FL.
1970 - 71	Attended University of West Florida, Pensacola, FL., majored in chemistry.
1971	B. S. Degree, University of West Florida, Pensacola, FL.
1971 - 72	Research technician, Entomology Division, U. S. Department of Agriculture
1972 - 77	Attended graduate school in chemistry, University of Florida, Gainesville, FL.
1977	Ph. D. Degree, University of Florida, Gainesville, FL.

I certify that I have read this study and that in my opinion it conforms to acceptable standards of scholarly presentation and is fully adequate, in scope and quality, as a dissertation for the degree of Doctor of Philosophy.

Edmond J. Gabbay, Chairman
Professor of Chemistry

I certify that I have read this study and that in my opinion it conforms to acceptable standards of scholarly presentation and is fully adequate, in scope and quality, as a dissertation for the degree of Doctor of Philosophy.

Paul Tarrant
Professor of Chemistry

I certify that I have read this study and that in my opinion it conforms to acceptable standards of scholarly presentation and is fully adequate, in scope and quality, as a dissertation for the degree of Doctor of Philosophy.

James A. Deyrup
Professor of Chemistry

I certify that I have read this study and that in my opinion it conforms to acceptable standards of scholarly presentation and is fully adequate, in scope and quality, as a dissertation for the degree of Doctor of Philosophy.

Willis B. Person
Professor of Chemistry

I certify that I have read this study and that in my opinion it conforms to acceptable standards of scholarly presentation and is fully adequate, in scope and quality, as a dissertation for the degree of Doctor of Philosophy.

Gary S. Stein
Associate Professor of Biochemistry

This dissertation was submitted to the Graduate Faculty of the Department of Chemistry in the College of Arts and Sciences and to the Graduate Council, and was accepted as partial fulfillment of the requirements for the degree of Doctor of Philosophy.

March 1977

Dean, Graduate School